Constraining the description of the nuclear force

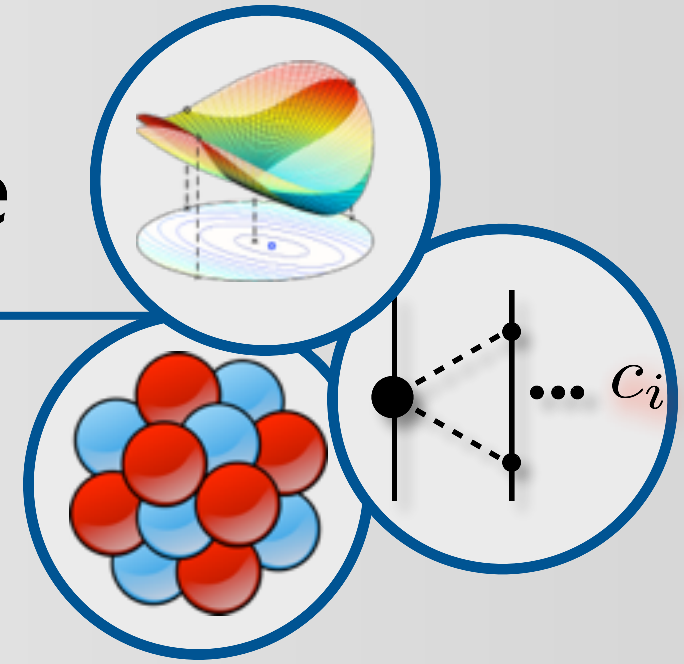

Andreas Ekström (UT/ORNL)

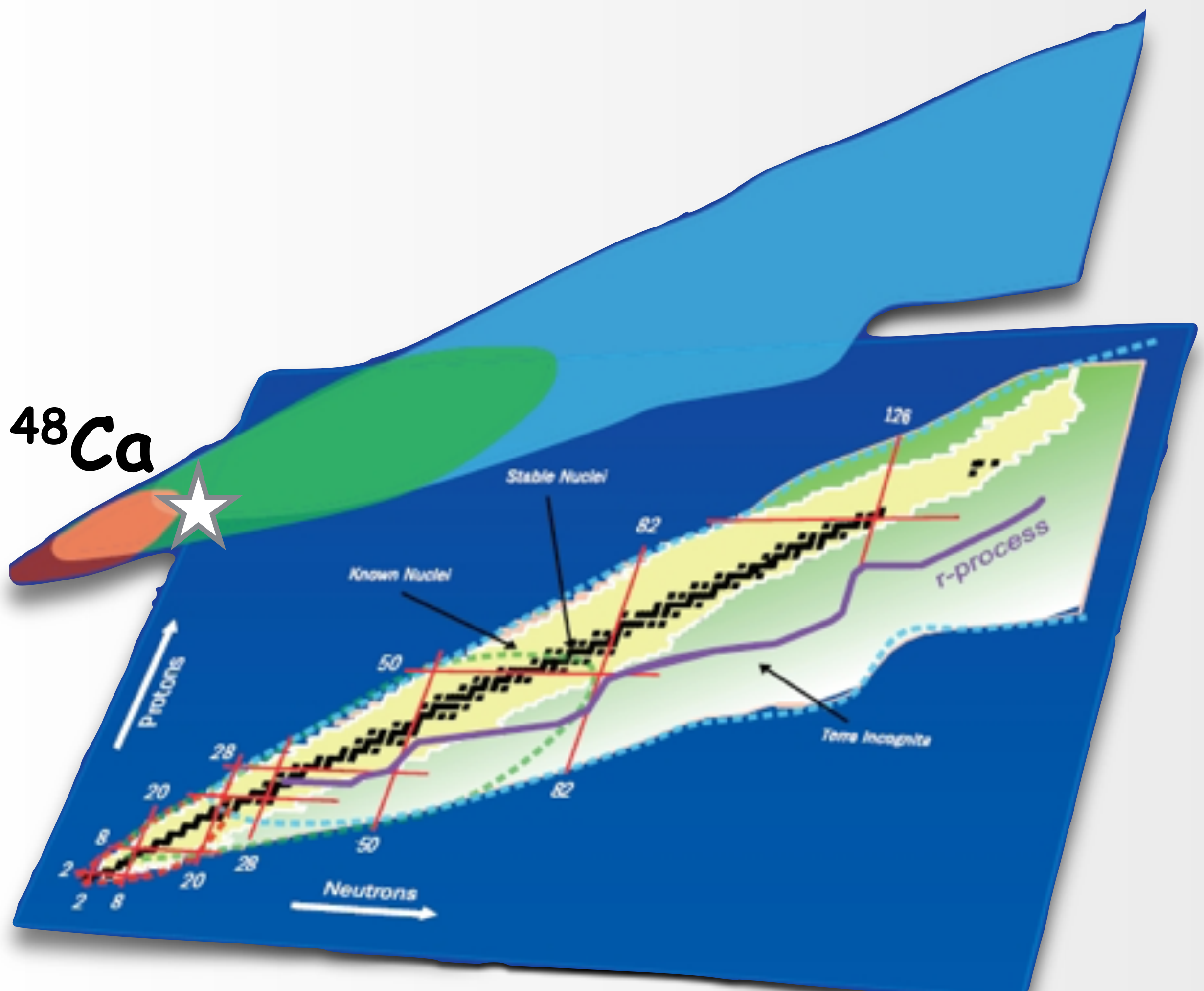

1. Overview
2. Precision and accuracy
3. Chiral effective field theory
4. New results: regression analysis
5. New results: $NNLO_{sat}$
6. Conclusions

Theory for open-shell nuclei near the limits of stability
May 11-29, 2015, East Lansing, MI, USA

Overview

- *Arrive at a Hamiltonian (a "standard model") of nuclear physics*
- *Understand the link between (Lattice) QCD and EFT and nuclei*
- *What are the limits for the existence of nuclei (i.e. drip line location)*
- *Explain collective phenomena from individual motion of nuclei*
- *Error estimates of computed quantities*
- *....*

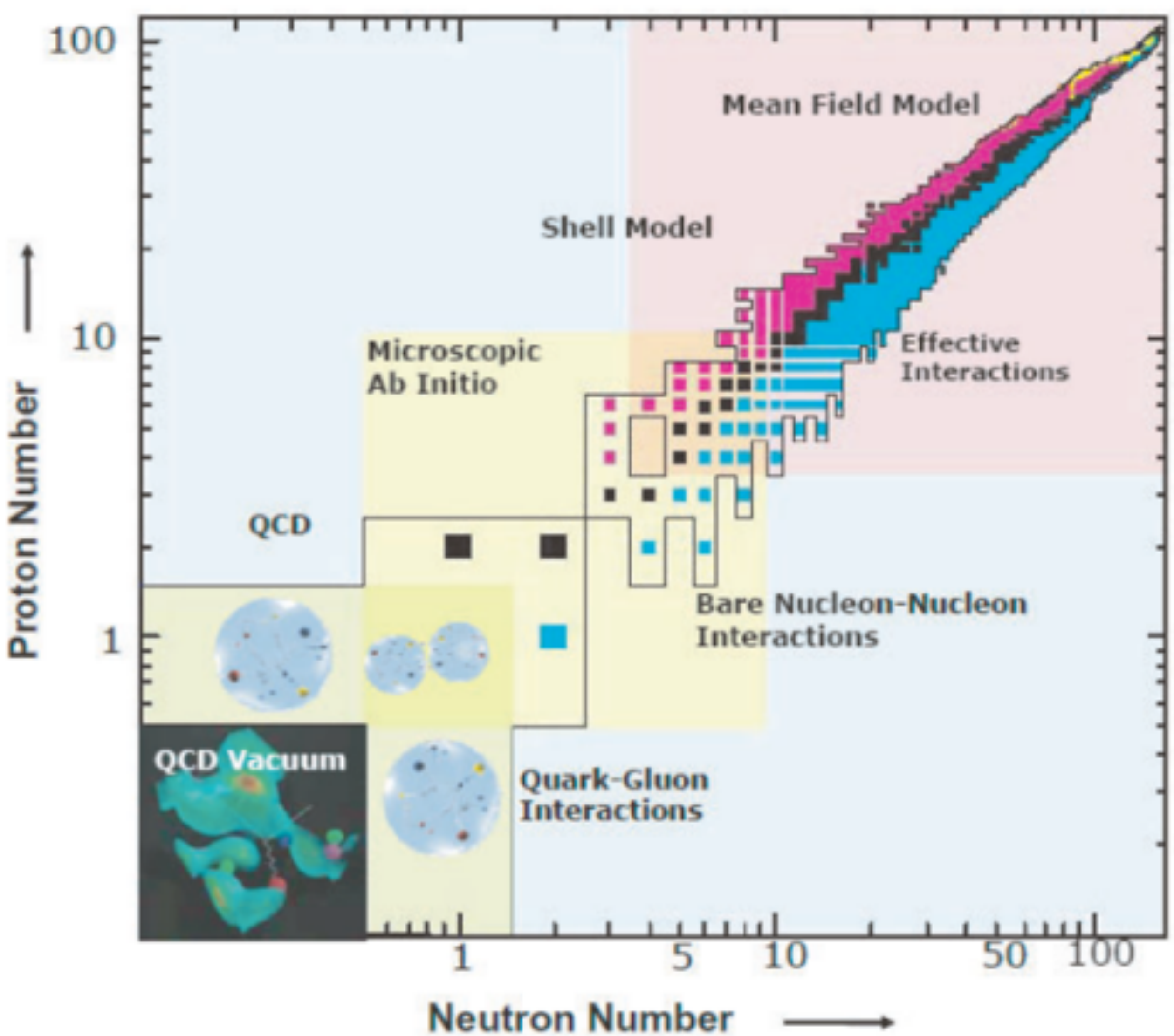

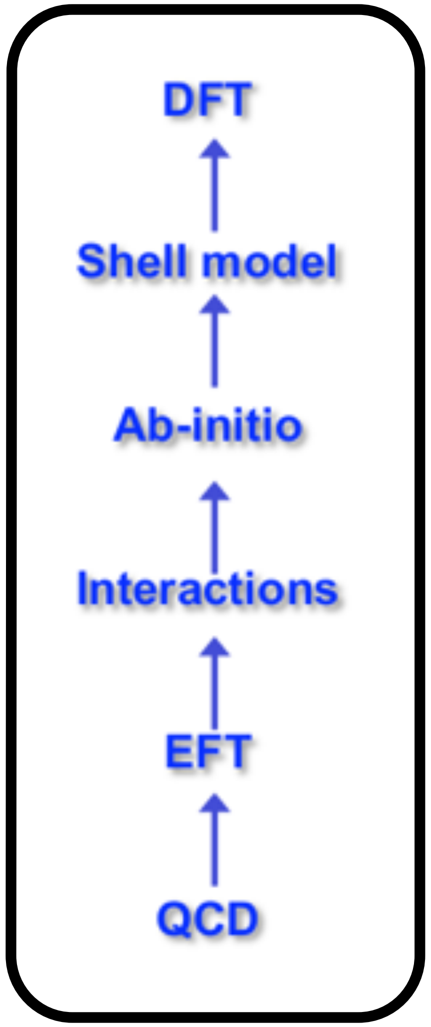

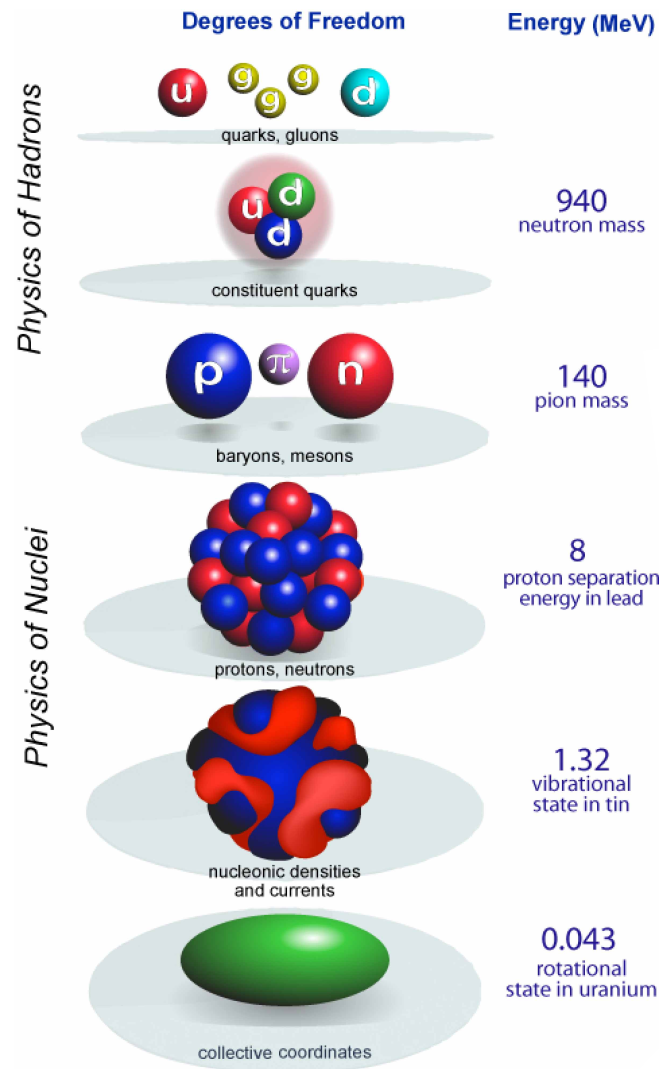

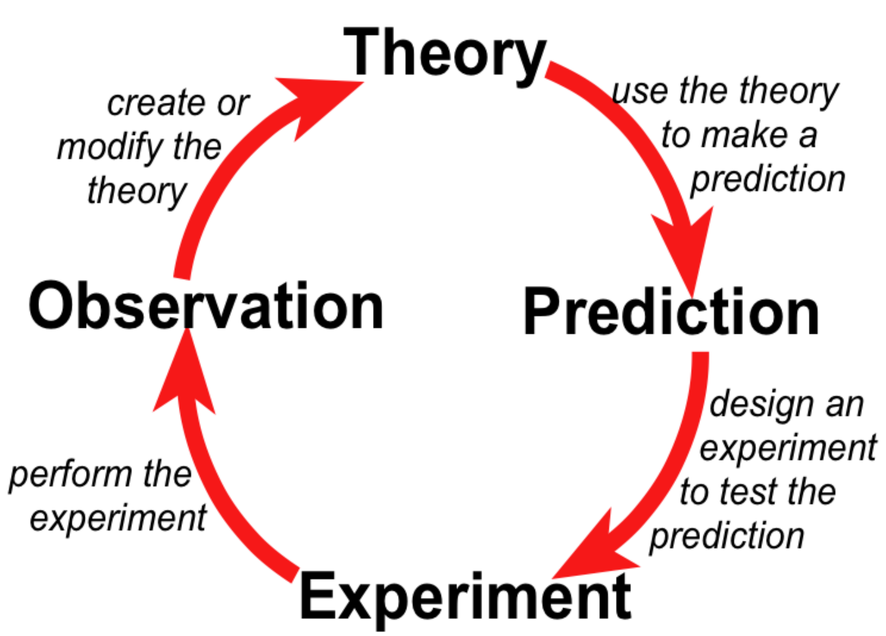

ab initio capabilities (a selection)

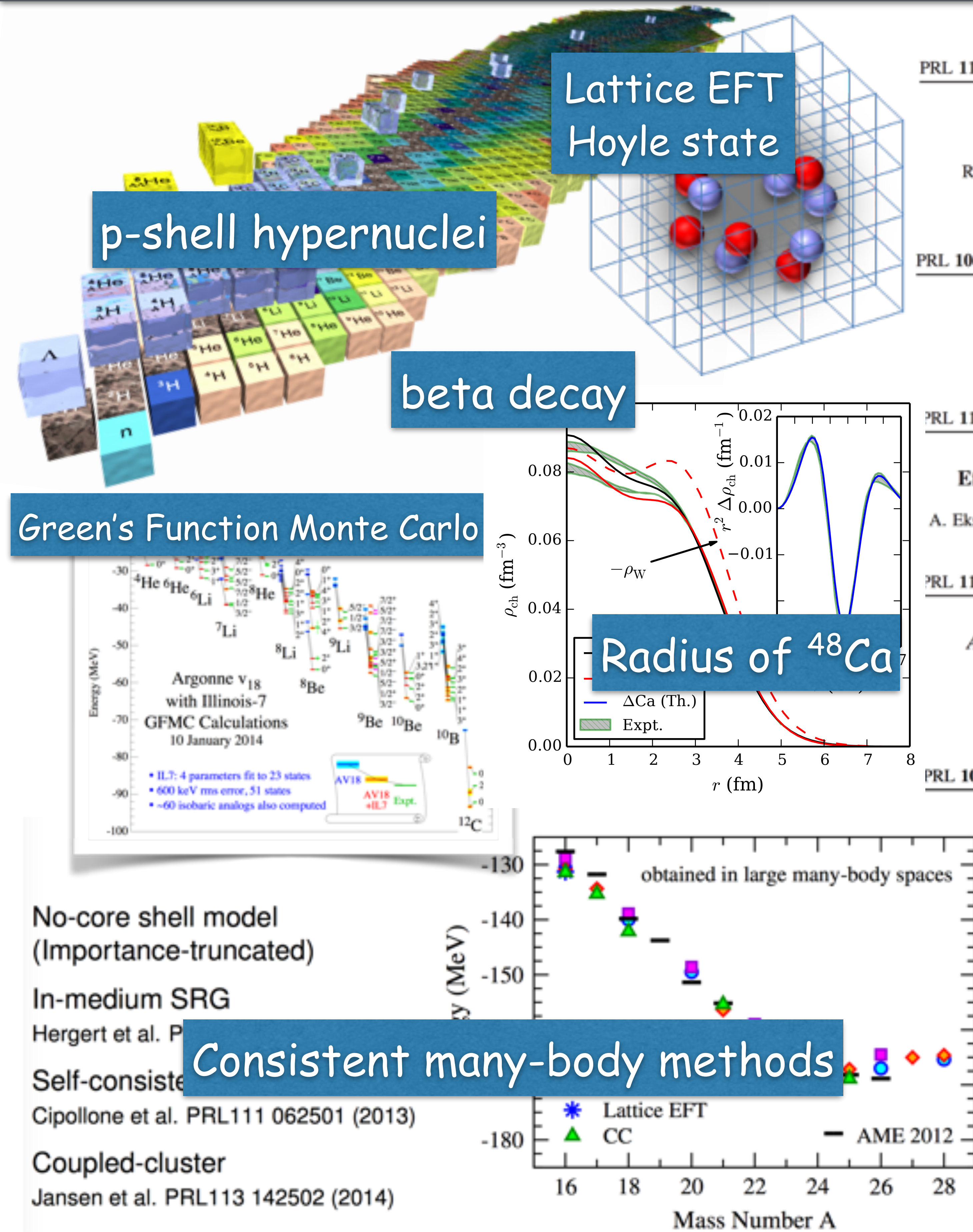

PRL 113, 192502 (2014) PHYSICAL REVIEW LETTERS week ending 7 NOVEMBER 2014

Ab Initio Description of p-Shell Hypernuclei

Roland Wirth,[1,*] Daniel Gazda,[2,3] Petr Navrátil,[4] Angelo Calci,[1] Joachim Langhammer,[1] and Robert Roth[1,†]

Selected for a Viewpoint in *Physics*

PRL 106, 192501 (2011) PHYSICAL REVIEW LETTERS week ending 13 MAY 2011

Ab Initio Calculation of the Hoyle State

Evgeny Epelbaum,[1] Hermann Krebs,[1] Dean Lee,[2] and Ulf-G. Meißner[3,4]

PRL 113, 262504 (2014) PHYSICAL REVIEW LETTERS week ending 31 DECEMBER 2014

Effects of Three-Nucleon Forces and Two-Body Currents on Gamow-Teller Strengths

A. Ekström,[1] G. R. Jansen,[2,3] K. A. Wendt,[3,2] G. Hagen,[2,3] T. Papenbrock,[3,2] S. Bacca,[4,5] B. Carlsson,[6] and D. Gazit[7]

PRL 113, 142502 (2014) PHYSICAL REVIEW LETTERS week ending 3 OCTOBER 2014

Ab Initio Coupled-Cluster Effective Interactions for the Shell Model: Application to Neutron-Rich Oxygen and Carbon Isotopes

G. R. Jansen,[1,2] J. Engel,[3] G. Hagen,[1,2] P. Navratil,[4] and A. Signoracci[1,2]

PRL 109, 032502 (2012) PHYSICAL REVIEW LETTERS week ending 20 JULY 2012

Evolution of Shell Structure in Neutron-Rich Calcium Isotopes

G. Hagen,[1,2] M. Hjorth-Jensen,[3,4] G. R. Jansen,[3] R. Machleidt,[5] and T. Papenbrock[1,2]

Many Many-Body Solvers:

Many-Body Perturbation Theory, Hyperspherical harmonics, NCSM-RGM, Gamow Shell Model, Continuum Shell-Model, Coupled Cluster, Self-Consistent Green's Functions, Faddeev, Bogoliubov CC, Gorkov SCGF, Monte Carlo Shell-Model, …

ab initio capabilities (a selection)

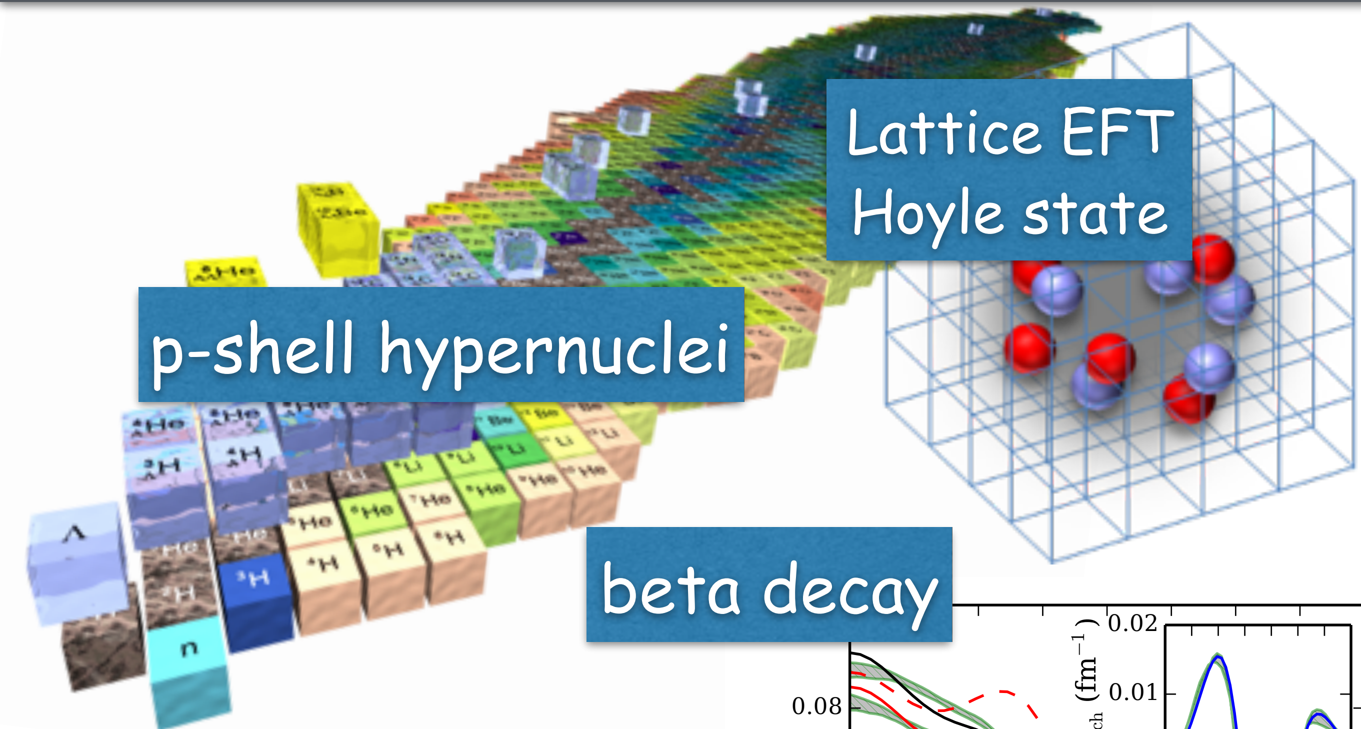

PRL 113, 192502 (2014) PHYSICAL REVIEW LETTERS week ending 7 NOVEMBER 2014

Ab Initio Description of p-Shell Hypernuclei

Roland Wirth,[1,*] Daniel Gazda,[2,3] Petr Navrátil,[4] Angelo Calci,[1] Joachim Langhammer,[1] and Robert Roth[1,†]

Selected for a Viewpoint in *Physics*

PRL 106, 192501 (2011) PHYSICAL REVIEW LETTERS week ending 13 MAY 2011

Ab Initio Calculation of the Hoyle State

Evgeny Epelbaum,[1] Hermann Krebs,[1] Dean Lee,[2] and Ulf-G. Meißner[3,4]

PRL 113, 262504 (2014) PHYSICAL REVIEW LETTERS week ending 31 DECEMBER 2014

Effects of Three-Nucleon Forces and Two-Body Currents on Gamow-Teller Strengths

A. Ekström,[1] G. R. Jansen,[2,3] K. A. Wendt,[3,2] G. Hagen,[2,3] T. Papenbrock,[3,2] S. Bacca,[4,5] B. Carlsson,[6] and D. Gazit[7]

PRL 113, 142502 (2014) PHYSICAL REVIEW LETTERS week ending 3 OCTOBER 2014

Ab Initio Coupled-Cluster Effective Interactions for the Shell Model: Application to Neutron-Rich Oxygen and Carbon Isotopes

G. R. Jansen,[1,2] J. Engel,[3] G. Hagen,[1,2] P. Navratil,[4] and A. Signoracci[1,2]

PRL 109, 032502 (2012) PHYSICAL REVIEW LETTERS week ending 20 JULY 2012

Green's Function Monte Carlo

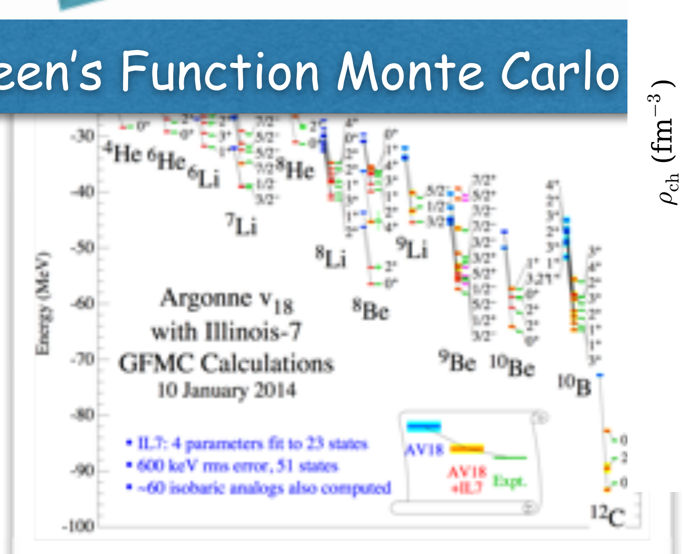

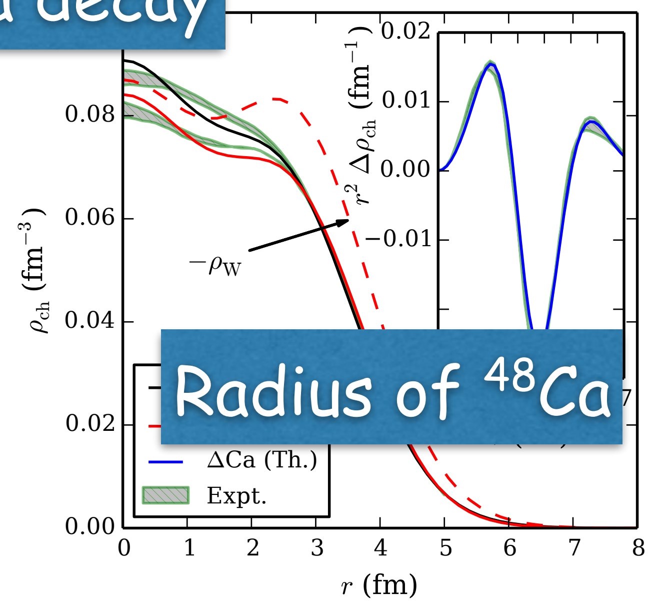

No-core shell model
(Importance-truncated)

In-medium SRG
Hergert et al. P

Self-consiste

Cipollone et al. PRL111 062501 (2013)

Coupled-cluster
Jansen et al. PRL113 142502 (2014)

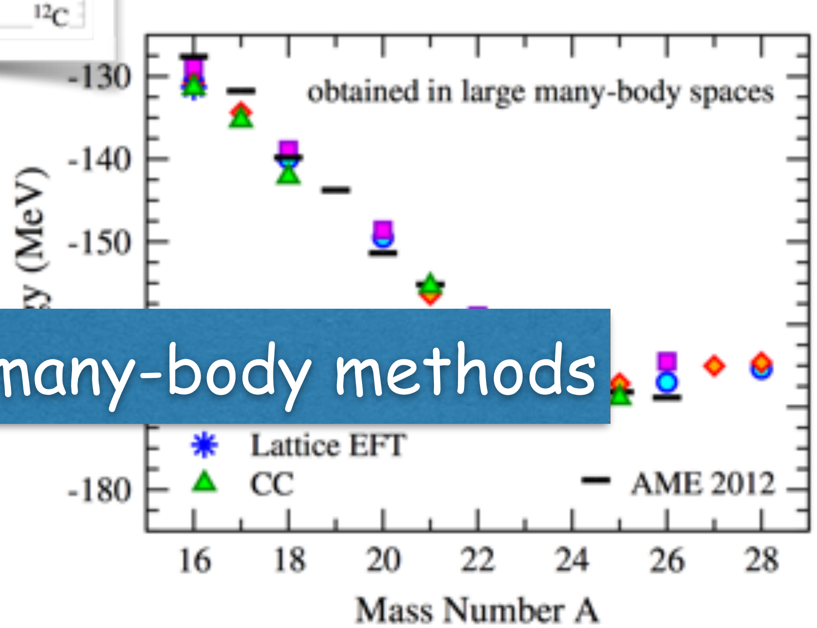

Numerically converged solutions to the Schrödinger equation signal deficiencies in the description of the nuclear force

Lattice QCD

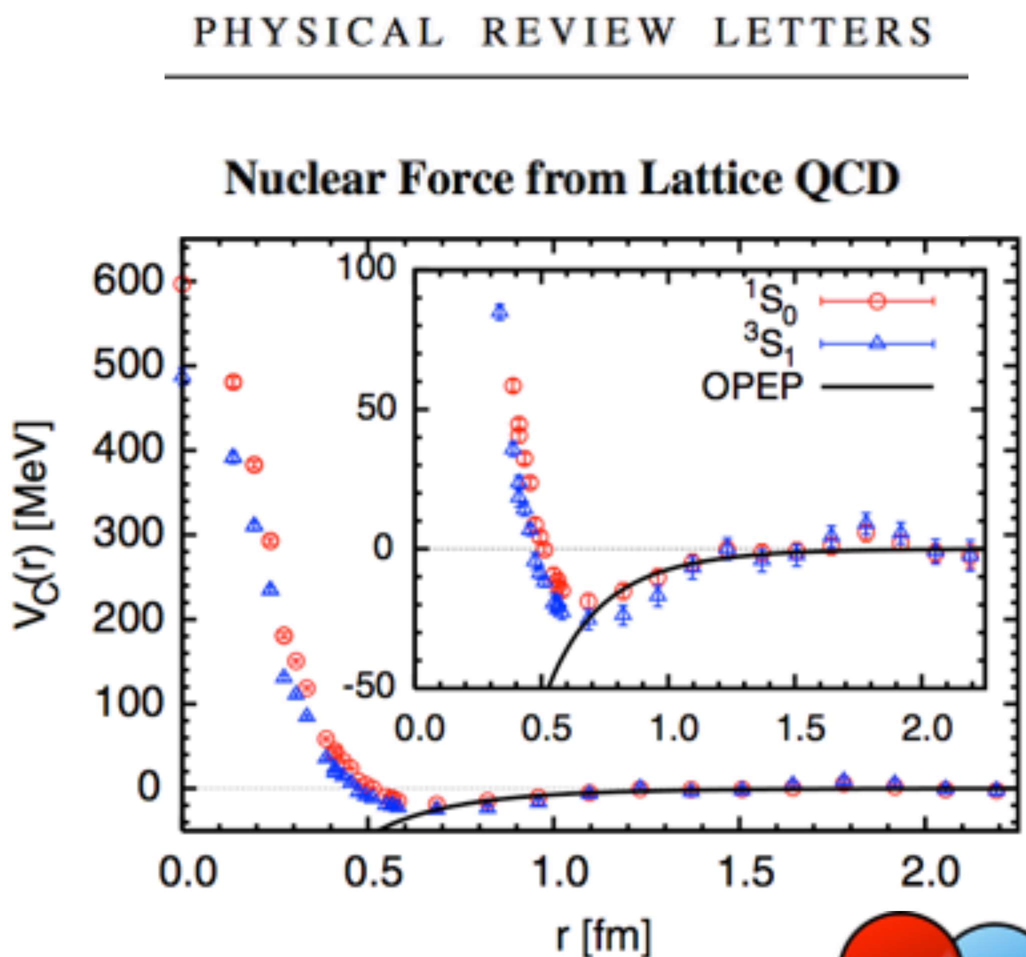

LQCD is computationally demanding

- unphysical pion masses right now
- requires larger lattices
- exponentially small signal-to-noise ratio
- difficult to identify bound states
- growth of Wick contractions for large number of quarks
- …. …. ….

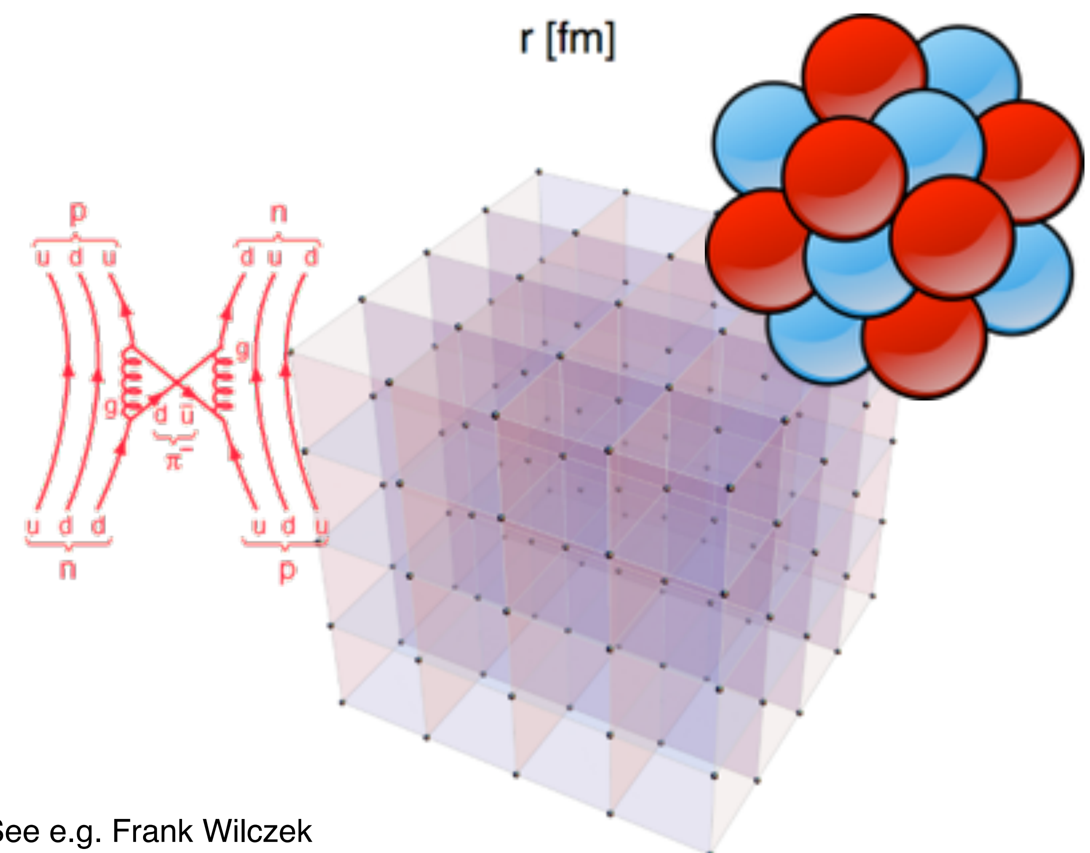

See e.g. Frank Wilczek
Nature Vol 445, January 2007

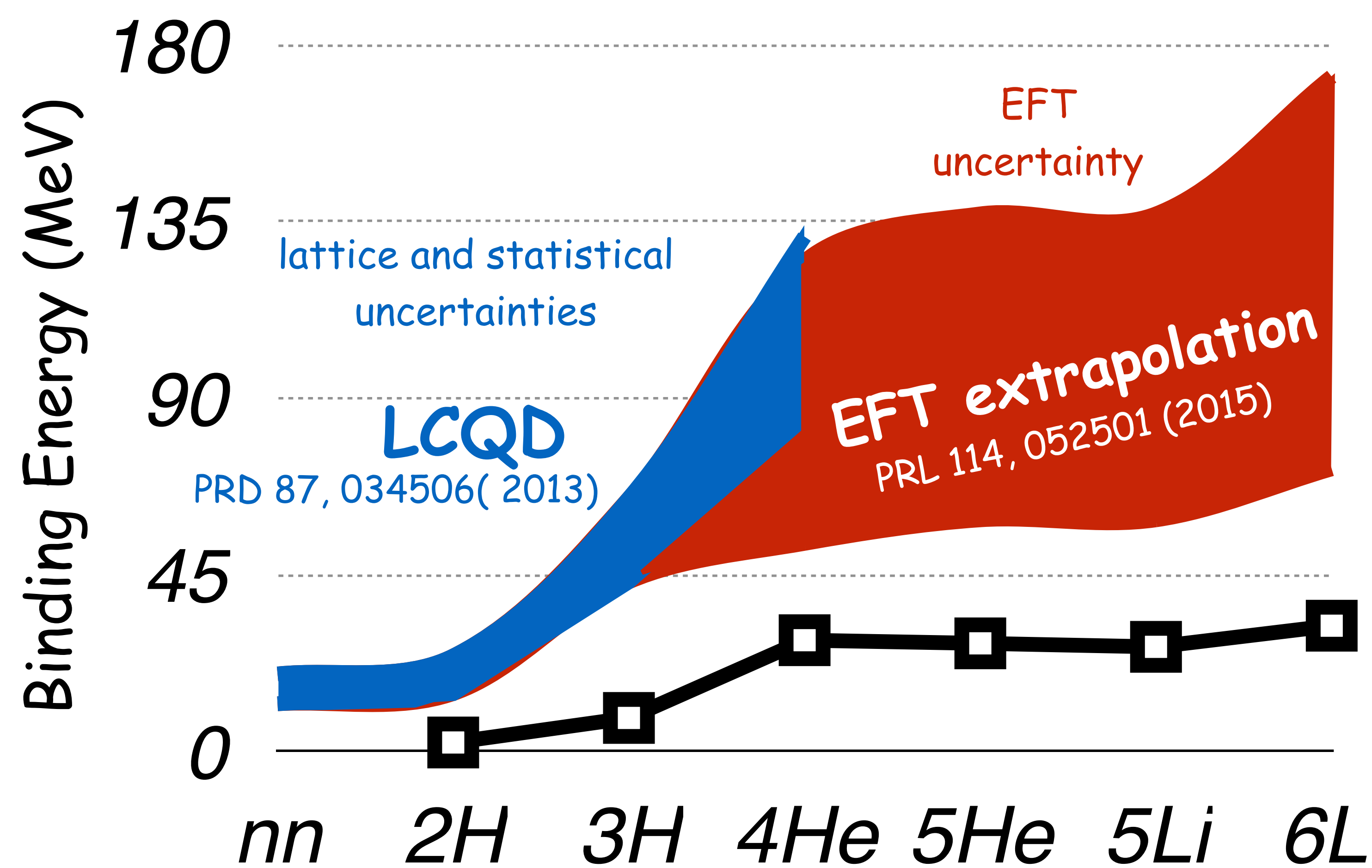

This talk will be about precision and accuracy

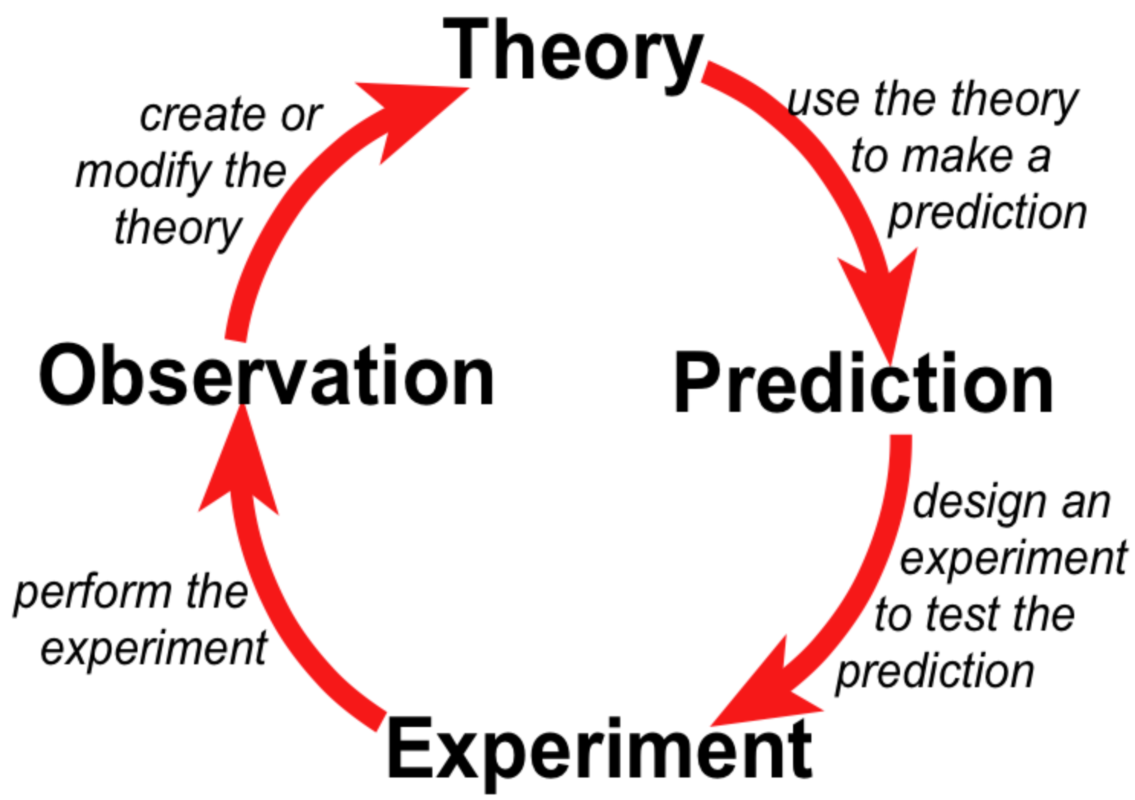

This talk will be about precision and accuracy

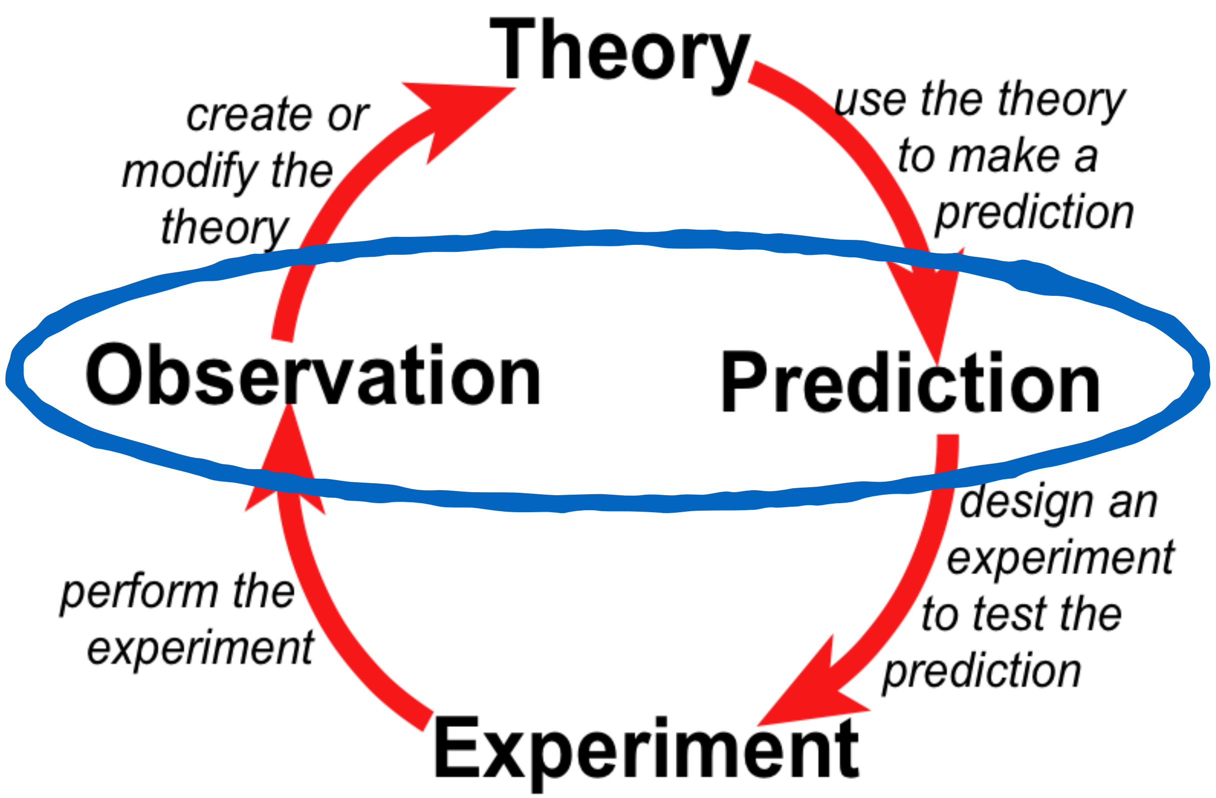

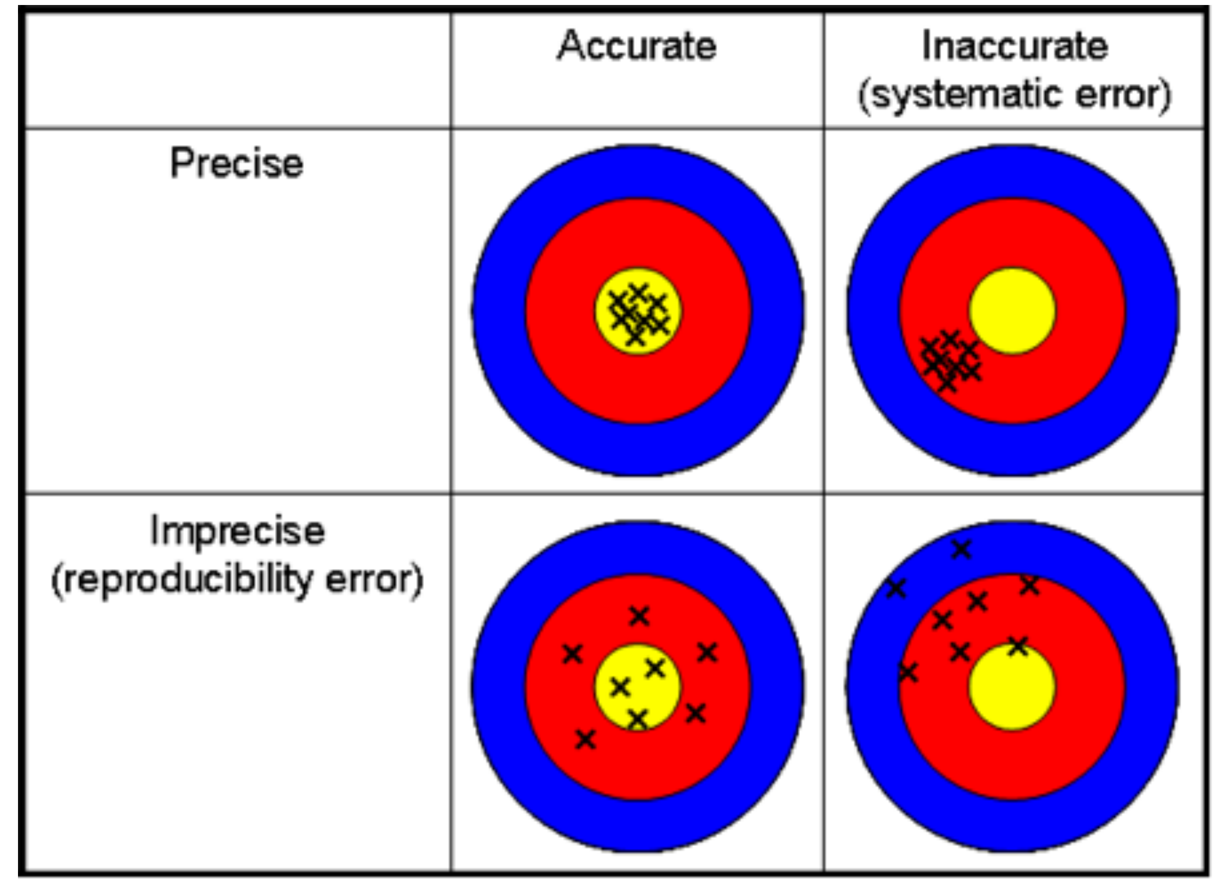

This talk will be about precision and accuracy

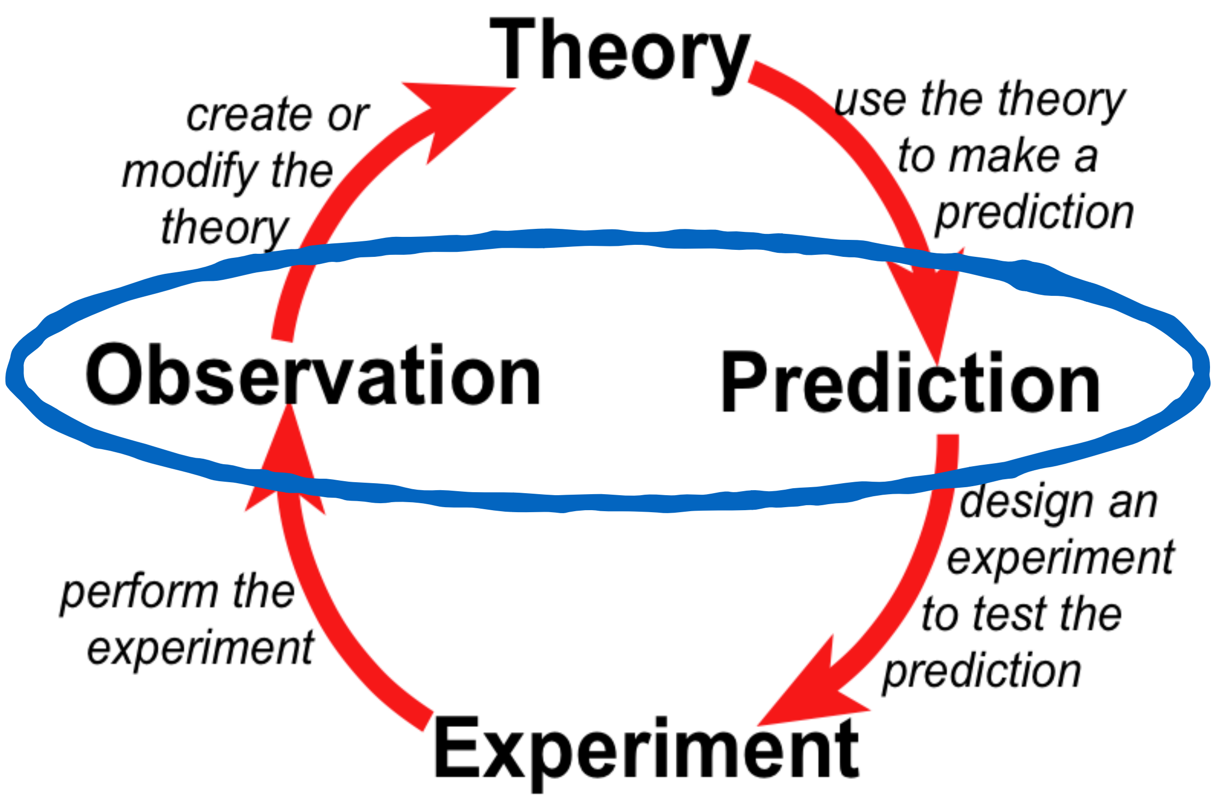

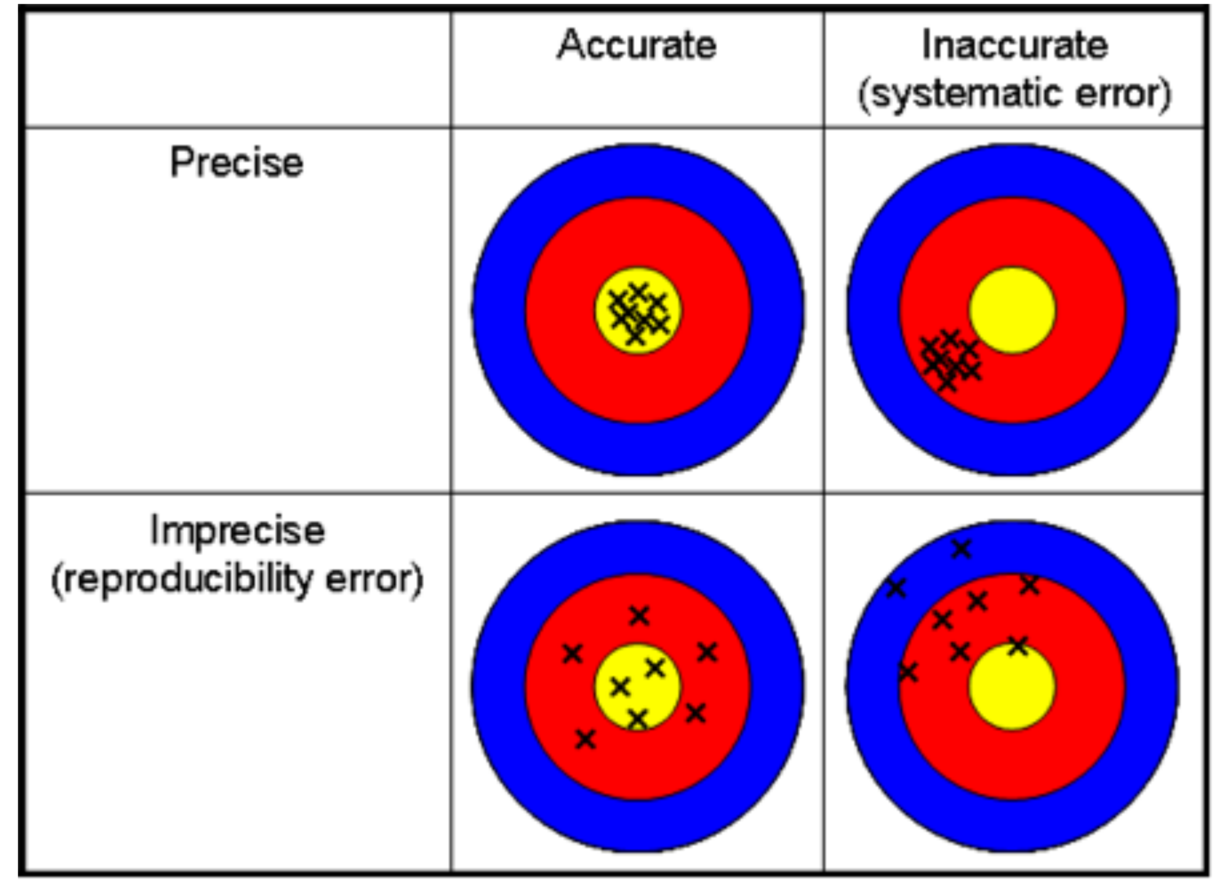

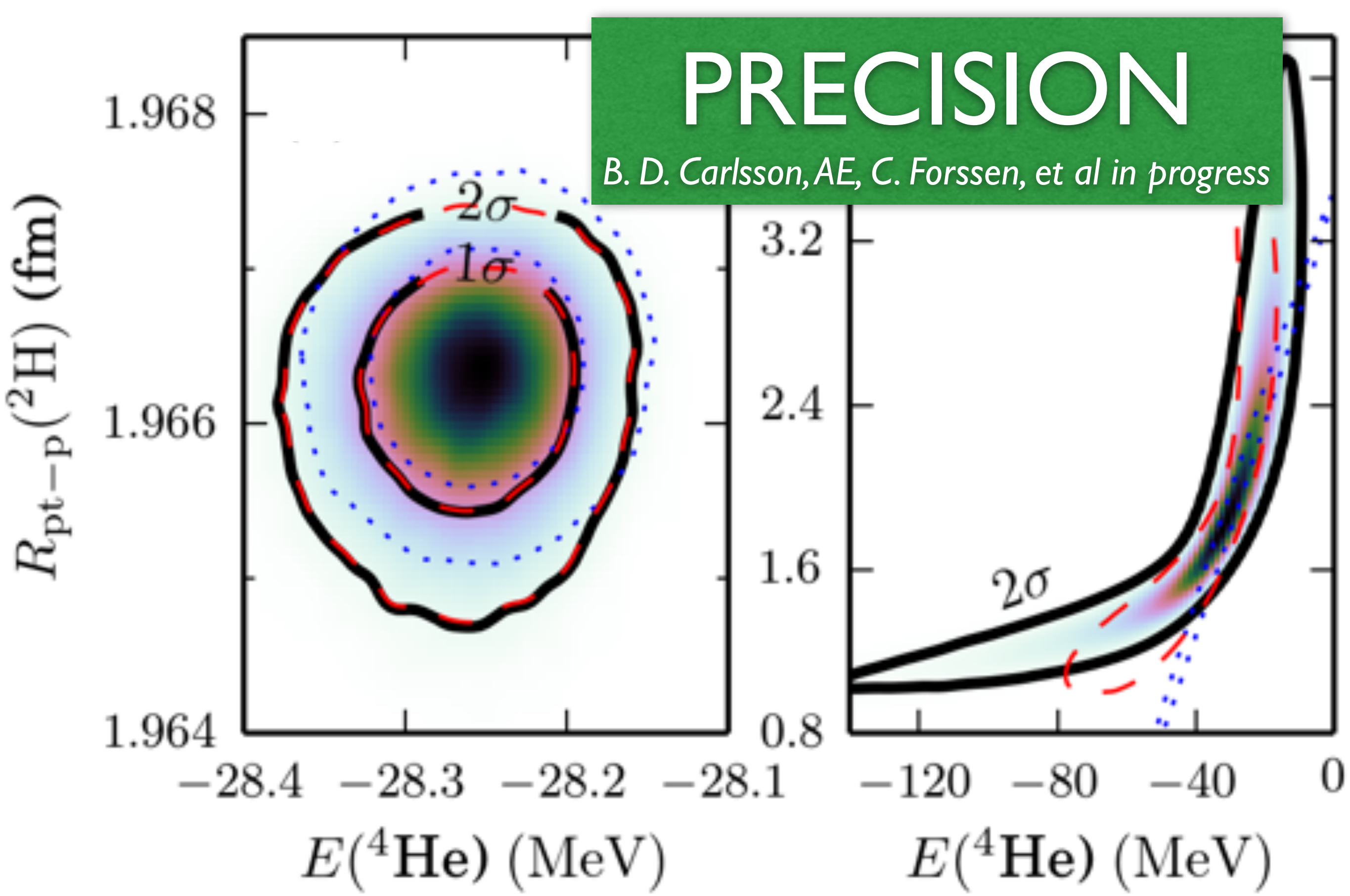

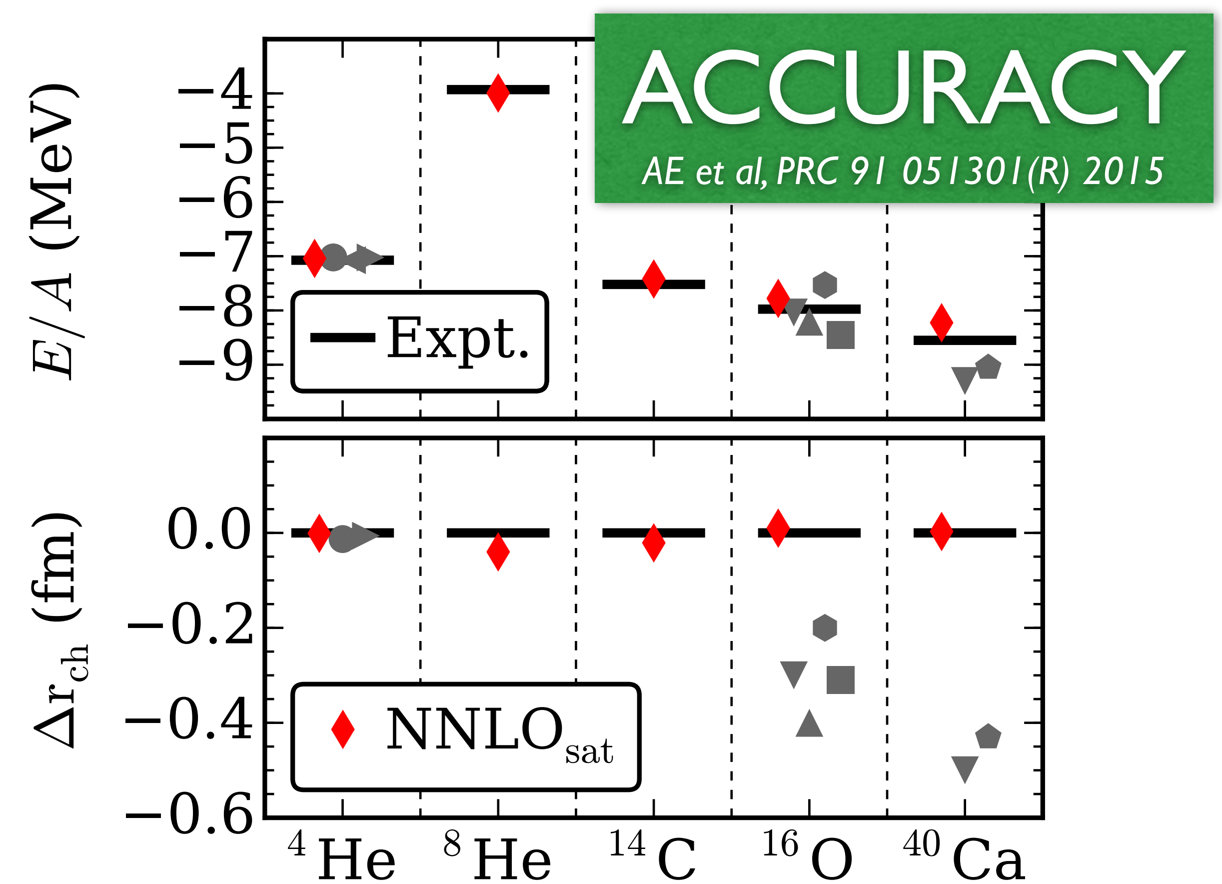

Chiral Effective Field Theory (χEFT)

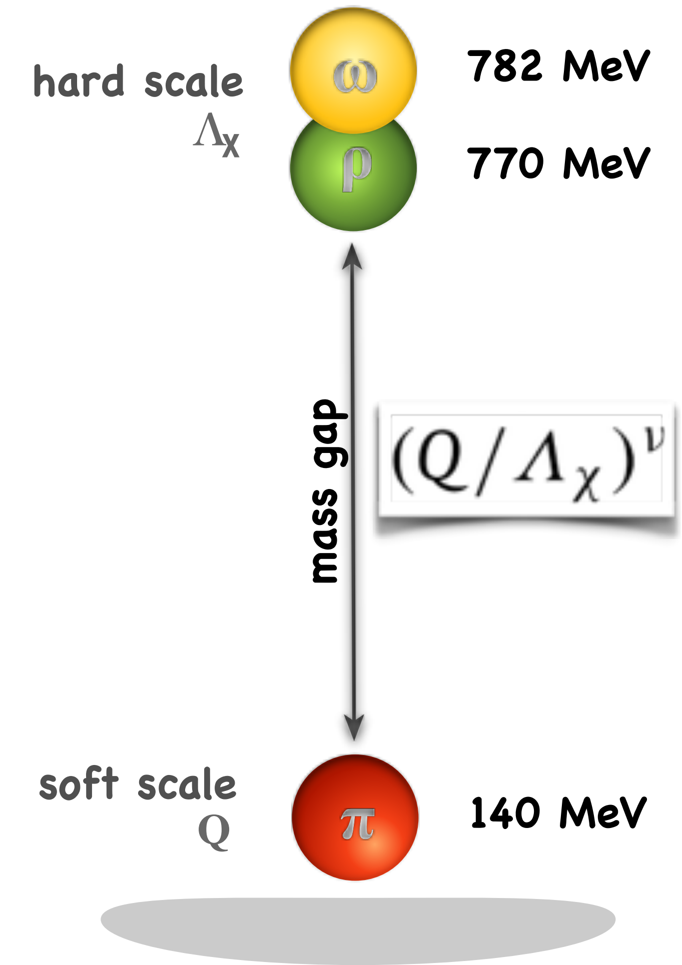

E. Epelbaum et al. Rev. Mod. Phys. 81, 1773 (2009)
R. Machleidt et al. Phys. Rep. 503, 1 (2011)

Chiral Effective Field Theory (χEFT)

LO

NLO

NNLO

N3LO

N4LO

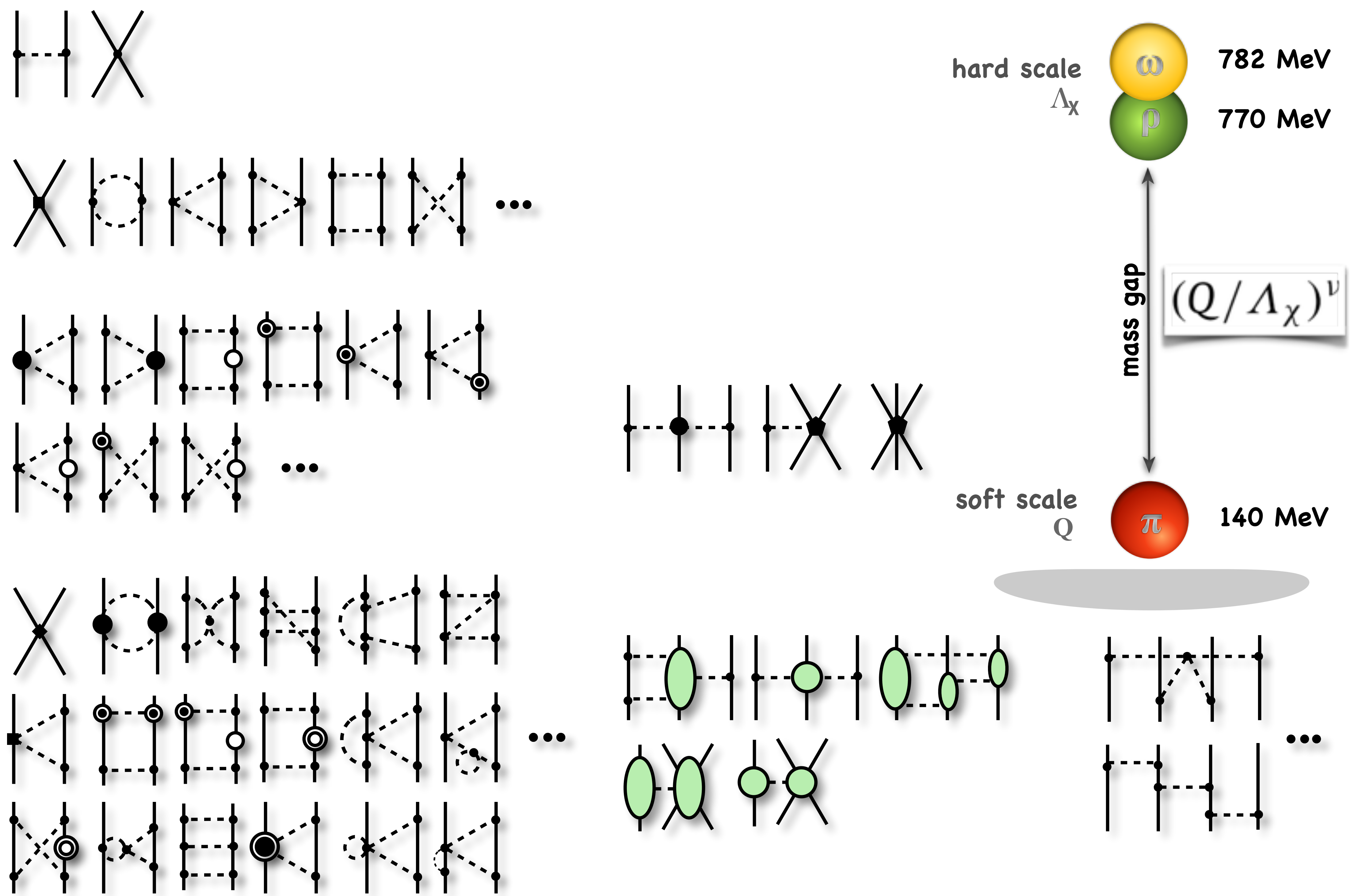

E. Epelbaum et al. Rev. Mod. Phys. 81, 1773 (2009)
R. Machleidt et al. Phys. Rep. 503, 1 (2011)

Chiral Effective Field Theory (xEFT)

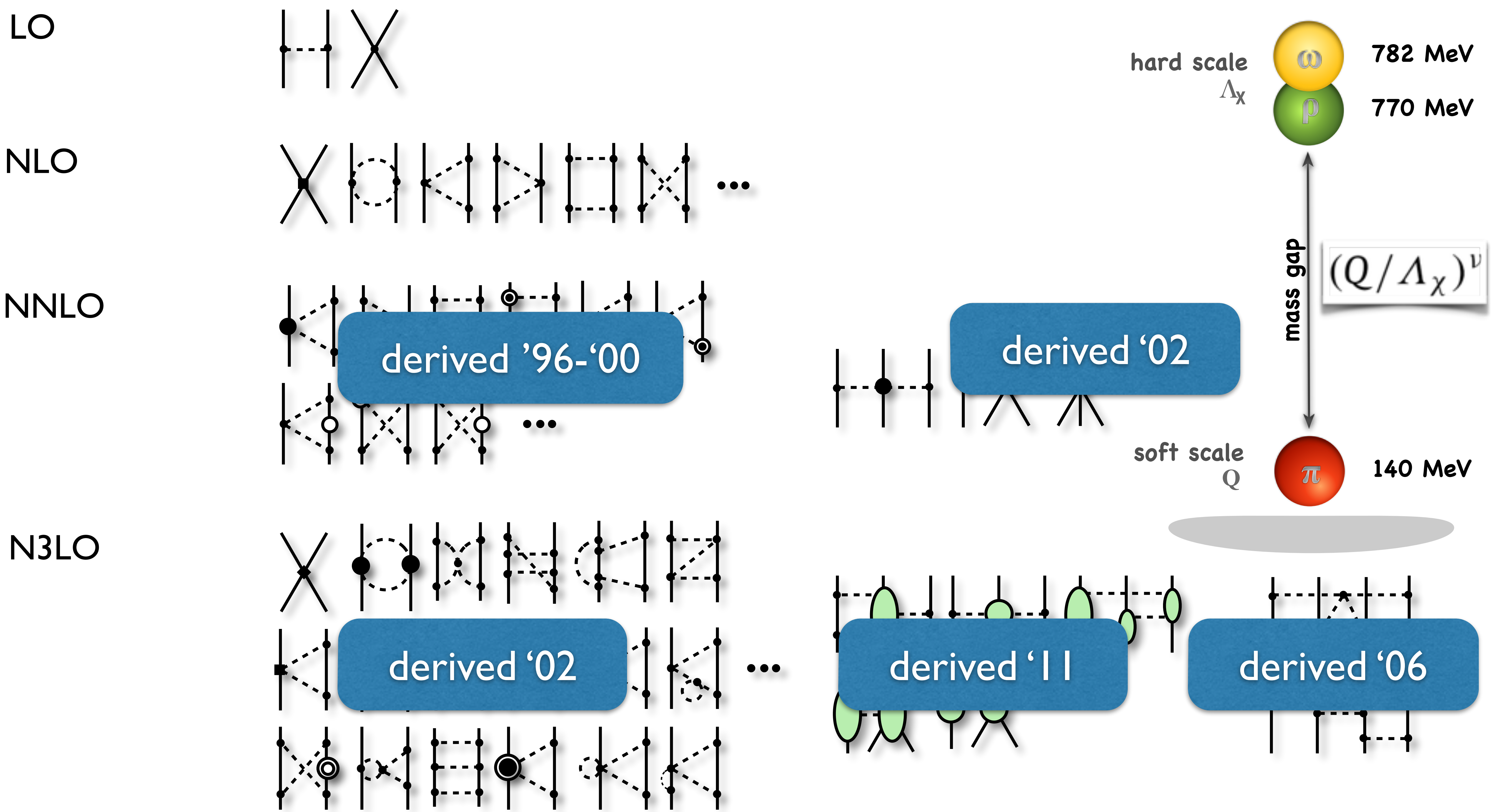

N4LO

derived '15

E. Epelbaum et al. Rev. Mod. Phys. 81, 1773 (2009)
R. Machleidt et al. Phys. Rep. 503, 1 (2011)

Chiral Effective Field Theory (χEFT)

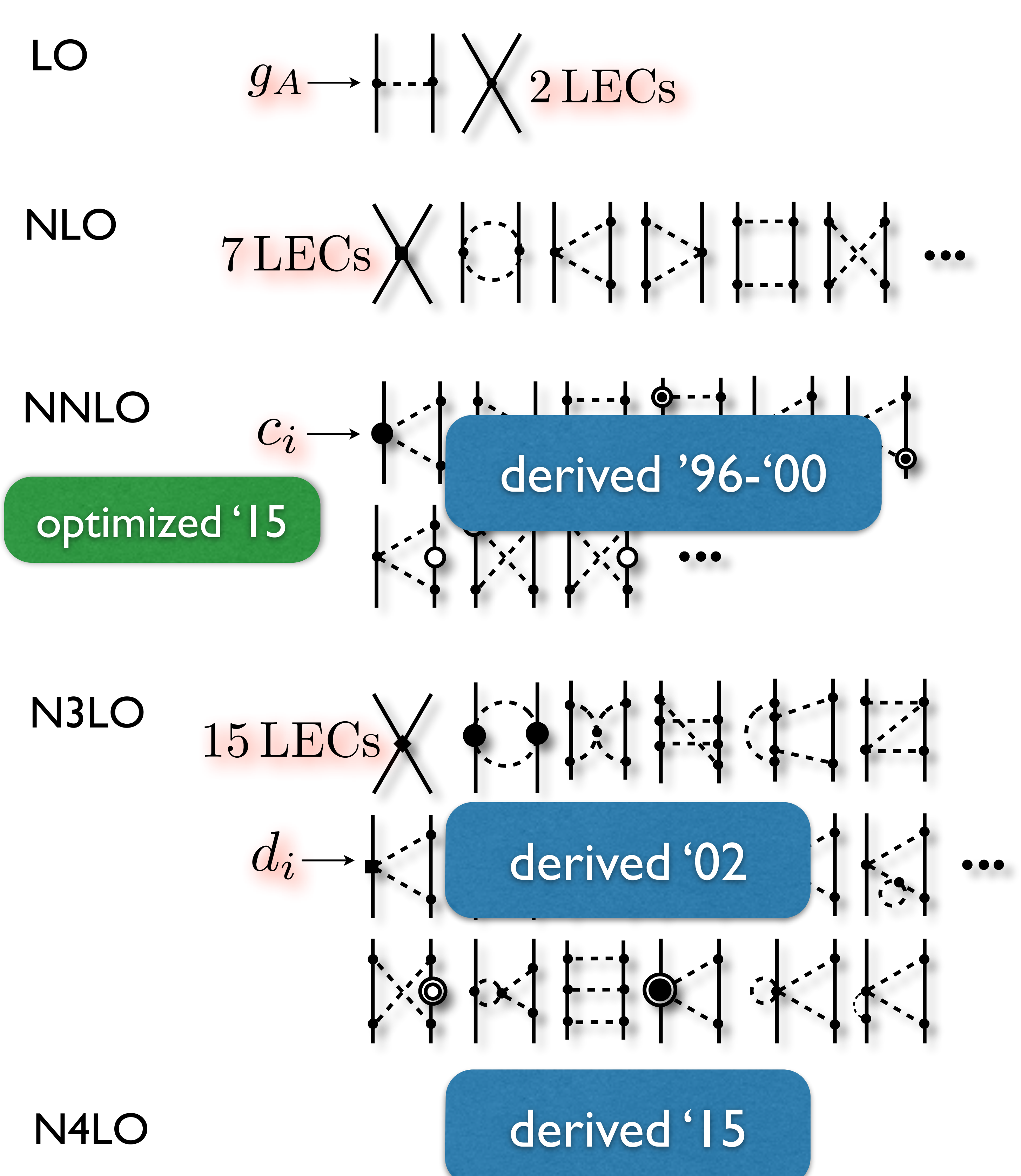

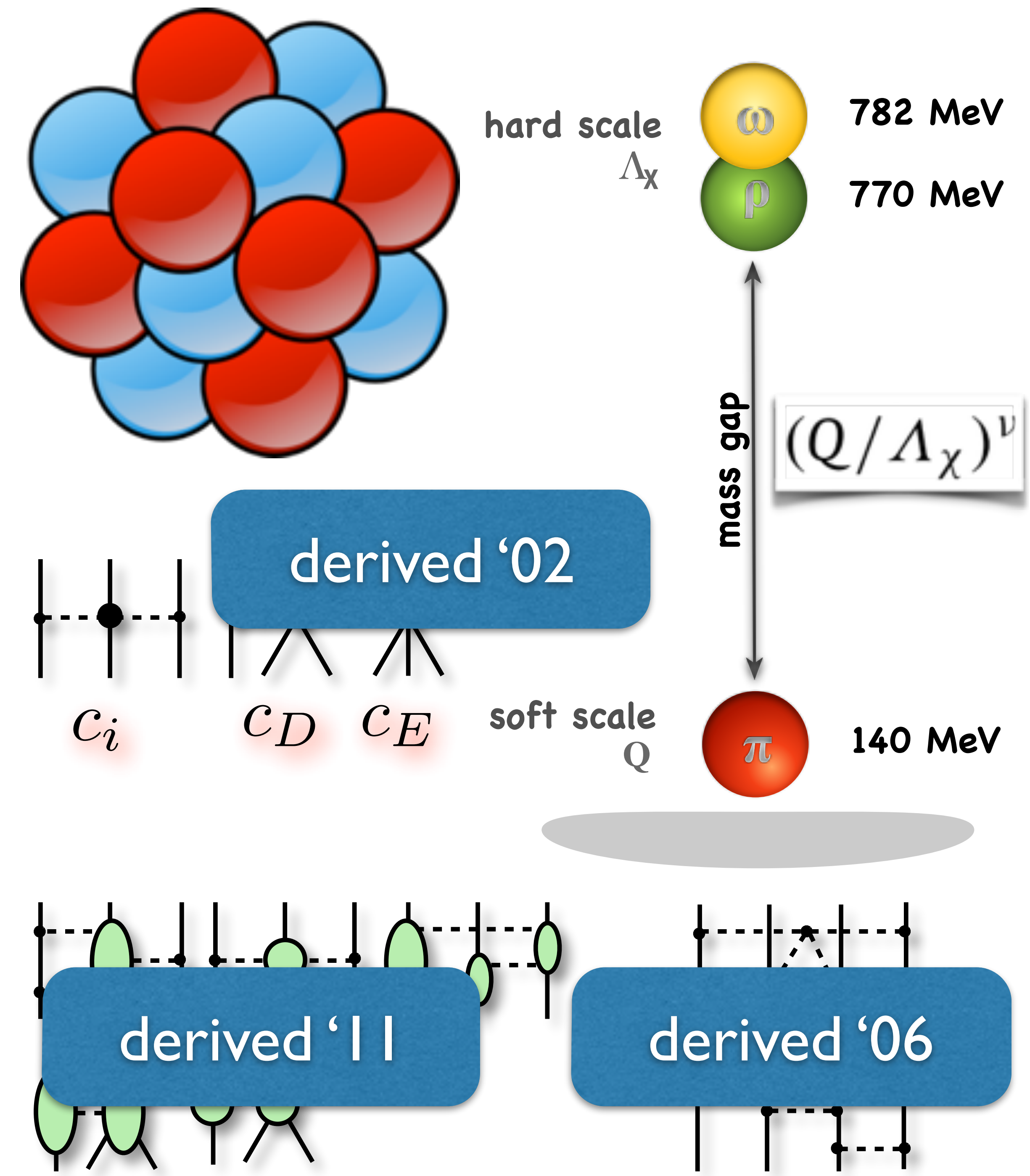

E. Epelbaum et al. Rev. Mod. Phys. 81, 1773 (2009)
R. Machleidt et al. Phys. Rep. 503, 1 (2011)

Chiral Effective Field Theory (χEFT)

LO

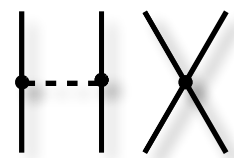

NLO

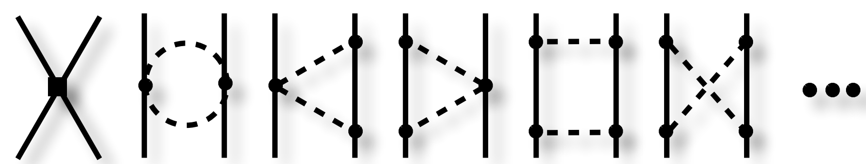

NNLO

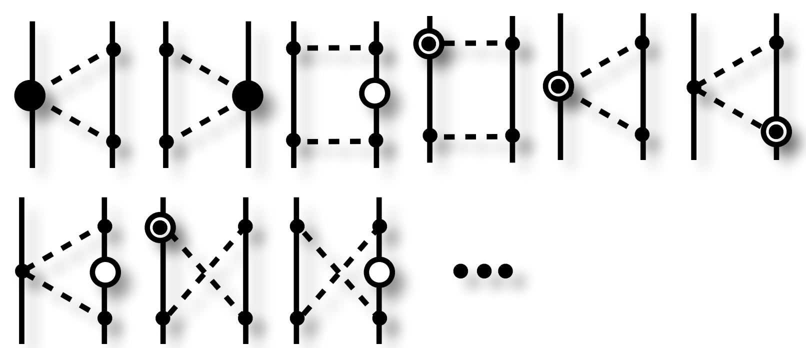

optimized '15

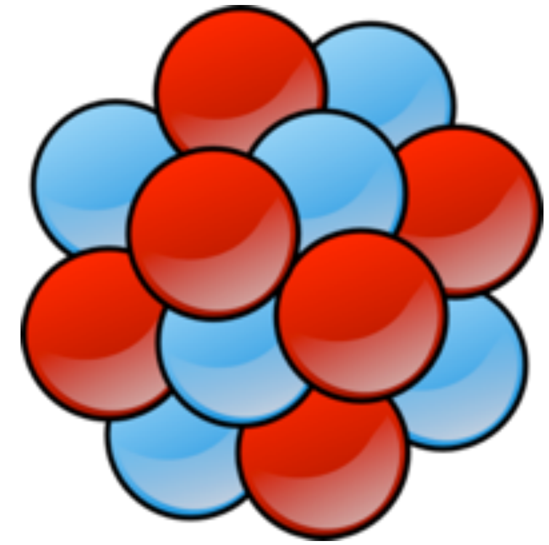

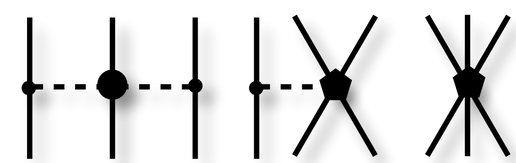

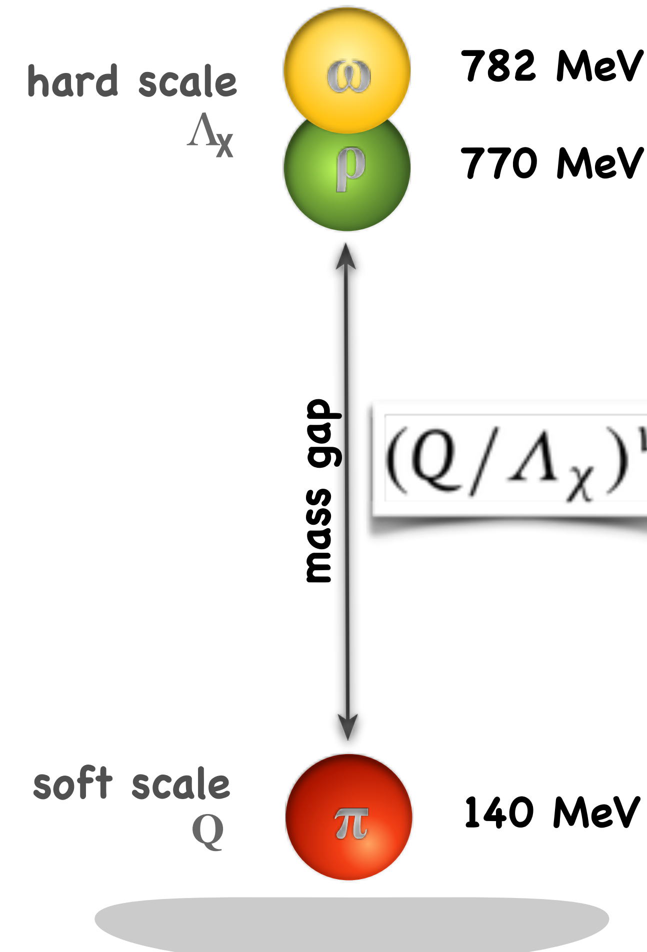

Nuclear physics at NNLO (AE et al PRL 110, 192502 (2013))
Statistical Uncertainties at NNLO (AE et al J. Phys. G. 42 034003 (2014))

Still many unresolved issues:

- **order-by-order convergence**
- **uncertainties**
- cutoff dependence
- power counting

Chiral Effective Field Theory (χEFT)

LO

NLO

NNLO

optimized '15

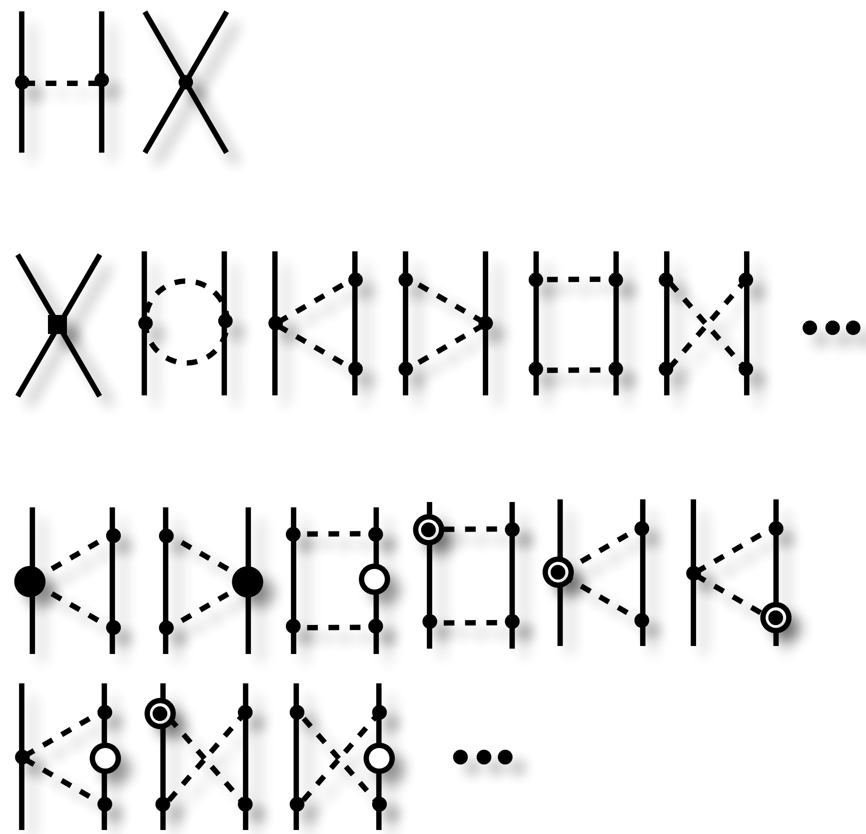

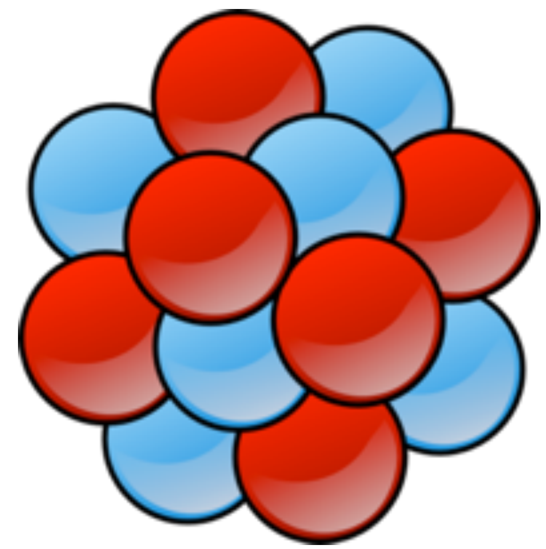

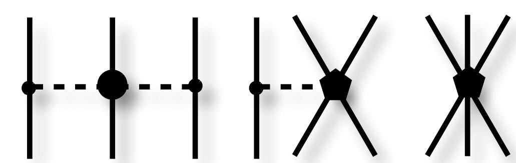

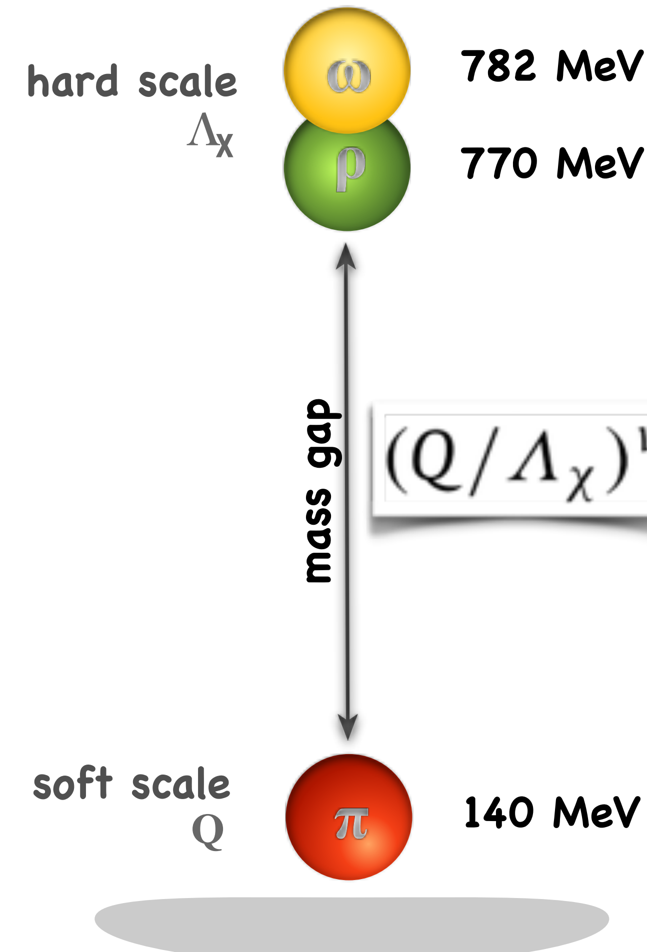

Nuclear physics at NNLO (AE et al PRL 110, 192502 (2013))

Statistical Uncertainties at NNLO (AE et al J. Phys. G. 42 034003 (2014))

Still many unresolved issues:

- **order-by-order convergence**
- **uncertainties**
- cutoff dependence
- power counting

mathematical optimization and statistical regression are indispensable tools

next-to-next-to-leading order (NNLO)

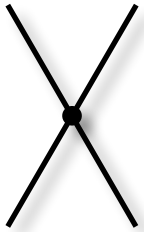

2 LECs

$$\tilde{C}^{pp}_{^1S_0} \quad \tilde{C}^{np}_{^1S_0} \quad \tilde{C}^{nn}_{^1S_0} \quad \tilde{C}_{^3S_1}$$

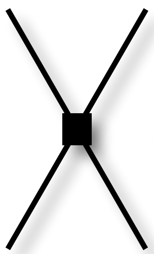

7 LECs

$$C_{^1S_0} \quad C_{^3P_0} \quad C_{^3P_1} \quad C_{^3P_2}$$
$$C_{^1P_1} \quad C_{^3S_1} \quad C_{^3S_1-^3D_1}$$

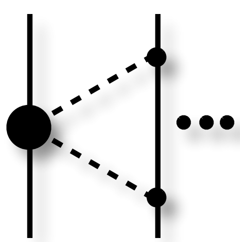

c_i

$$c_1 \quad c_3 \quad c_4$$

$$\chi^2(\mathbf{p}) = \sum_{i \in \mathbb{M}} \left(\frac{\mathcal{O}_i^{\text{theo}}(\mathbf{p}) - \mathcal{O}_i^{\text{exp}}}{\sigma_i^{\text{total}}} \right)^2$$

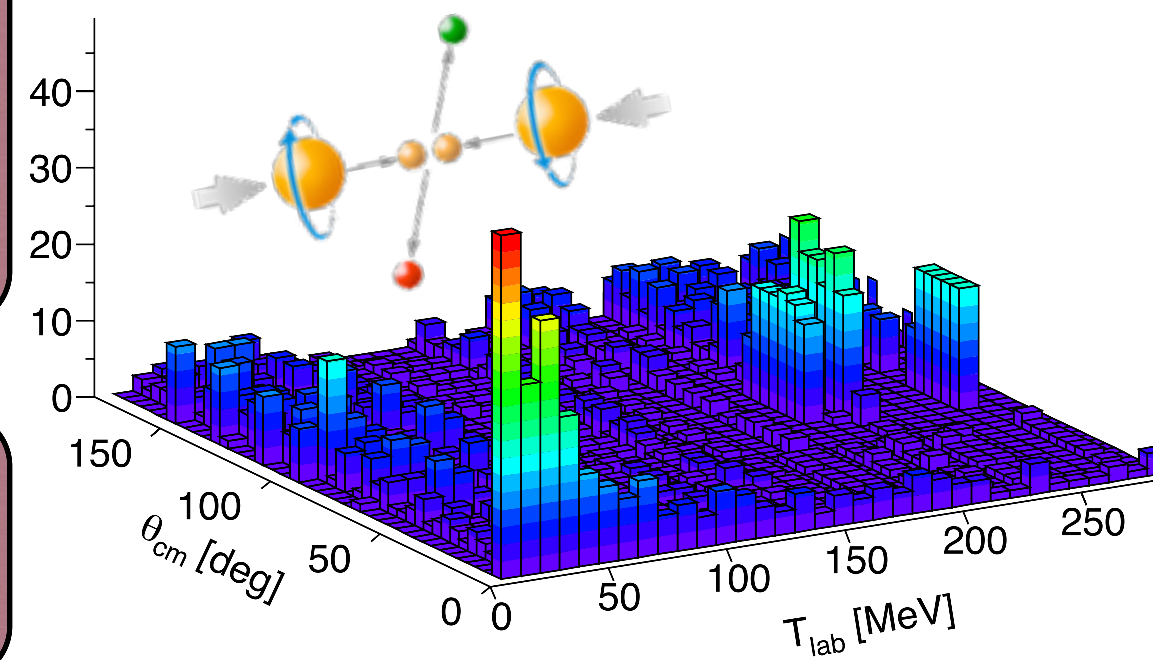

Tlab (MeV)	Idaho-N3LO	AV18
0-100	1.06	0.95
100-190	1.08	1.1
190-290	1.15	1.11
0-290	**1.10**	**1.04**

next-to-next-to-leading order (NNLO)

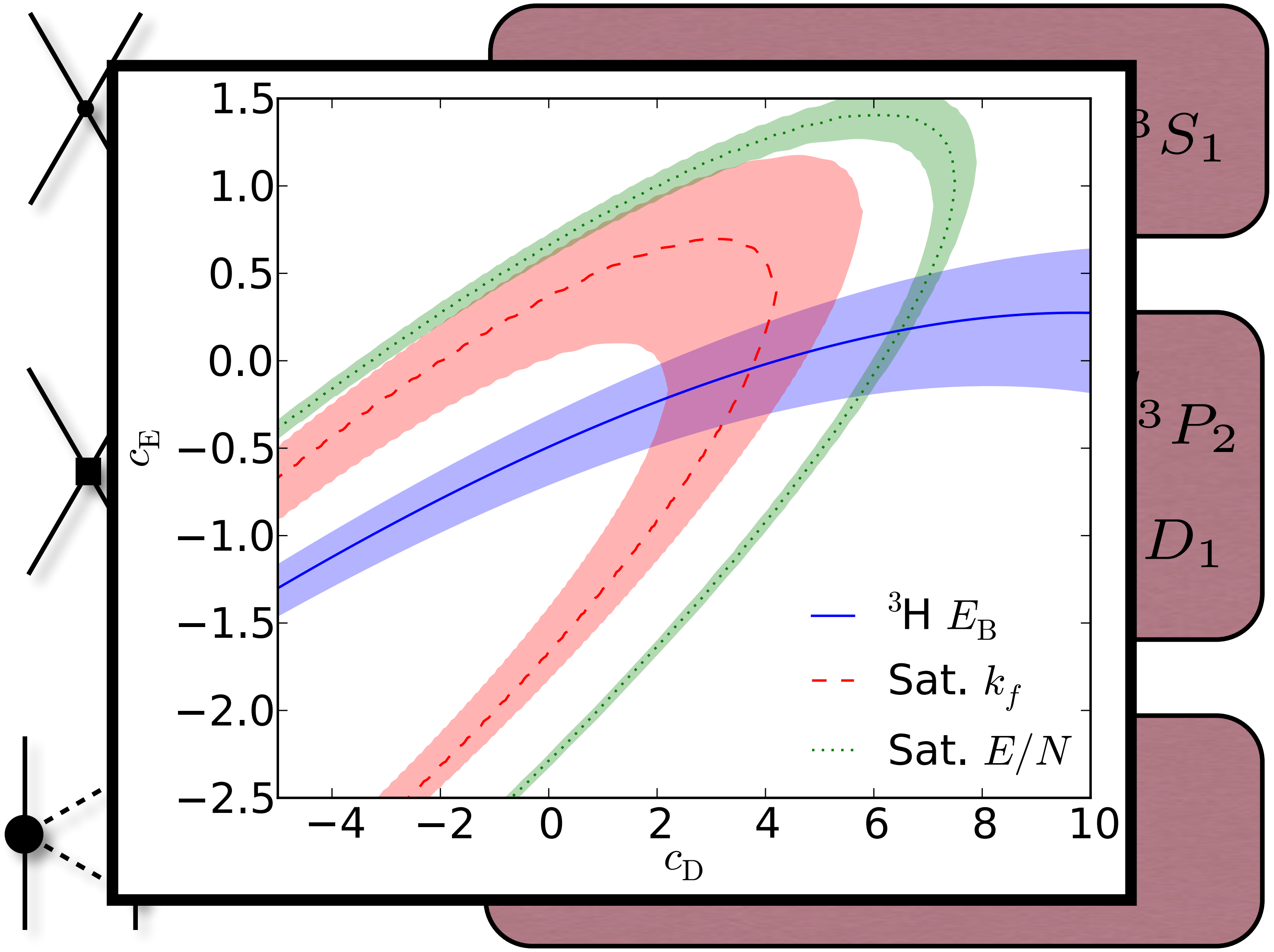

$$\chi^2(\mathbf{p}) = \sum_{i\in\mathbb{M}} \left(\frac{\mathcal{O}_i^{\mathrm{theo}}(\mathbf{p}) - \mathcal{O}_i^{\mathrm{exp}}}{\sigma_i^{\mathrm{total}}} \right)^2$$

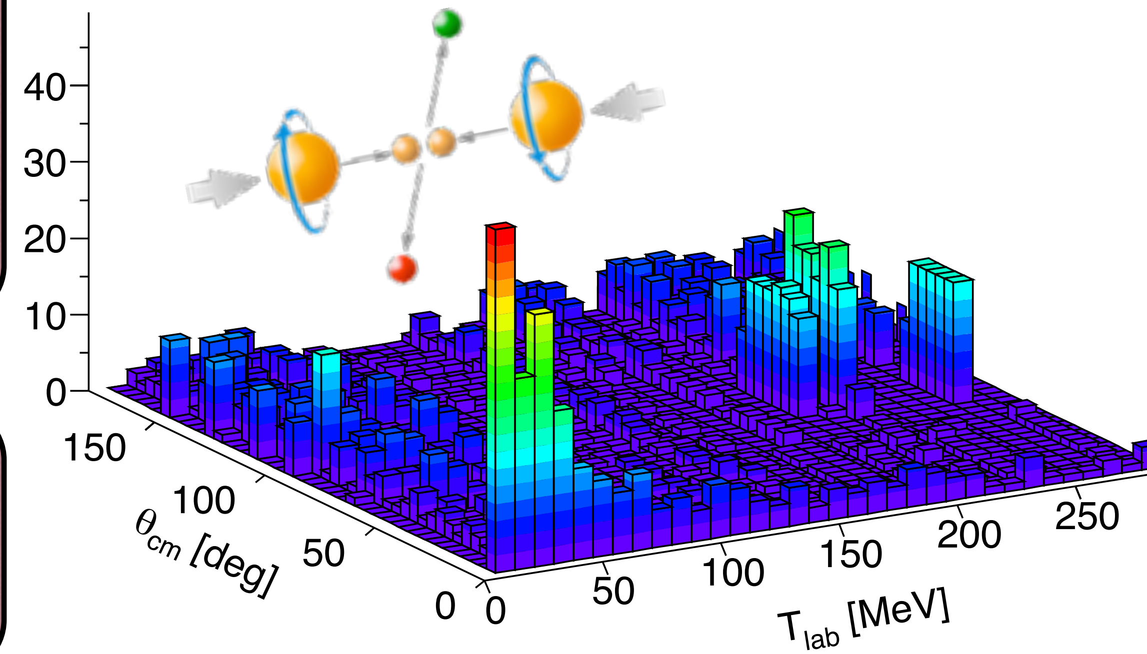

Tlab (MeV)	Idaho-N3LO	AV18
0-100	1.06	0.95
100-190	1.08	1.1
190-290	1.15	1.11
0-290	**1.10**	**1.04**

next-to-next-to-leading order (NNLO)

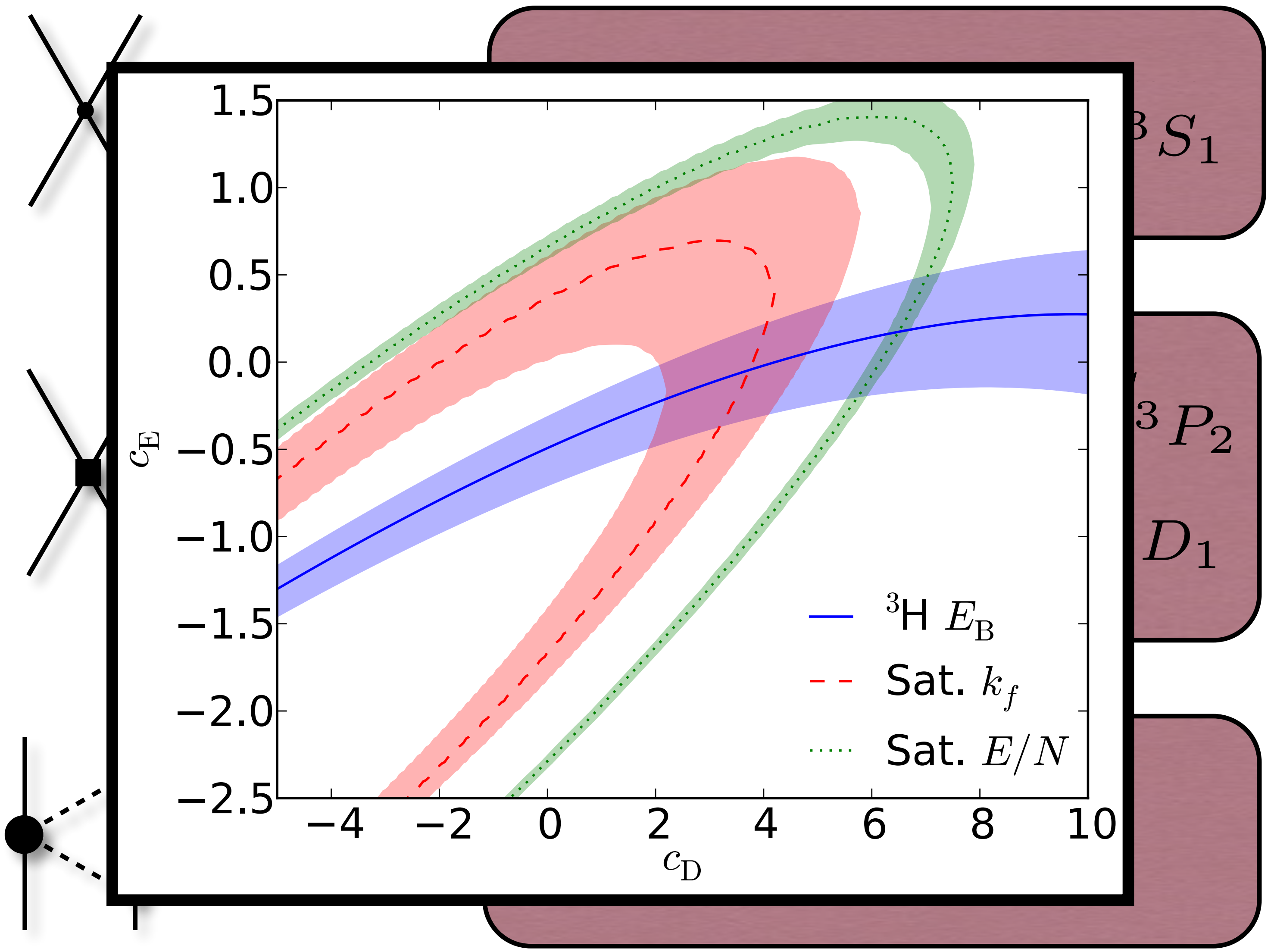

$$\chi^2(\mathbf{p}) = \sum_{i \in \mathbb{M}} \left(\frac{\mathcal{O}_i^{\mathrm{theo}}(\mathbf{p}) - \mathcal{O}_i^{\mathrm{exp}}}{\sigma_i^{\mathrm{total}}} \right)^2$$

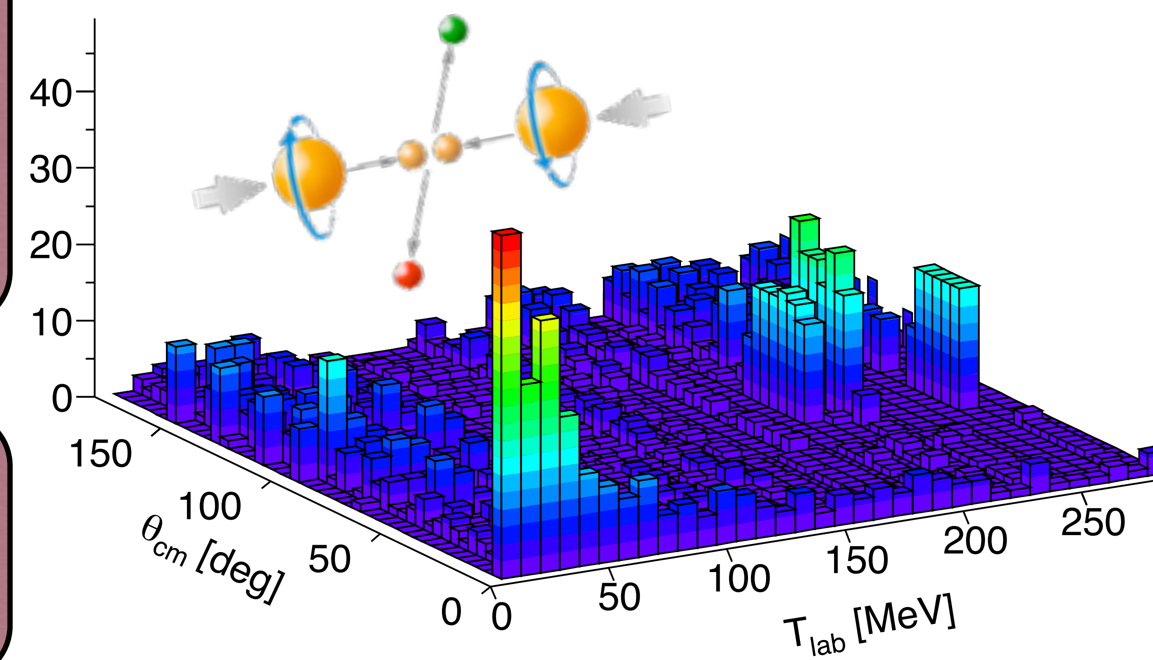

- NNN-force always fitted to an existing NN-force.

Tlab (MeV)	Idaho-N3LO	AV18
0-100	1.06	0.95
100-190	1.08	1.1
190-290	1.15	1.11
0-290	**1.10**	**1.04**

next-to-next-to-leading order (NNLO)

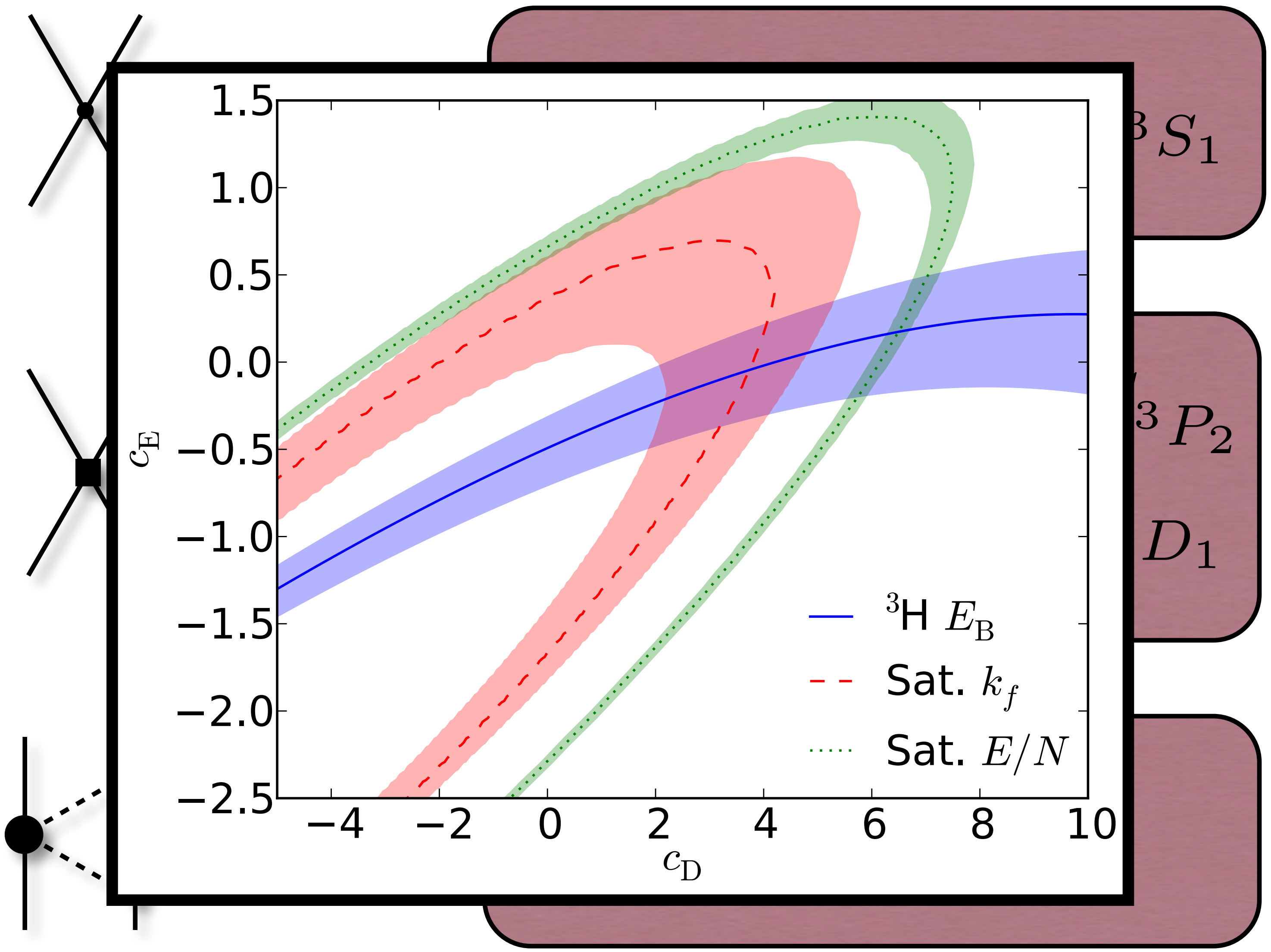

$$\chi^2(\mathbf{p}) = \sum_{i \in \mathbb{M}} \left(\frac{\mathcal{O}_i^{\text{theo}}(\mathbf{p}) - \mathcal{O}_i^{\text{exp}}}{\sigma_i^{\text{total}}} \right)^2$$

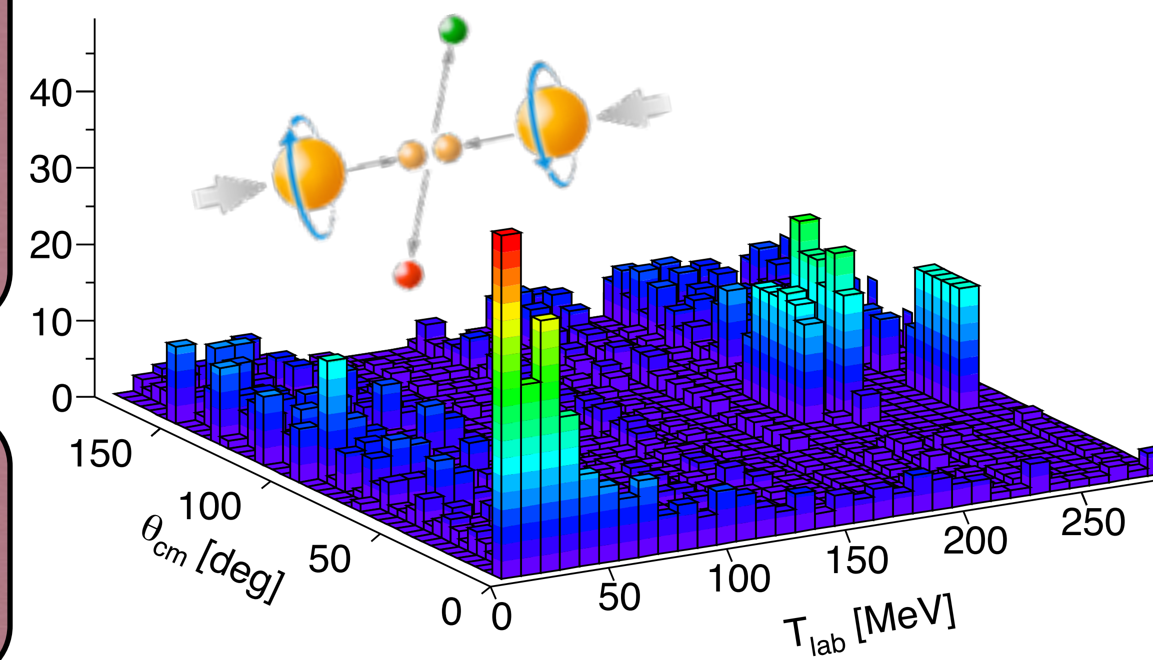

- NNN-force always fitted to an existing NN-force.
- Sub-leading pion-nucleon LECs taken from separate pion-nucleon analysis.

Tlab (MeV)	Idaho-N3LO	AV18
0-100	1.06	0.95
100-190	1.08	1.1
190-290	1.15	1.11
0-290	**1.10**	**1.04**

next-to-next-to-leading order (NNLO)

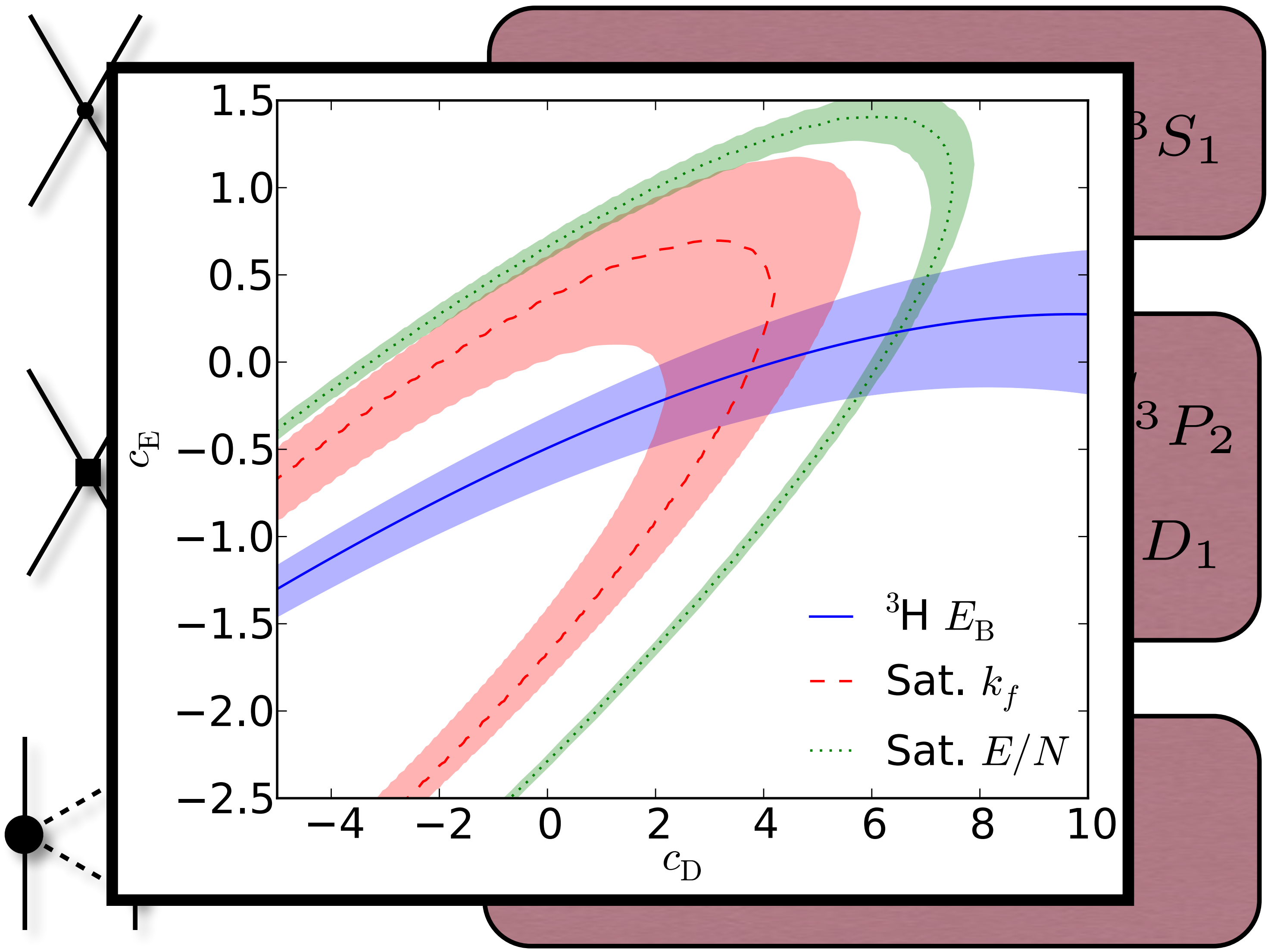

$$\chi^2(\mathbf{p}) = \sum_{i \in \mathbb{M}} \left(\frac{\mathcal{O}_i^{\text{theo}}(\mathbf{p}) - \mathcal{O}_i^{\text{exp}}}{\sigma_i^{\text{total}}} \right)^2$$

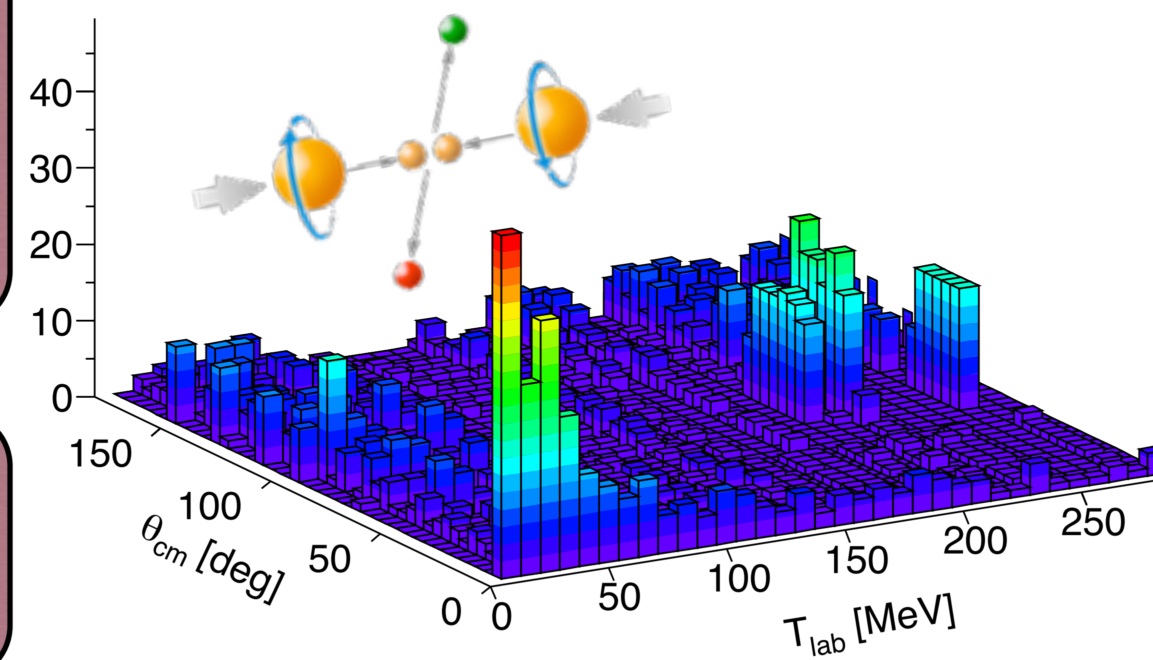

- NNN-force always fitted to an existing NN-force.
- Sub-leading pion-nucleon LECs taken from separate pion-nucleon analysis.
- Several choices in what scattering database to use.

Tlab (MeV)	Idaho-N3LO	AV18
0-100	1.06	0.95
100-190	1.08	1.1
190-290	1.15	1.11
0-290	**1.10**	**1.04**

next-to-next-to-leading order (NNLO)

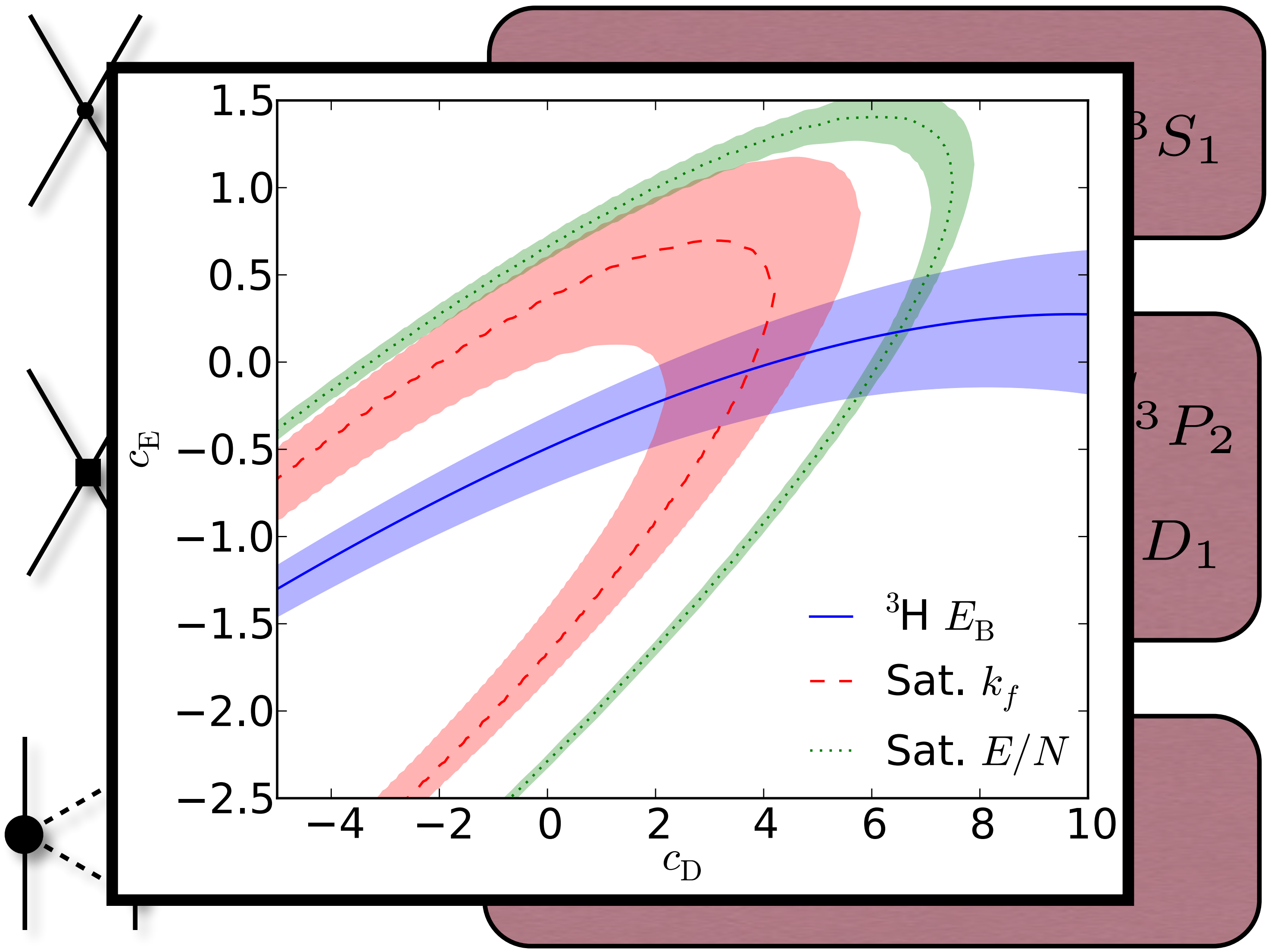

$$\chi^2(\mathbf{p}) = \sum_{i \in \mathbb{M}} \left(\frac{\mathcal{O}_i^{\rm theo}(\mathbf{p}) - \mathcal{O}_i^{\rm exp}}{\sigma_i^{\rm total}} \right)^2$$

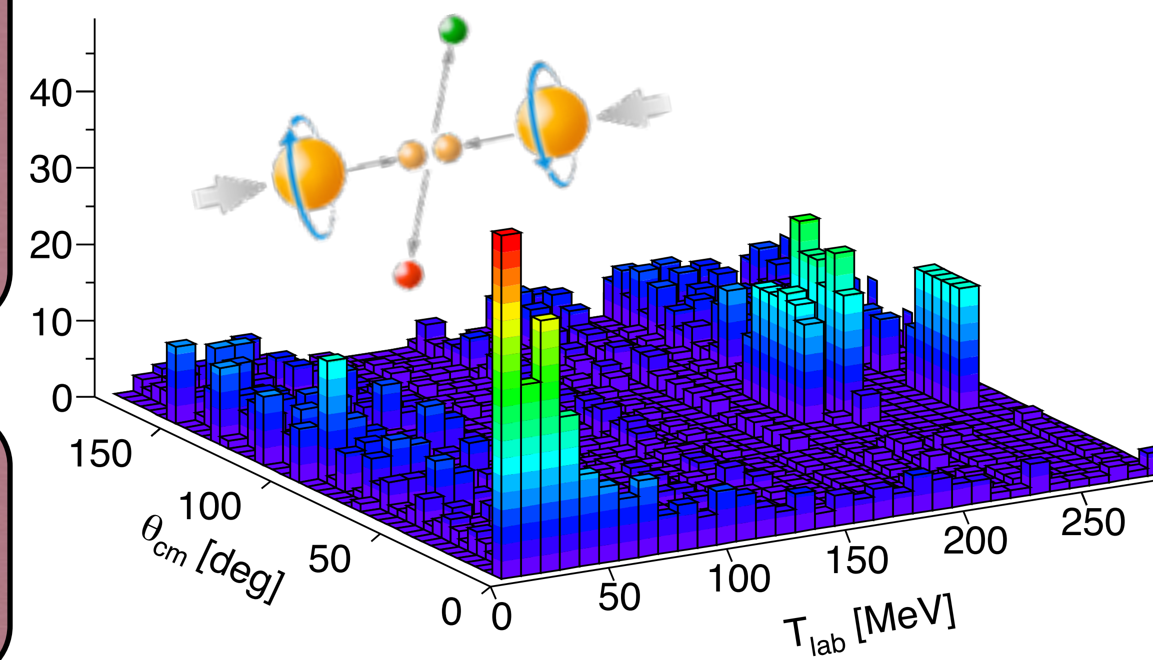

- NNN-force always fitted to an existing NN-force.
- Sub-leading pion-nucleon LECs taken from separate pion-nucleon analysis.
- Several choices in what scattering database to use.
- Low-energy and high-energy data weighted equally.

Tlab (MeV)	Idaho-N3LO	AV18
0-100	1.06	0.95
100-190	1.08	1.1
190-290	1.15	1.11
0-290	**1.10**	**1.04**

next-to-next-to-leading order (NNLO)

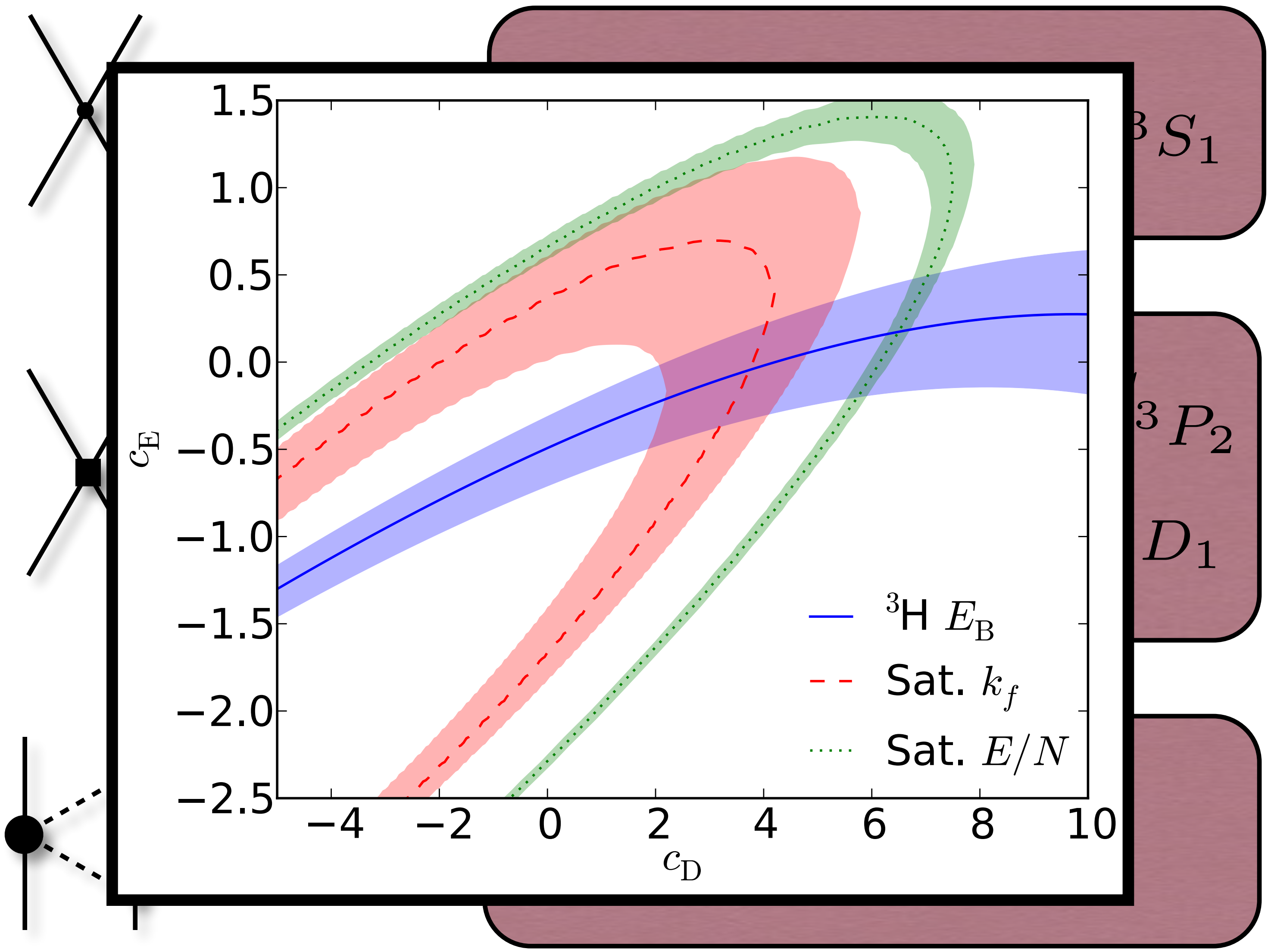

$$\chi^2(\mathbf{p}) = \sum_{i \in \mathbb{M}} \left(\frac{\mathcal{O}_i^{\text{theo}}(\mathbf{p}) - \mathcal{O}_i^{\text{exp}}}{\sigma_i^{\text{total}}} \right)^2$$

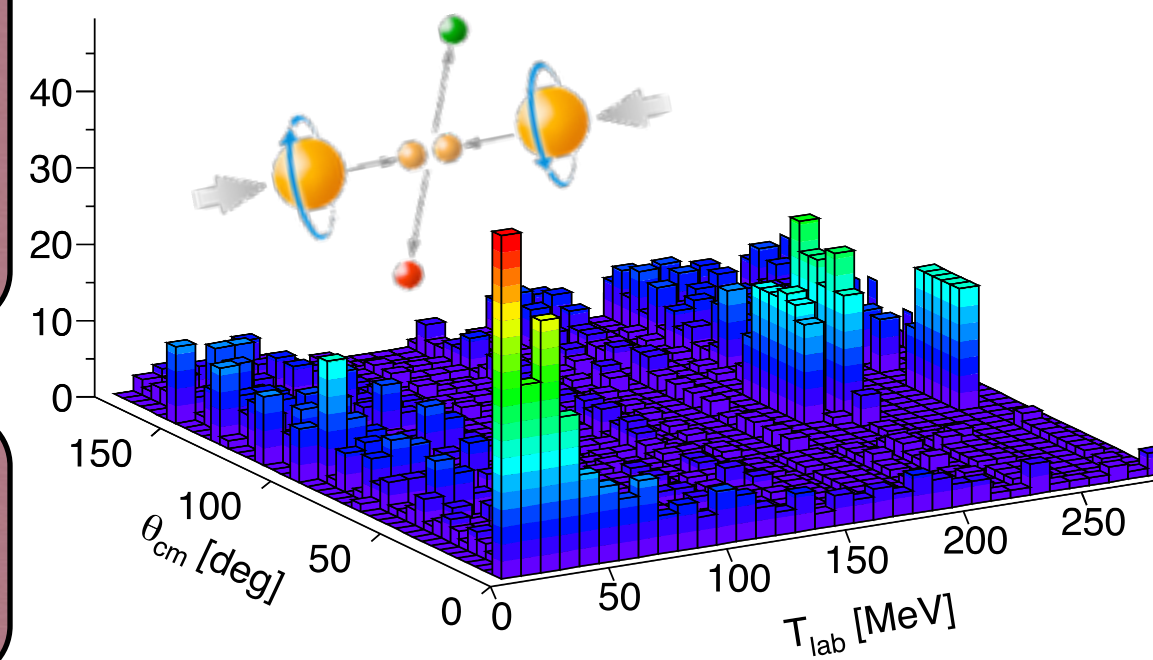

- NNN-force always fitted to an existing NN-force.
- Sub-leading pion-nucleon LECs taken from separate pion-nucleon analysis.
- Several choices in what scattering database to use.
- Low-energy and high-energy data weighted equally.
- Electromagnetic effects sometimes neglected.

Tlab (MeV)	Idaho-N3LO	AV18
0-100	1.06	0.95
100-190	1.08	1.1
190-290	1.15	1.11
0-290	**1.10**	**1.04**

next-to-next-to-leading order (NNLO)

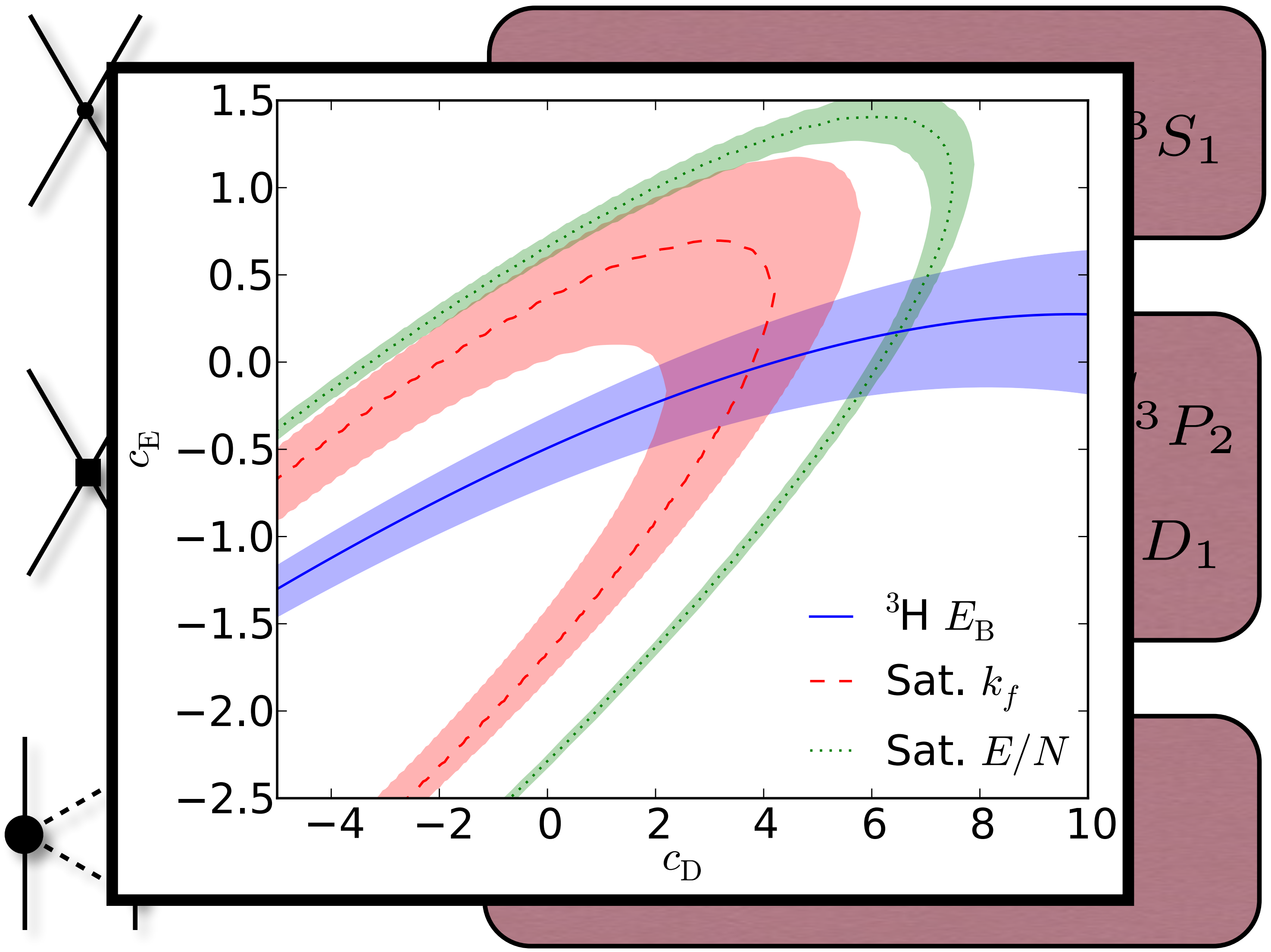

$$\chi^2(\mathbf{p}) = \sum_{i\in\mathbb{M}} \left(\frac{\mathcal{O}_i^{\text{theo}}(\mathbf{p}) - \mathcal{O}_i^{\text{exp}}}{\sigma_i^{\text{total}}} \right)^2$$

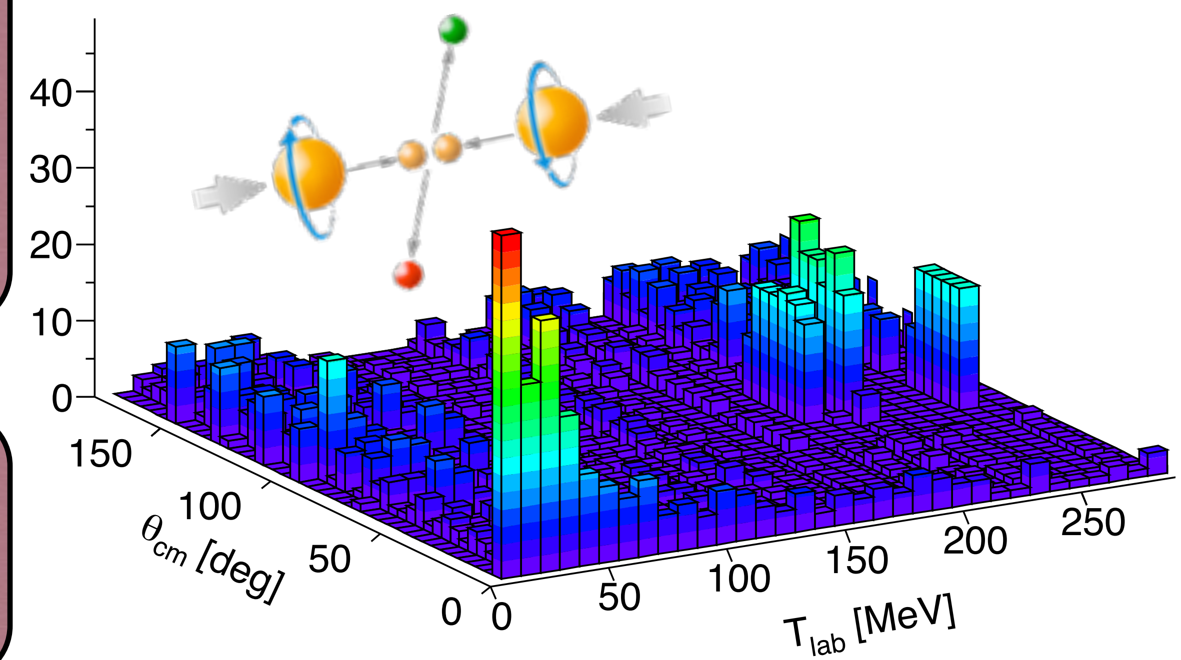

- NNN-force always fitted to an existing NN-force.
- Sub-leading pion-nucleon LECs taken from separate pion-nucleon analysis.
- Several choices in what scattering database to use.
- Low-energy and high-energy data weighted equally.
- Electromagnetic effects sometimes neglected.
- LECs tuned by hand more often than not.

Tlab (MeV)	Idaho-N3LO	AV18
0-100	1.06	0.95
100-190	1.08	1.1
190-290	1.15	1.11
0-290	**1.10**	**1.04**

next-to-next-to-leading order (NNLO)

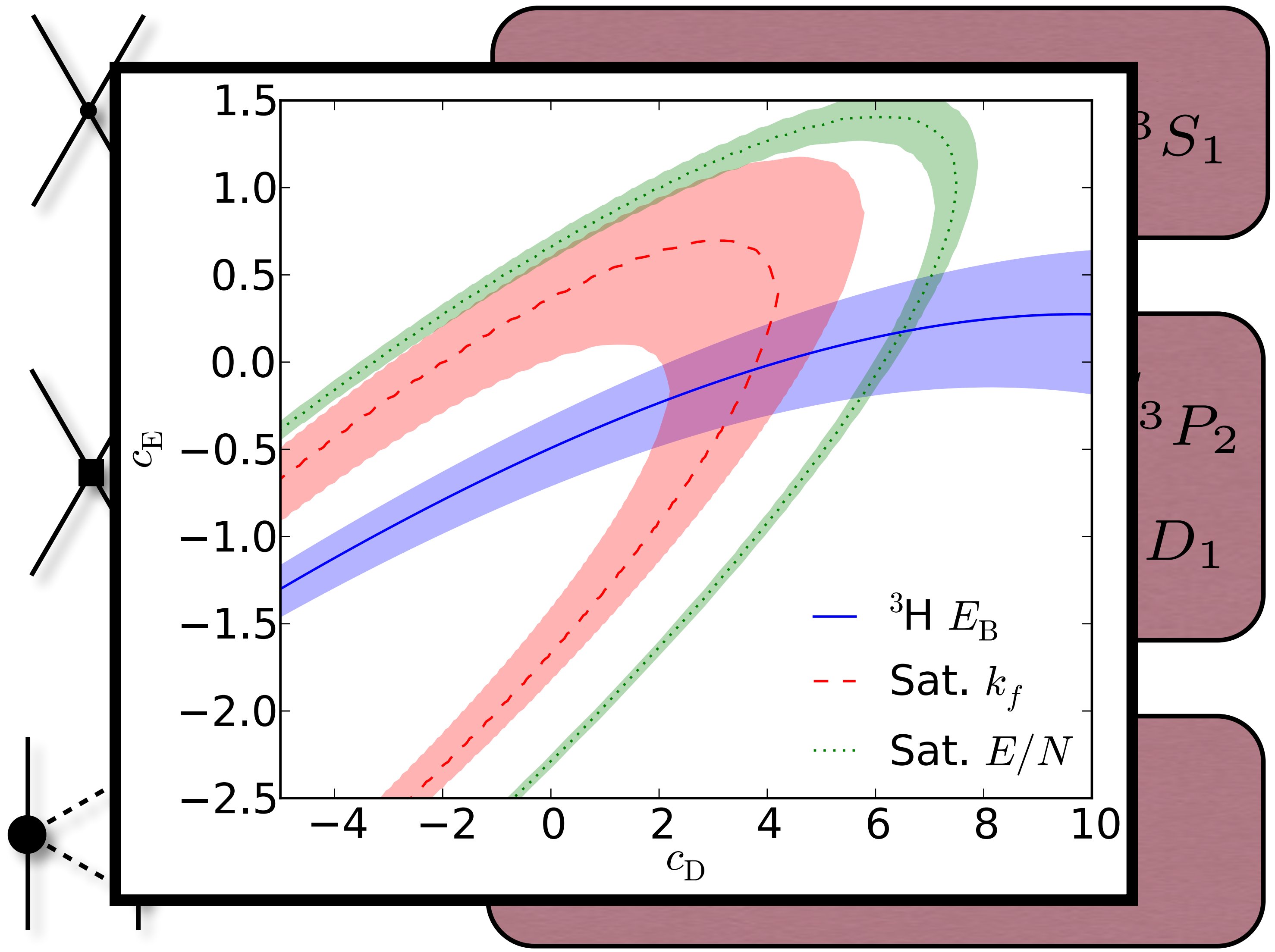

$$\chi^2(\mathbf{p}) = \sum_{i \in \mathbb{M}} \left(\frac{\mathcal{O}_i^{\mathrm{theo}}(\mathbf{p}) - \mathcal{O}_i^{\mathrm{exp}}}{\sigma_i^{\mathrm{total}}} \right)^2$$

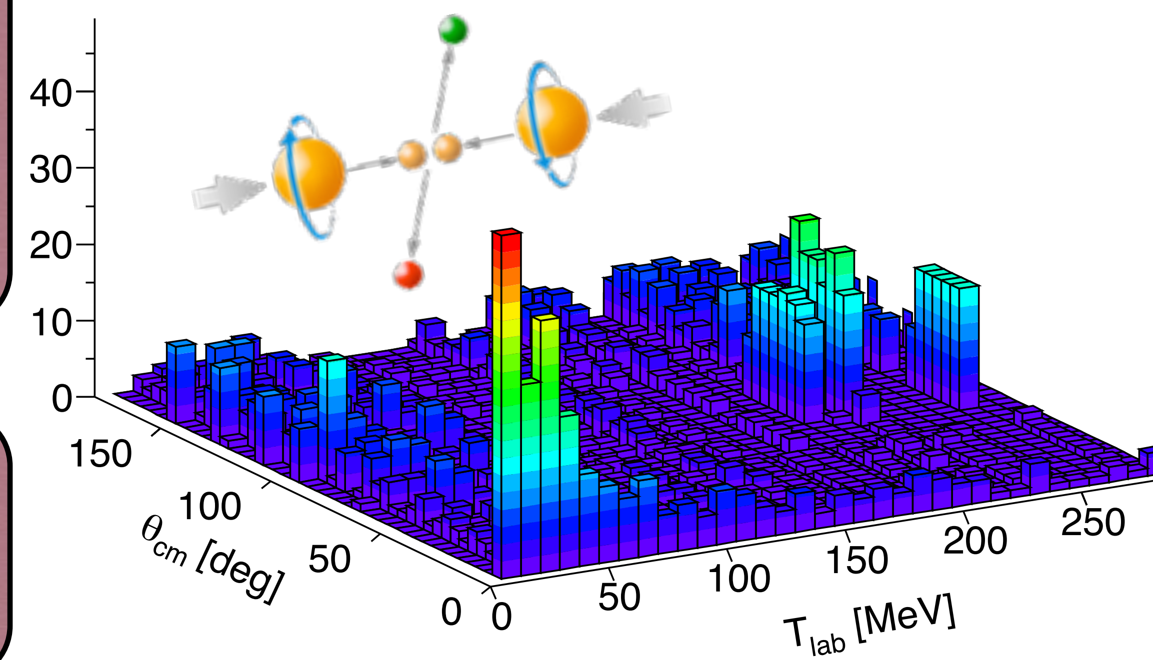

- NNN-force always fitted to an existing NN-force.
- Sub-leading pion-nucleon LECs taken from separate pion-nucleon analysis.
- Several choices in what scattering database to use.
- Low-energy and high-energy data weighted equally.
- Electromagnetic effects sometimes neglected.
- LECs tuned by hand more often than not.
- What are the resulting uncertainties (and there are several of them….)

Tlab (MeV)	Idaho-N3LO	AV18
0-100	1.06	0.95
100-190	1.08	1.1
190-290	1.15	1.11
0-290	**1.10**	**1.04**

next-to-next-to-leading order (NNLO)

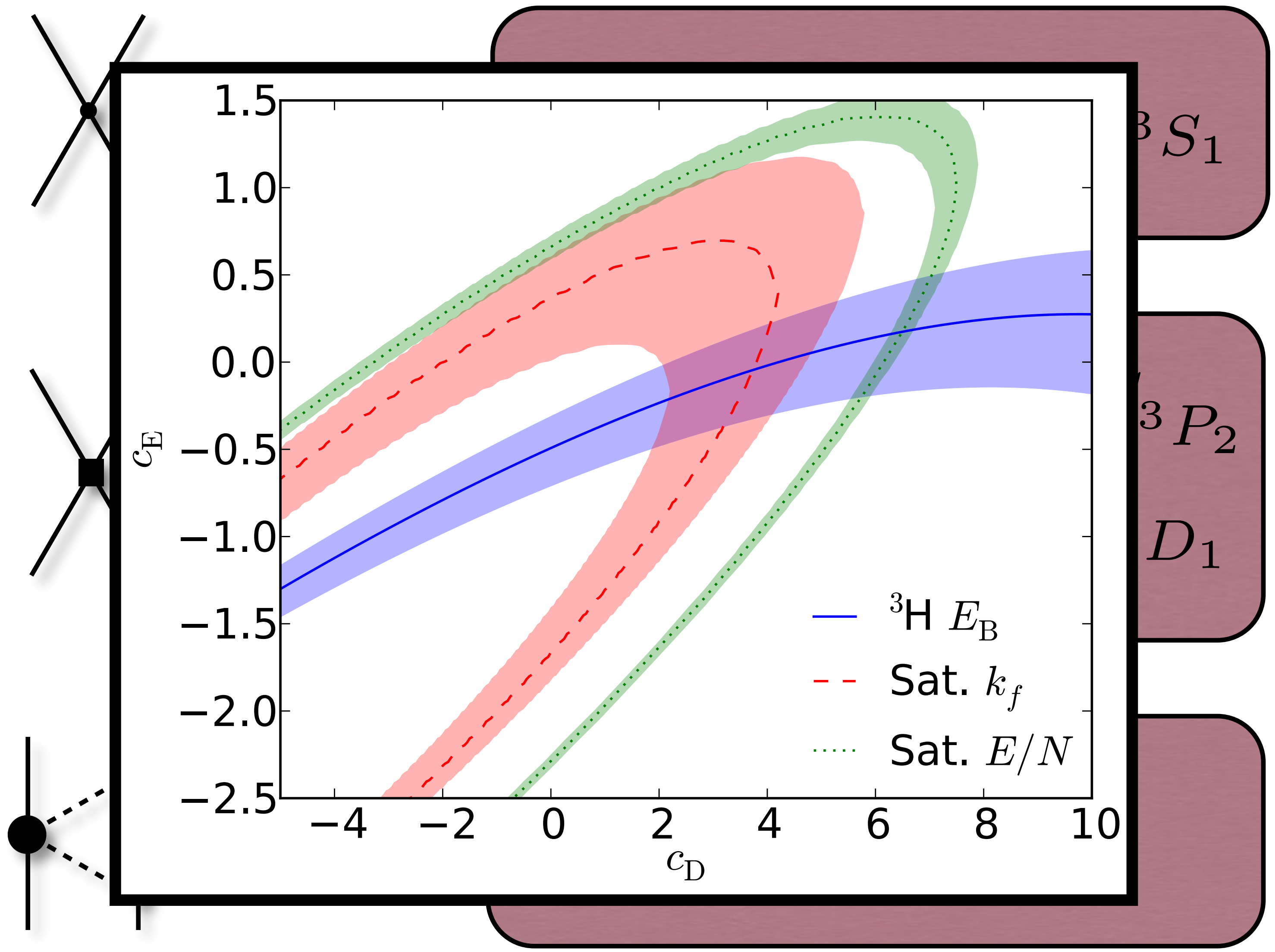

$$\chi^2(\mathbf{p}) = \sum_{i\in\mathbb{M}} \left(\frac{\mathcal{O}_i^{\text{theo}}(\mathbf{p}) - \mathcal{O}_i^{\text{exp}}}{\sigma_i^{\text{total}}} \right)^2$$

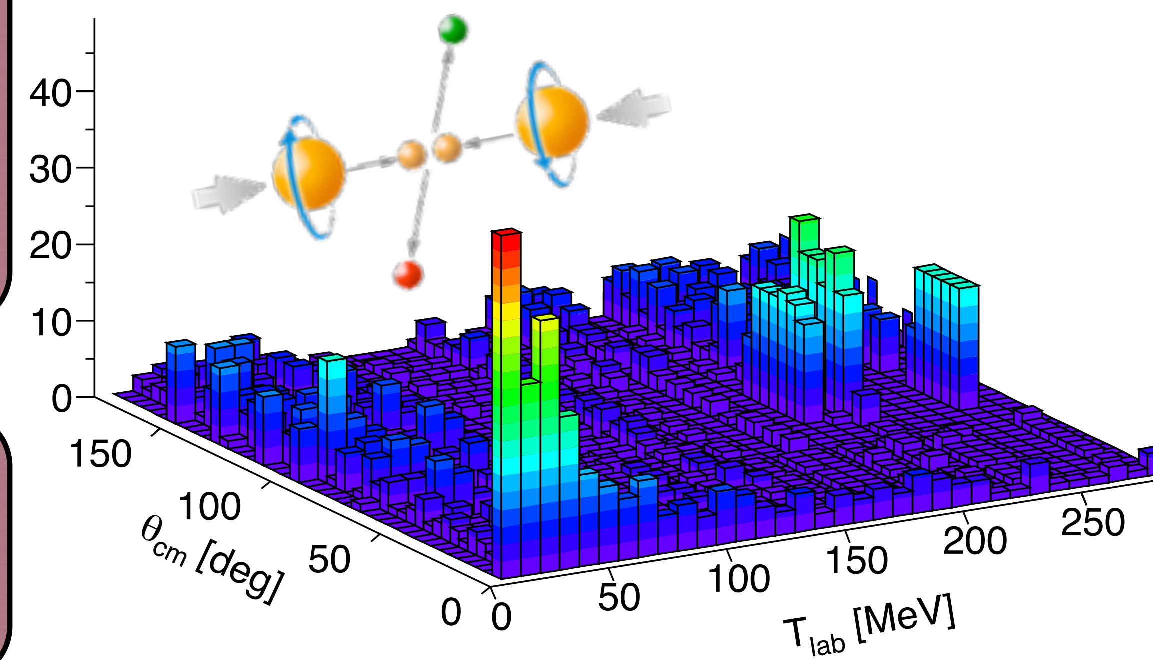

- NNN-force always fitted to an existing NN-force.
- Sub-leading pion-nucleon LECs taken from separate pion-nucleon analysis.
- Several choices in what scattering database to use.
- Low-energy and high-energy data weighted equally.
- Electromagnetic effects sometimes neglected.
- LECs tuned by hand more often than not.
- What are the resulting uncertainties (and there are several of them….)

Tlab (MeV)	Idaho-N3LO	AV18
0-100	1.06	0.95
100-190	1.08	1.1
190-290	1.15	1.11
0-290	**1.10**	**1.04**

next-to-next-to-leading order (NNLO)

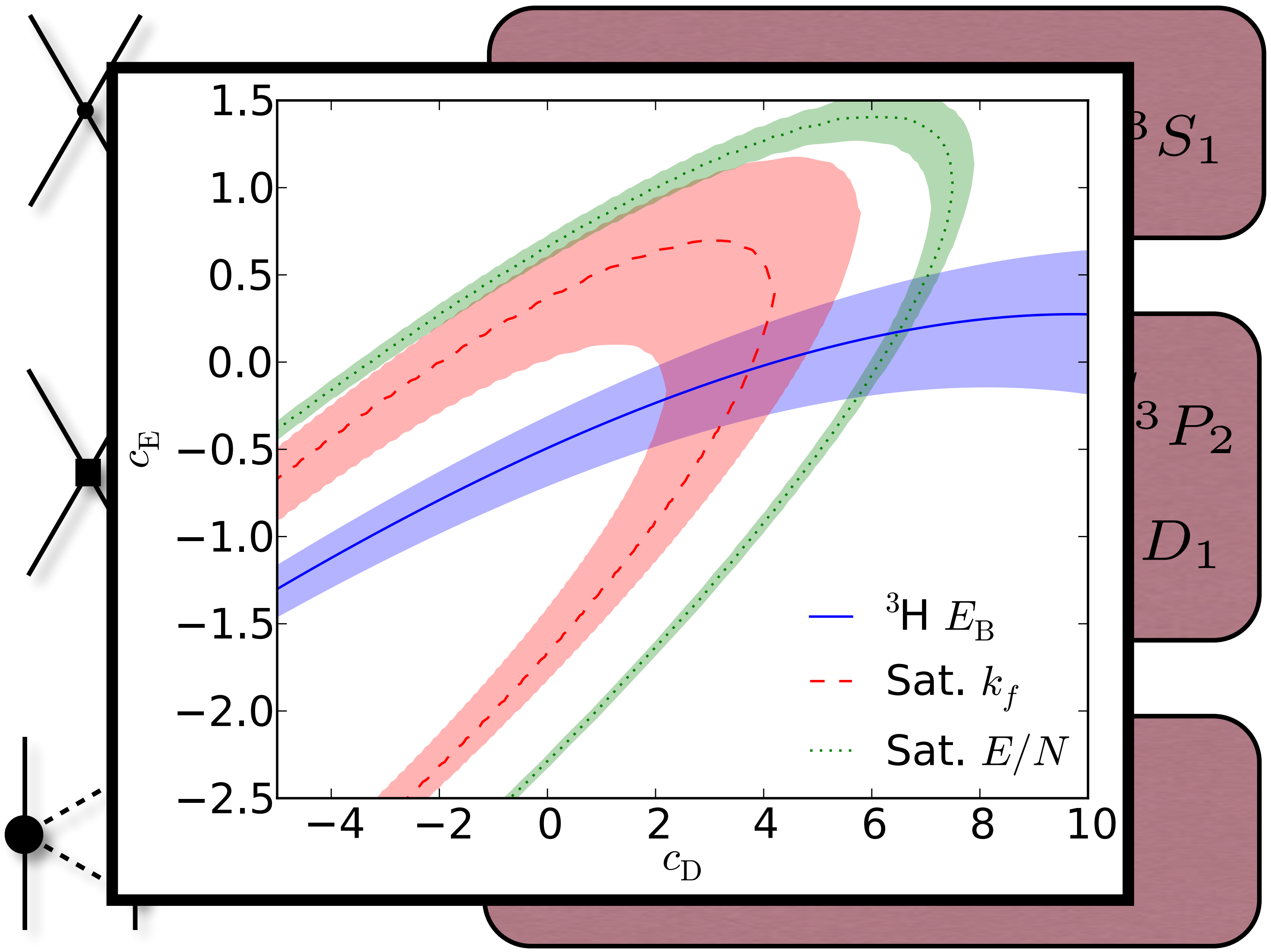

$$\chi^2(\mathbf{p}) = \sum_{i\in\mathbb{M}} \left(\frac{\mathcal{O}_i^{\text{theo}}(\mathbf{p}) - \mathcal{O}_i^{\text{exp}}}{\sigma_i^{\text{total}}} \right)^2$$

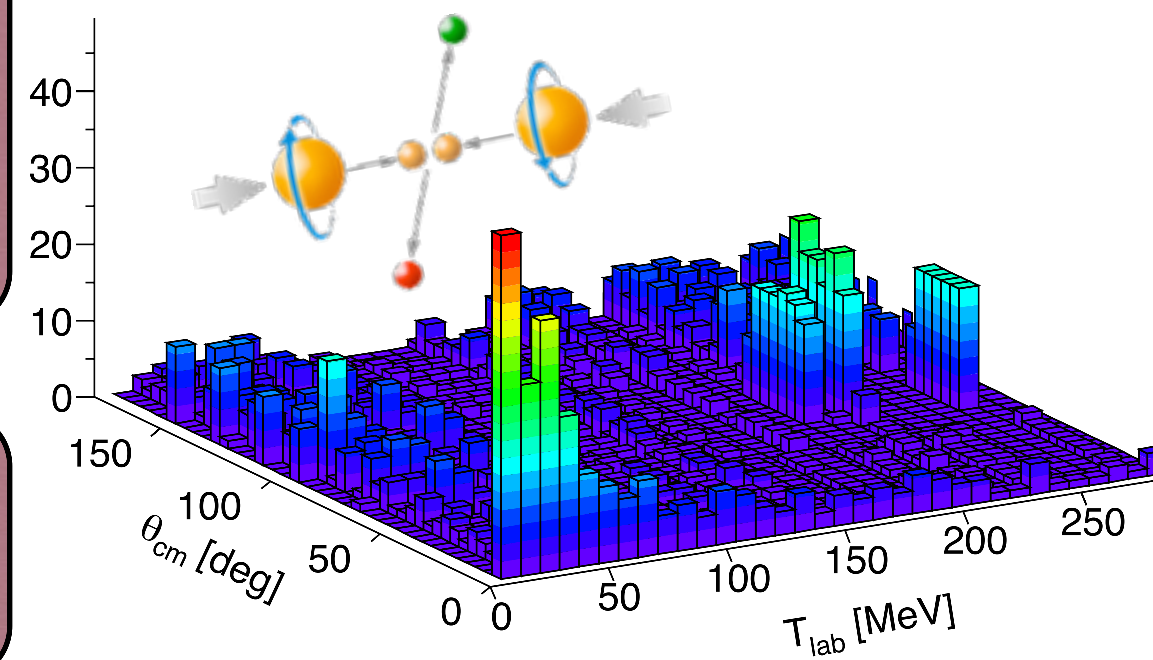

- NNN-force always fitted to an existing NN-force.
- Sub-leading pion-nucleon LECs taken from separate pion-nucleon analysis.
- Several choices in what scattering database to use.
- Low-energy and high-energy data weighted equally.
- Electromagnetic effects sometimes neglected.
- LECs tuned by hand more often than not.
- What are the resulting uncertainties (and there are several of them....)

Tlab (MeV)	Idaho-N3LO	AV18
0-100	1.06	0.95
100-190	1.08	1.1
190-290	1.15	1.11
0-290	**1.10**	**1.04**

Let's adress these points

A Simultaneous Objective Function

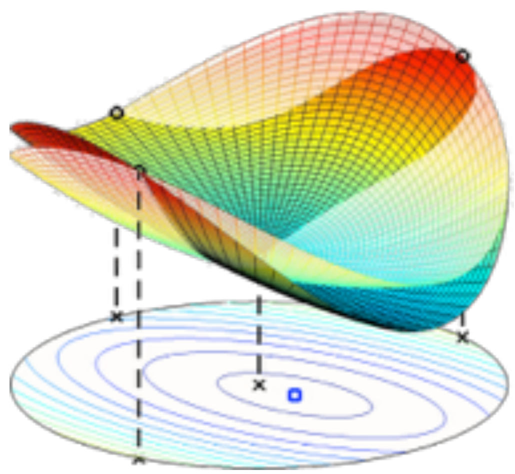

$$\chi^2(\mathbf{p}) = \sum_{i\in\mathbb{M}} \left(\frac{\mathcal{O}_i^{\text{theo}}(\mathbf{p}) - \mathcal{O}_i^{\text{exp}}}{\sigma_i^{\text{total}}} \right)^2 = \sum_{i\in\mathbb{M}} R_i^2(\mathbf{p})$$

$$\chi^2(\mathbf{p}) \equiv \sum_{i\in\mathbb{M}} R_i^2(\mathbf{p}) = \sum_{j\in\mathrm{NN}} R_j^2(\mathbf{p}) + \sum_{k\in\pi\mathrm{N}} R_k^2(\mathbf{p}) + \sum_{l\in\mathrm{NNN}} R_l^2(\mathbf{p})$$

A Simultaneous Objective Function

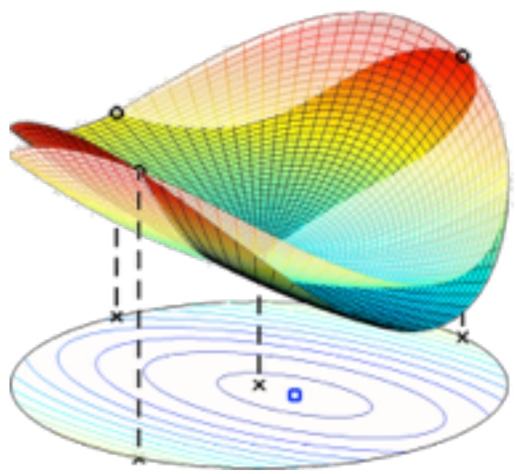

$$\chi^2(\mathbf{p}) = \sum_{i\in\mathbb{M}} \left(\frac{\mathcal{O}_i^{\mathrm{theo}}(\mathbf{p}) - \mathcal{O}_i^{\exp}}{\sigma_i^{\mathrm{total}}} \right)^2 = \sum_{i\in\mathbb{M}} R_i^2(\mathbf{p})$$

$$\chi^2(\mathbf{p}) \equiv \sum_{i\in\mathbb{M}} R_i^2(\mathbf{p}) = \sum_{j\in\mathrm{NN}} R_j^2(\mathbf{p}) + \sum_{k\in\pi\mathrm{N}} R_k^2(\mathbf{p}) + \sum_{l\in\mathrm{NNN}} R_l^2(\mathbf{p})$$

Observable	LO	NLO	NNLO
NN scattering	X	X	X
^{2}H: E_{gs}, $r_{pt\text{-}p}$, Q	X	X	X
πN scattering			X
^{3}He: E_{gs}, $r_{pt\text{-}p}$			X
^{3}H: E_{gs}, $r_{pt\text{-}p}$, $T_{1/2}$			X

A Simultaneous Objective Function

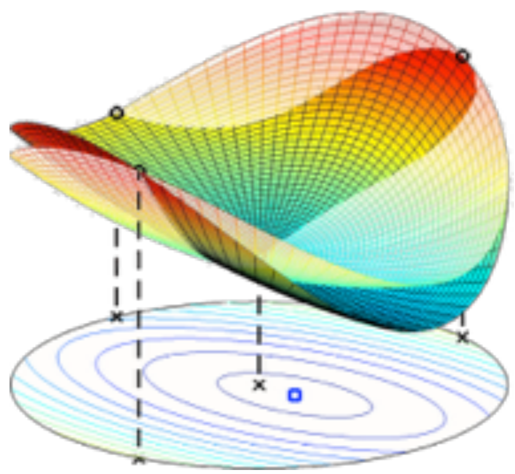

$$\chi^2(\mathbf{p}) = \sum_{i\in\mathbb{M}} \left(\frac{\mathcal{O}_i^{\text{theo}}(\mathbf{p}) - \mathcal{O}_i^{\text{exp}}}{\sigma_i^{\text{total}}} \right)^2 = \sum_{i\in\mathbb{M}} R_i^2(\mathbf{p})$$

$$\chi^2(\mathbf{p}) \equiv \sum_{i\in\mathbb{M}} R_i^2(\mathbf{p}) = \sum_{j\in\text{NN}} R_j^2(\mathbf{p}) + \sum_{k\in\pi\text{N}} R_k^2(\mathbf{p}) + \sum_{l\in\text{NNN}} R_l^2(\mathbf{p})$$

Sequential

Observable	LO	NLO	NNLO	
NN scattering	X	X	X	NN
^{2}H: E_{gs}, $r_{pt\text{-}p}$, Q	X	X	X	
πN scattering			X	πN
^{3}He: E_{gs}, $r_{pt\text{-}p}$			X	NNN
^{3}H: E_{gs}, $r_{pt\text{-}p}$, $T_{1/2}$			X	

A Simultaneous Objective Function

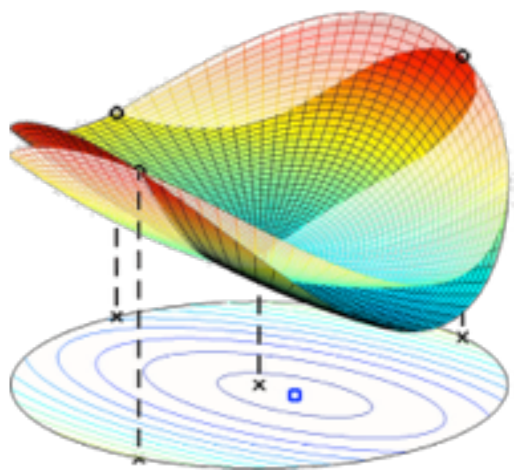

$$\chi^2(\mathbf{p}) = \sum_{i\in\mathbb{M}} \left(\frac{\mathcal{O}_i^{\text{theo}}(\mathbf{p}) - \mathcal{O}_i^{\text{exp}}}{\sigma_i^{\text{total}}} \right)^2 = \sum_{i\in\mathbb{M}} R_i^2(\mathbf{p})$$

$$\chi^2(\mathbf{p}) \equiv \sum_{i\in\mathbb{M}} R_i^2(\mathbf{p}) = \sum_{j\in\text{NN}} R_j^2(\mathbf{p}) + \sum_{k\in\pi\text{N}} R_k^2(\mathbf{p}) + \sum_{l\in\text{NNN}} R_l^2(\mathbf{p})$$

Simultaneous

Observable	LO	NLO	NNLO
NN scattering	X	X	X
^{2}H: E_{gs}, r_{pt-p}, Q	X	X	X
πN scattering			X
^{3}He: E_{gs}, r_{pt-p}			X
^{3}H: E_{gs}, r_{pt-p}, $T_{1/2}$			X

NN

πN

NNN

A Simultaneous Objective Function

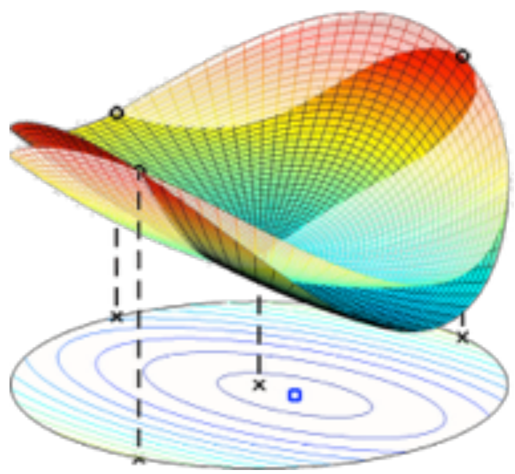

$$\chi^2(\mathbf{p}) = \sum_{i\in\mathbb{M}} \left(\frac{\mathcal{O}_i^{\text{theo}}(\mathbf{p}) - \mathcal{O}_i^{\text{exp}}}{\sigma_i^{\text{total}}} \right)^2 = \sum_{i\in\mathbb{M}} R_i^2(\mathbf{p})$$

$$\chi^2(\mathbf{p}) \equiv \sum_{i\in\mathbb{M}} R_i^2(\mathbf{p}) = \sum_{j\in\text{NN}} R_j^2(\mathbf{p}) + \sum_{k\in\pi\text{N}} R_k^2(\mathbf{p}) + \sum_{l\in\text{NNN}} R_l^2(\mathbf{p})$$

Simultaneous

Observable	LO	NLO	NNLO
NN scattering	X	X	X
^{2}H: E_{gs}, $r_{pt\text{-}p}$, Q	X	X	X
πN scattering			X
^{3}He: E_{gs}, $r_{pt\text{-}p}$			X
^{3}H: E_{gs}, $r_{pt\text{-}p}$, $T_{1/2}$			X

NN

πN

NNN

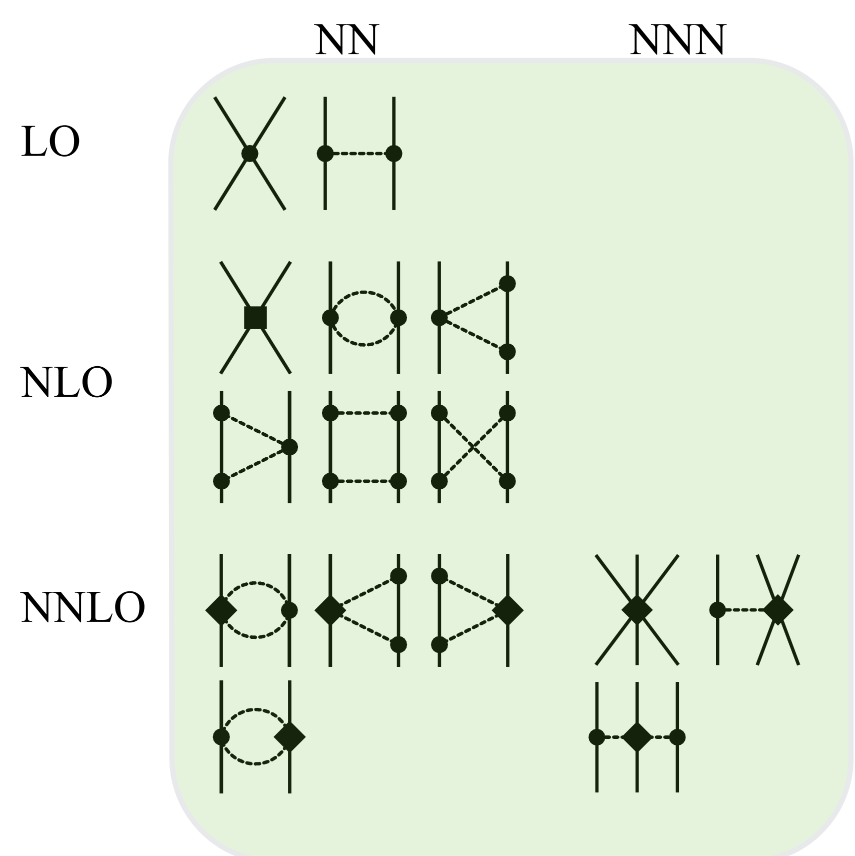

A Simultaneous Objective Function

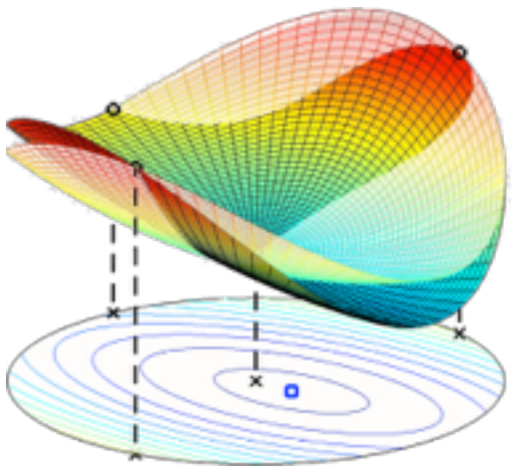

Simultaneous optimization critical in order to

- find the optimal set of LECs
- capture all relevant correlations between them
- reduce the statistical uncertainty.

Within such an approach we find that statistical errors are, in general, small, and that the total error budget is dominated by systematic errors.

$$\sum_{i\in\mathbb{M}} R_i^2(\mathbf{p})$$

$$\chi^2(\mathbf{p}) \equiv \sum_{i\in\mathbb{M}} R \;\cdots\; \sum_{l\in\mathrm{NNN}} R_l^2(\mathbf{p})$$

Simultaneous

Observable	LO	NLO	NNLO
NN scattering	X	X	X
^{2}H: E_{gs}, $r_{pt\text{-}p}$, Q	X	X	X
πN scattering			X
^{3}He: E_{gs}, $r_{pt\text{-}p}$			X
^{3}H: E_{gs}, $r_{pt\text{-}p}$, $T_{1/2}$			X

NN

πN

NNN

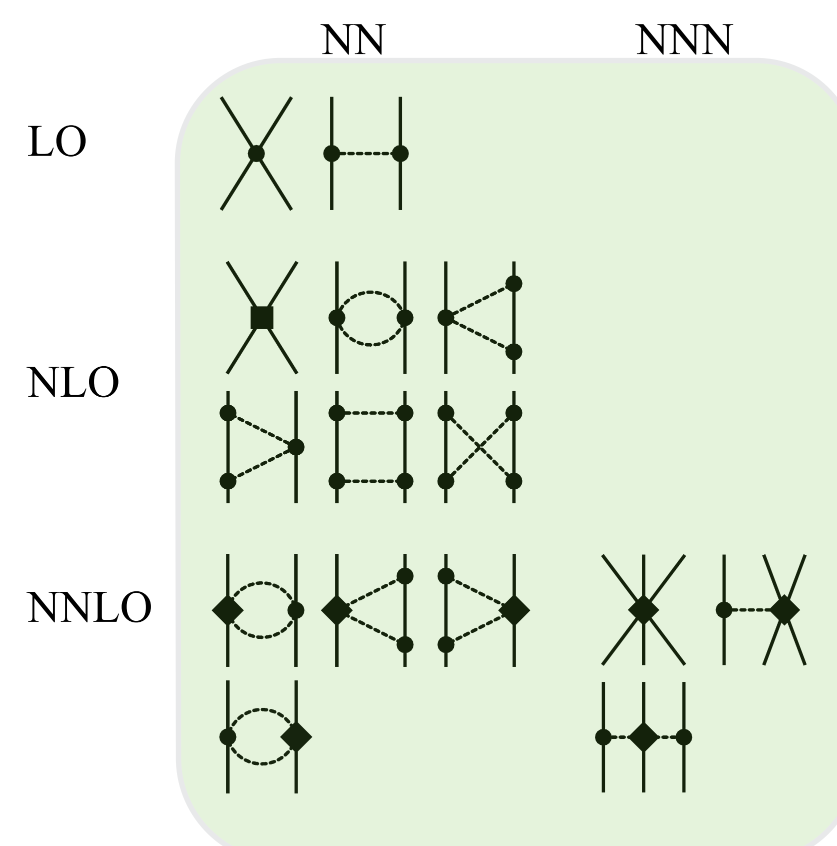

Optimization Algorithm

POUNDerS — Levenberg-Marquardt — Newtons Method

Approximate Hessian ⟵ Exact Hessian

$$\chi^2(\mathbf{p}) \qquad \frac{\partial \chi^2(\mathbf{p})}{\partial p_i} \qquad \frac{\partial \chi^2(\mathbf{p})}{\partial p_i}, \ \frac{\partial^2 \chi^2(\mathbf{p})}{\partial p_i \partial p_j}$$

Optimization Algorithm

POUNDerS — Levenberg-Marquardt — Newtons Method

Approximate Hessian ← Exact Hessian

$$\chi^2(\mathbf{p}) \qquad \frac{\partial \chi^2(\mathbf{p})}{\partial p_i} \qquad \frac{\partial \chi^2(\mathbf{p})}{\partial p_i}, \frac{\partial^2 \chi^2(\mathbf{p})}{\partial p_i \partial p_j}$$

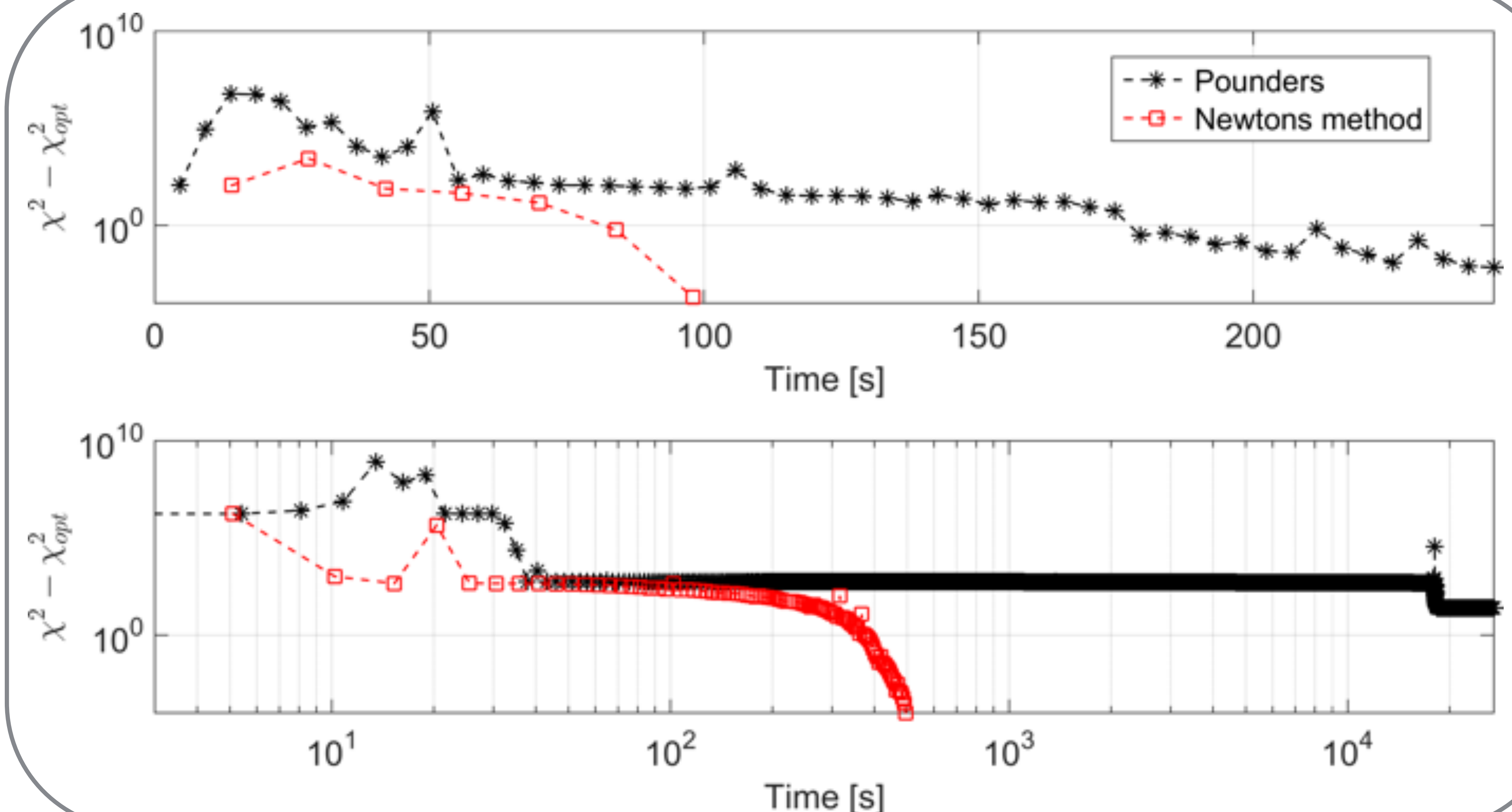

Computing derivatives

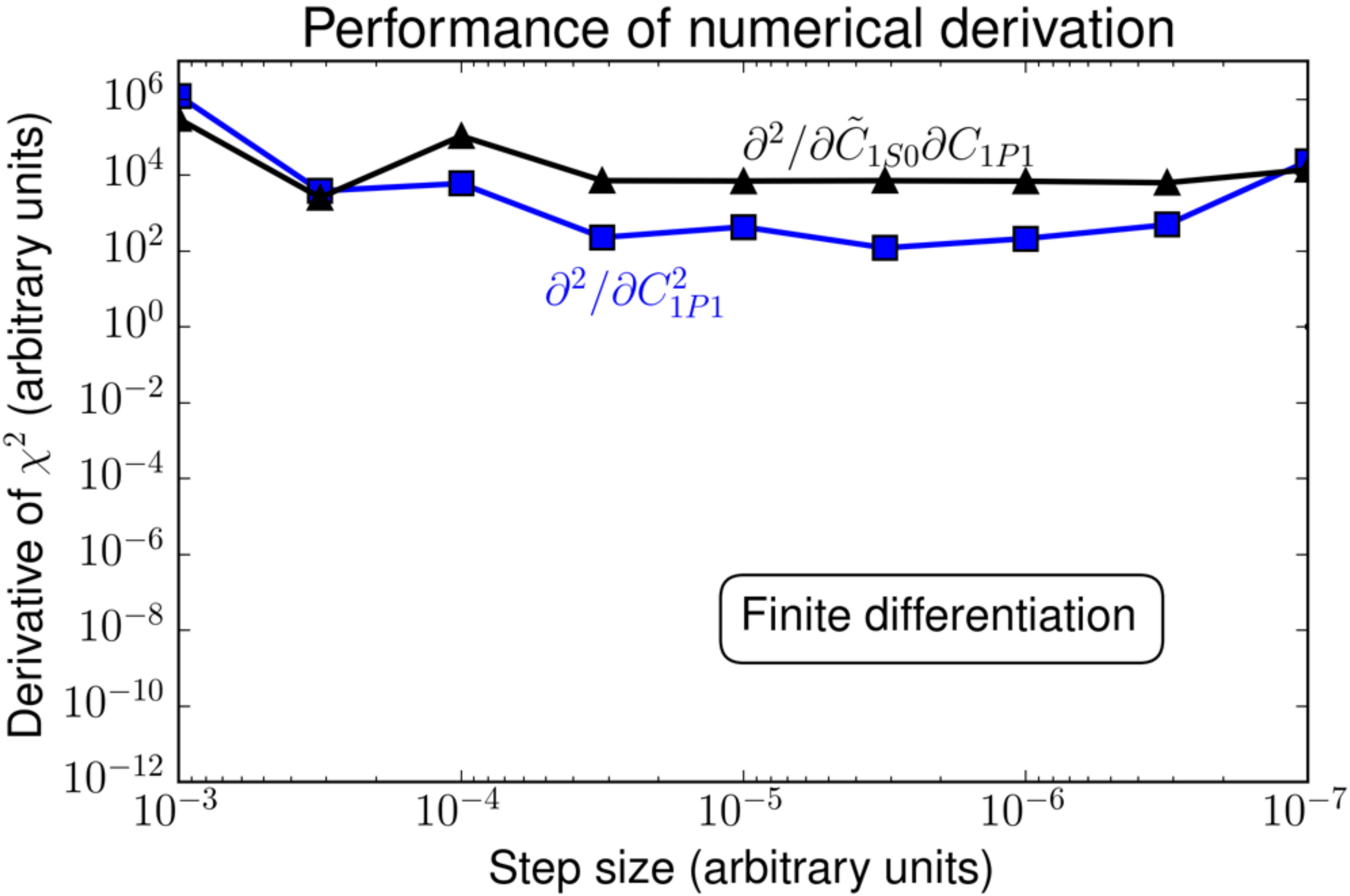

Computing derivatives

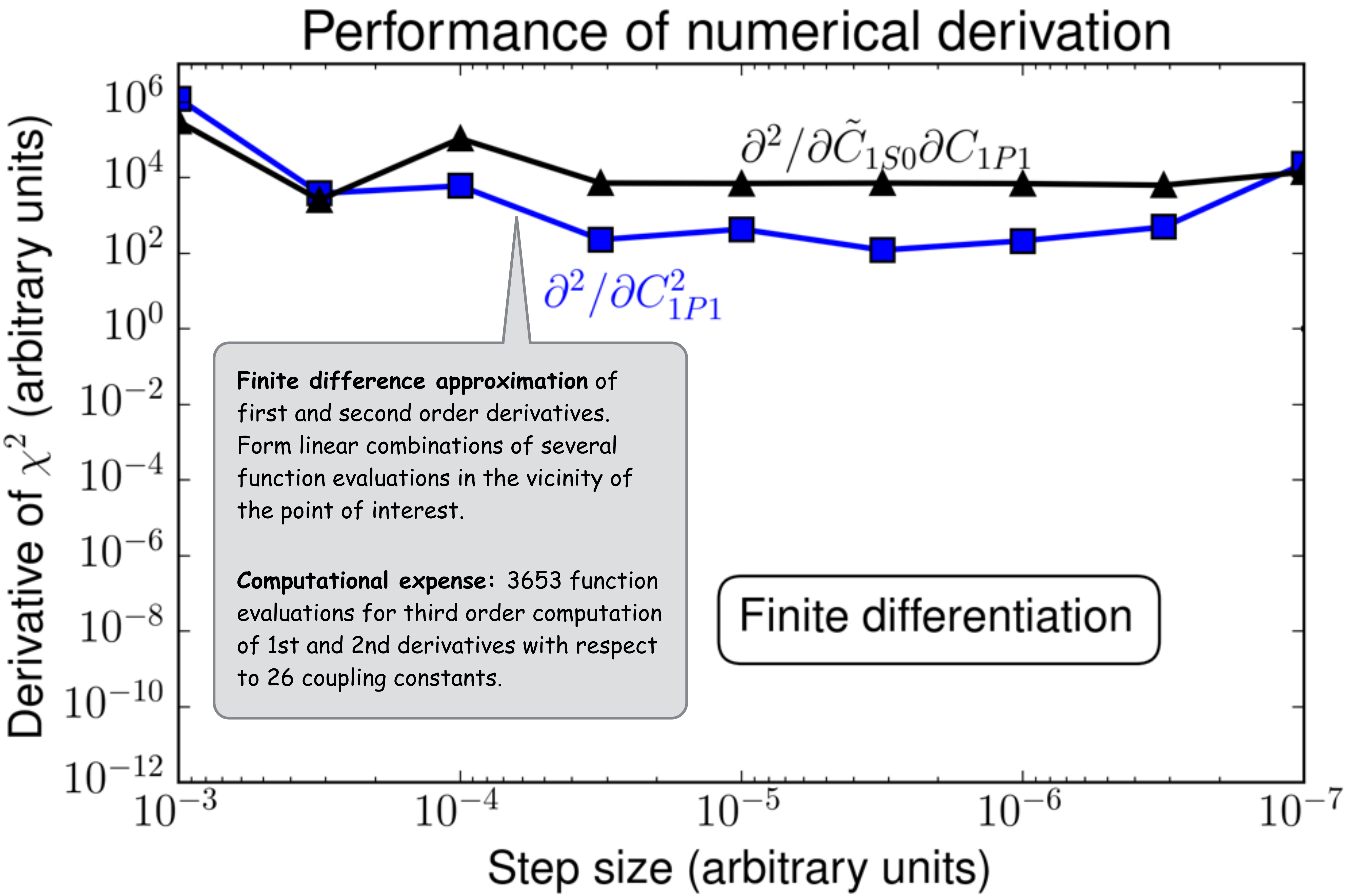

Finite difference approximation of first and second order derivatives. Form linear combinations of several function evaluations in the vicinity of the point of interest.

Computational expense: 3653 function evaluations for third order computation of 1st and 2nd derivatives with respect to 26 coupling constants.

Precision

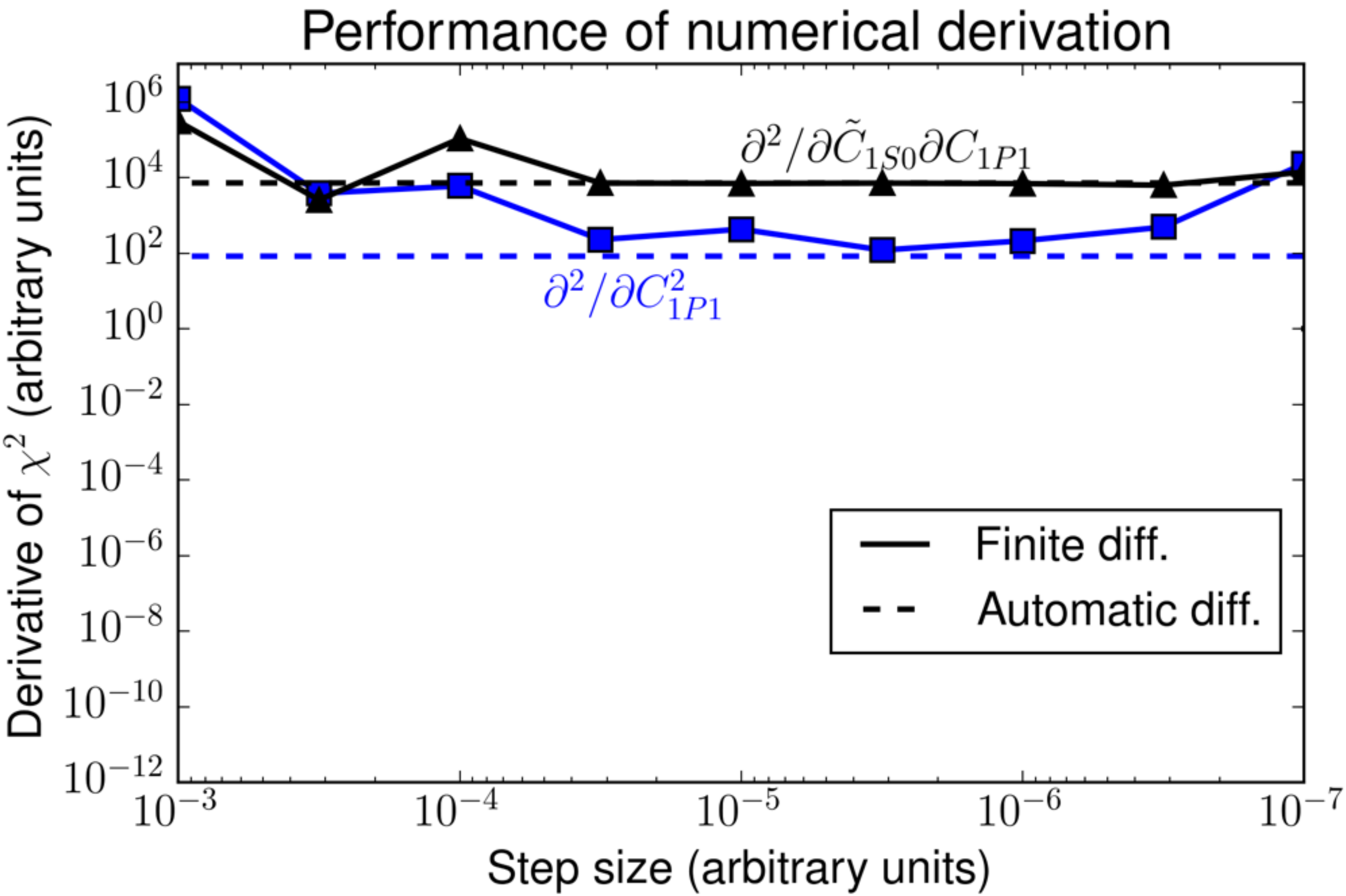
Performance of numerical derivation
Derivative of χ^2 (arbitrary units)
Step size (arbitrary units)
10^{6}
10^{4}
10^{2}
10^{0}
10^{-2}
10^{-4}
10^{-6}
10^{-8}
10^{-10}
10^{-12}
10^{-3}
10^{-4}
10^{-5}
10^{-6}
10^{-7}
$\partial^2/\partial\tilde{C}_{1S0}\partial C_{1P1}$
$\partial^2/\partial C_{1P1}^2$
Finite diff.
Automatic diff.

Precision

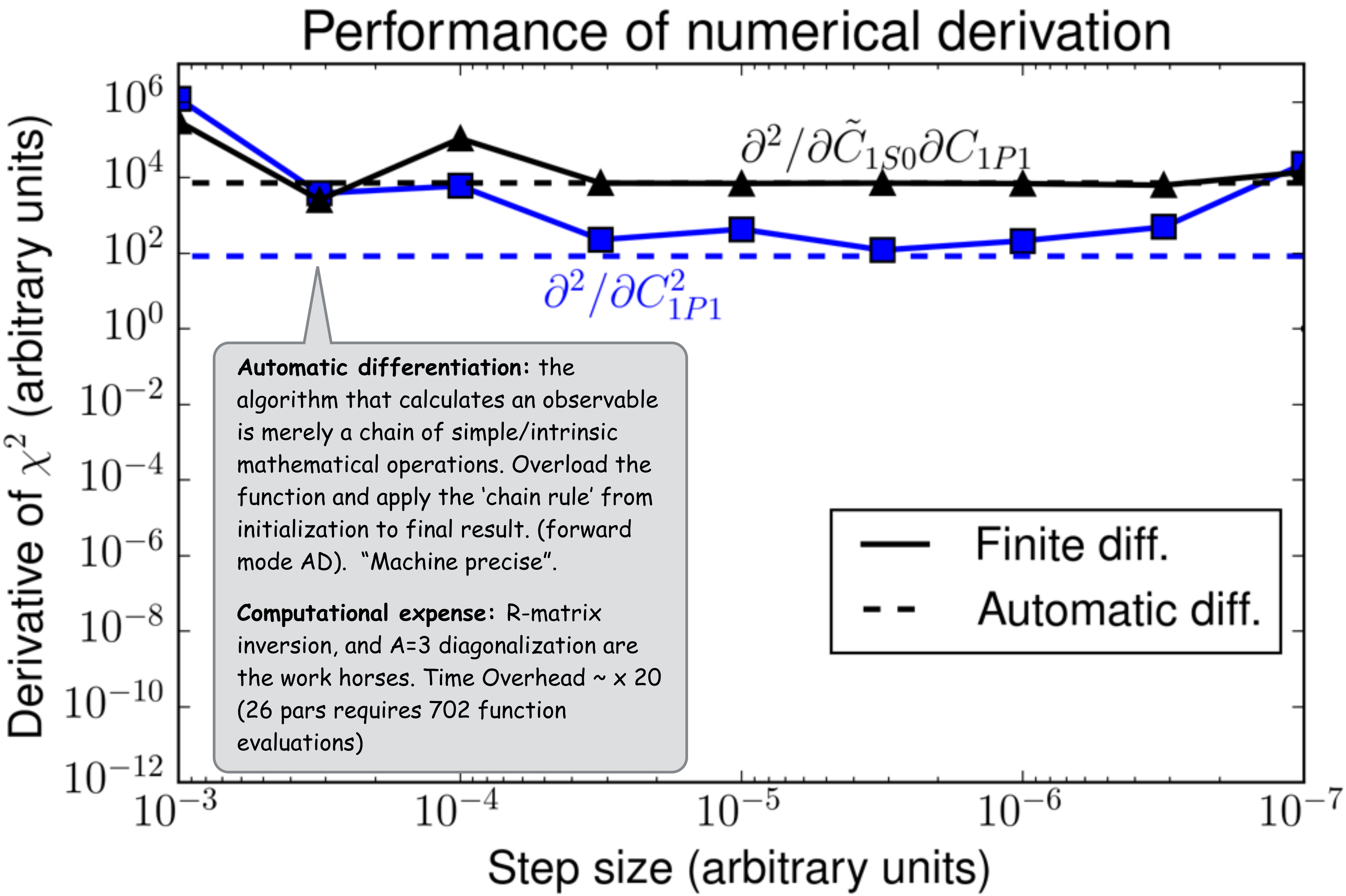

Automatic differentiation: the algorithm that calculates an observable is merely a chain of simple/intrinsic mathematical operations. Overload the function and apply the 'chain rule' from initialization to final result. (forward mode AD). "Machine precise".

Computational expense: R-matrix inversion, and A=3 diagonalization are the work horses. Time Overhead ~ x 20 (26 pars requires 702 function evaluations)

Precision

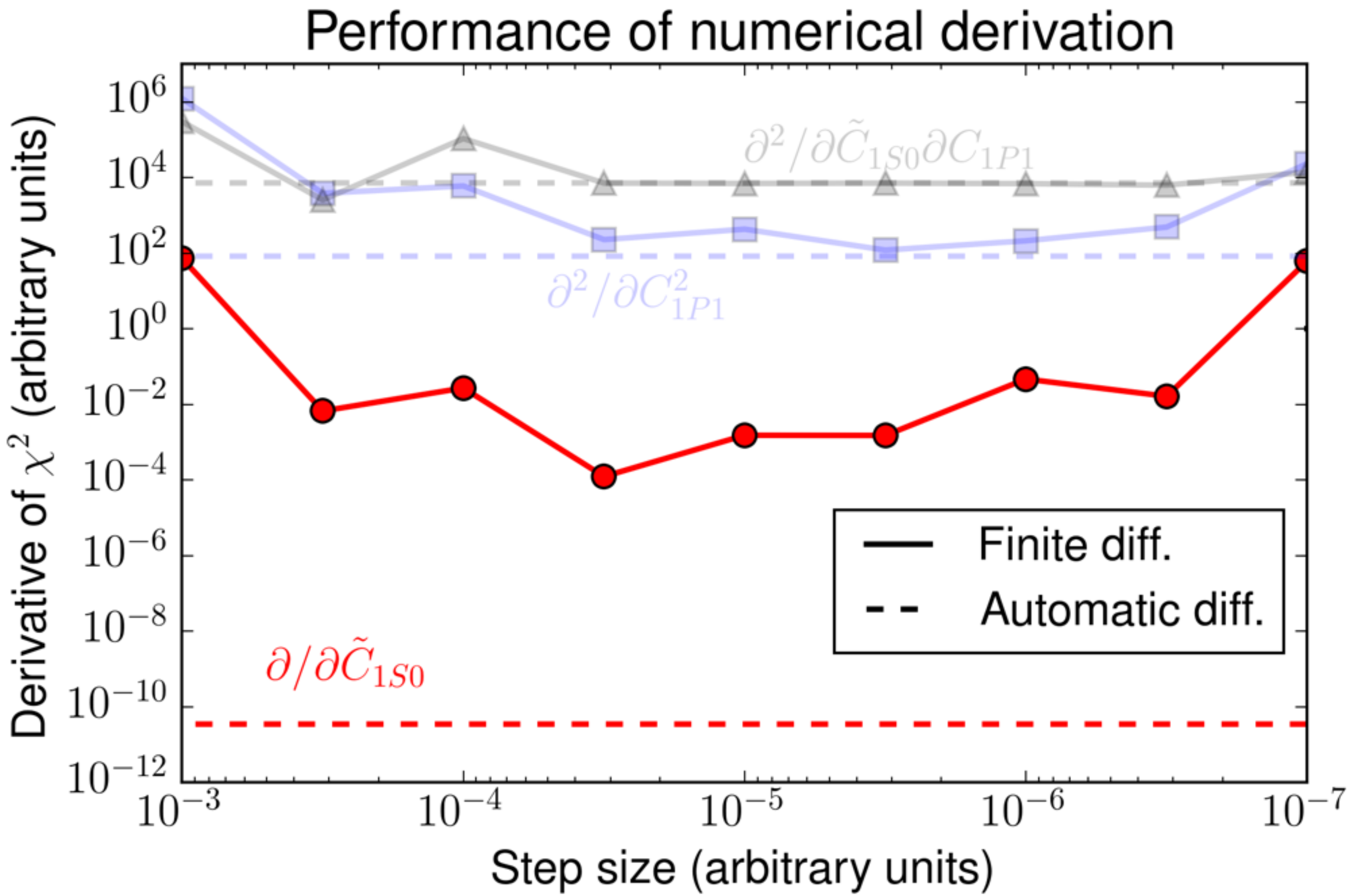

Performance of numerical derivation
Derivative of χ^2 (arbitrary units)
Step size (arbitrary units)
10^{6}
10^{4}
10^{2}
10^{0}
10^{-2}
10^{-4}
10^{-6}
10^{-8}
10^{-10}
10^{-12}
10^{-3}
10^{-4}
10^{-5}
10^{-6}
10^{-7}
$\partial^2/\partial\tilde{C}_{1S0}\partial C_{1P1}$
$\partial^2/\partial C_{1P1}^2$
$\partial/\partial\tilde{C}_{1S0}$
Finite diff.
Automatic diff.

Our Error Budget

theoretical error sources:
- systematic uncertainty (incorrect assumptions)
- statistical uncertainty (fitting)
- numerical uncertainty

$$\sigma^2_{\text{total}} = \sigma^2_{\text{experiment}} + \sigma^2_{\text{theory}}$$

Our Error Budget

theoretical error sources:

- systematic uncertainty (incorrect assumptions)
- statistical uncertainty (fitting)
- numerical uncertainty

$$\sigma^2_{\text{total}} = \boxed{\sigma^2_{\text{experiment}}} + \sigma^2_{\text{theory}}$$

Our Error Budget

theoretical error sources:

- systematic uncertainty (incorrect assumptions)
- statistical uncertainty (fitting)
- numerical uncertainty

$$\sigma^2_{\text{total}} = \boxed{\sigma^2_{\text{experiment}}} + \boxed{\sigma^2_{\text{theory}}}$$

Our Error Budget

theoretical error sources:

- systematic uncertainty (incorrect assumptions)
- statistical uncertainty (fitting)
- numerical uncertainty

$$\sigma^2_{\text{total}} = \boxed{\sigma^2_{\text{experiment}}} + \boxed{\sigma^2_{\text{theory}}}$$

$$\boxed{\sigma^2_{\text{theory}}} = \sigma^2_{\text{numerical}} + \sigma^2_{\text{method}} + \sigma^2_{\text{model}}$$

Our Error Budget

theoretical error sources:

- systematic uncertainty (incorrect assumptions)
- statistical uncertainty (fitting)
- numerical uncertainty

$$\sigma^2_{\text{total}} = \boxed{\sigma^2_{\text{experiment}}} + \boxed{\sigma^2_{\text{theory}}}$$

$$\boxed{\sigma^2_{\text{theory}}} = \boxed{\sigma^2_{\text{numerical}}} + \sigma^2_{\text{method}} + \sigma^2_{\text{model}}$$

Our Error Budget

theoretical error sources:

- systematic uncertainty (incorrect assumptions)
- statistical uncertainty (fitting)
- numerical uncertainty

$$\sigma^2_{\text{total}} = \boxed{\sigma^2_{\text{experiment}}} + \boxed{\sigma^2_{\text{theory}}}$$

$$\boxed{\sigma^2_{\text{theory}}} = \boxed{\sigma^2_{\text{numerical}}} + \sigma^2_{\text{method}} + \sigma^2_{\text{model}}$$

Algorithmic origin, due to approximations in the implementation of the computer model. (Machine epsilon of float 10^{-16})

We safely neglect this.

Our Error Budget

theoretical error sources:

- systematic uncertainty (incorrect assumptions)
- statistical uncertainty (fitting)
- numerical uncertainty

$$\sigma^2_{\text{total}} = \boxed{\sigma^2_{\text{experiment}}} + \boxed{\sigma^2_{\text{theory}}}$$

$$\boxed{\sigma^2_{\text{theory}}} = \boxed{\sigma^2_{\text{numerical}}} + \boxed{\sigma^2_{\text{method}}} + \sigma^2_{\text{model}}$$

Algorithmic origin, due to approximations in the implementation of the computer model. (Machine epsilon of float 10^{-16})

We safely neglect this.

Our Error Budget

theoretical error sources:

- systematic uncertainty (incorrect assumptions)
- statistical uncertainty (fitting)
- numerical uncertainty

$$\sigma^2_{\text{total}} = \sigma^2_{\text{experiment}} + \sigma^2_{\text{theory}}$$

Due to approximations in the solution of the Schrodinger equation. We estimate these using exponential extrapolation. The S-matrix for two-nucleon scattering states is constructed to sufficient precision using L=30 partial-waves.

$$\sigma^2_{\text{theory}} = \sigma^2_{\text{numerical}} + \sigma^2_{\text{method}} + \sigma^2_{\text{model}}$$

Algorithmic origin, due to approximations in the implementation of the computer model. (Machine epsilon of float 10^{-16})

We safely neglect this.

Our Error Budget

theoretical error sources:

- systematic uncertainty (incorrect assumptions)
- statistical uncertainty (fitting)
- numerical uncertainty

$$\sigma^2_{\text{total}} = \boxed{\sigma^2_{\text{experiment}}} + \boxed{\sigma^2_{\text{theory}}}$$

Due to approximations in the solution of the Schrodinger equation. We estimate these using exponential extrapolation. The S-matrix for two-nucleon scattering states is constructed to sufficient precision using L=30 partial-waves.

	Exp. value	Ref.	$\sigma_{\text{exp+method}}$
$E(^2\text{H})$	$-2.22456627(46)^{a}$	[38]	$0.47 \cdot 10^{-6}$
$E(^3\text{H})$	$-8.4817987(25)^{a}$	[38]	$3.3 \cdot 10^{-3}$
$E(^3\text{He})$	$-7.7179898(24)^{a}$	[38]	$3.8 \cdot 10^{-3}$
$E(^4\text{He})$	$-28.2956099(11)^{a}$	[38]	$6.5 \cdot 10^{-3}$
$r_{\text{pt-p}}(^2\text{H})$	$1.97559(78)^{b}$	[65, 73]	$0.78 \cdot 10^{-3}$
$r_{\text{pt-p}}(^3\text{H})$	1.587(41)	[65]	0.041
$r_{\text{pt-p}}(^3\text{He})$	1.7659(54)	[65]	0.013
$r_{\text{pt-p}}(^4\text{He})$	1.4552(62)	[65]	0.0071
Q_{d}	$0.27(1)^{c}$		0.01
$E^1_A(^3\text{H})$	0.6848(11)	[68]	0.0011

$$\boxed{\sigma^2_{\text{theory}}} = \boxed{\sigma^2_{\text{numerical}}} + \boxed{\sigma^2_{\text{method}}} + \sigma^2_{\text{model}}$$

Algorithmic origin, due to approximations in the implementation of the computer model. (Machine epsilon of float 10^{-16})

We safely neglect this.

Our Error Budget

theoretical error sources:

- systematic uncertainty (incorrect assumptions)
- statistical uncertainty (fitting)
- numerical uncertainty

$$\sigma^2_{\text{total}} = \sigma^2_{\text{experiment}} + \sigma^2_{\text{theory}}$$

Due to approximations in the solution of the Schrodinger equation. We estimate these using exponential extrapolation. The S-matrix for two-nucleon scattering states is constructed to sufficient precision using L=30 partial-waves.

	Exp. value	Ref.	$\sigma_{\text{exp+method}}$
$E(^2\text{H})$	$-2.22456627(46)^{a}$	[38]	$0.47 \cdot 10^{-6}$
$E(^3\text{H})$	$-8.4817987(25)^{a}$	[38]	$3.3 \cdot 10^{-3}$
$E(^3\text{He})$	$-7.7179898(24)^{a}$	[38]	$3.8 \cdot 10^{-3}$
$E(^4\text{He})$	$-28.2956099(11)^{a}$	[38]	$6.5 \cdot 10^{-3}$
$r_{\text{pt-p}}(^2\text{H})$	$1.97559(78)^{b}$	[65, 73]	$0.78 \cdot 10^{-3}$
$r_{\text{pt-p}}(^3\text{H})$	1.587(41)	[65]	0.041
$r_{\text{pt-p}}(^3\text{He})$	1.7659(54)	[65]	0.013
$r_{\text{pt-p}}(^4\text{He})$	1.4552(62)	[65]	0.0071
Q_{d}	$0.27(1)^{c}$		0.01
$E^1_A(^3\text{H})$	0.6848(11)	[68]	0.0011

$$\sigma^2_{\text{theory}} = \sigma^2_{\text{numerical}} + \sigma^2_{\text{method}} + \sigma^2_{\text{model}}$$

Algorithmic origin, due to approximations in the implementation of the computer model. (Machine epsilon of float 10^{-16})

We safely neglect this.

Our Error Budget

theoretical error sources:
- systematic uncertainty (incorrect assumptions)
- statistical uncertainty (fitting)
- numerical uncertainty

$$\sigma^2_{\text{total}} = \sigma^2_{\text{experiment}} + \sigma^2_{\text{theory}}$$

Due to approximations in the solution of the Schrodinger equation. We estimate these using exponential extrapolation. The S-matrix for two-nucleon scattering states is constructed to sufficient precision using L=30 partial-waves.

	Exp. value	Ref.	$\sigma_{\text{exp+method}}$
$E(^2\text{H})$	$-2.22456627(46)^a$	[38]	$0.47 \cdot 10^{-6}$
$E(^3\text{H})$	$-8.4817987(25)^a$	[38]	$3.3 \cdot 10^{-3}$
$E(^3\text{He})$	$-7.7179898(24)^a$	[38]	$3.8 \cdot 10^{-3}$
$E(^4\text{He})$	$-28.2956099(11)^a$	[38]	$6.5 \cdot 10^{-3}$
$r_{\text{pt-p}}(^2\text{H})$	$1.97559(78)^b$	[65, 73]	$0.78 \cdot 10^{-3}$
$r_{\text{pt-p}}(^3\text{H})$	$1.587(41)$	[65]	0.041
$r_{\text{pt-p}}(^3\text{He})$	$1.7659(54)$	[65]	0.013
$r_{\text{pt-p}}(^4\text{He})$	$1.4552(62)$	[65]	0.0071
Q_d	$0.27(1)^c$		0.01
$E^1_A(^3\text{H})$	$0.6848(11)$	[68]	0.0011

$$\sigma^2_{\text{theory}} = \sigma^2_{\text{numerical}} + \sigma^2_{\text{method}} + \sigma^2_{\text{model}}$$

Algorithmic origin, due to approximations in the implementation of the computer model. (Machine epsilon of float 10^{-16})

We safely neglect this.

Imperfect modeling and missing physics in the construction of the nuclear interaction. We estimate this from the rest term in the xEFT expansion:

$$\sigma^{(\text{amplitude})}_{\text{model,x}} = \mathcal{C}_x \left(\frac{Q}{\Lambda}\right)^{\nu+1}, \; x \in \{\text{NN}, \pi\text{N}\}$$

Estimating the model error

$$\chi^2(\mathbf{p}) = \sum_{i\in\mathbb{M}} \left(\frac{\mathcal{O}_i^{\mathrm{theo}}(\mathbf{p}) - \mathcal{O}_i^{\mathrm{exp}}}{\sigma_i^{\mathrm{total}}} \right)^2 = \sum_{i\in\mathbb{M}} R_i^2(\mathbf{p})$$

Estimating the model error

$$\chi^2(\mathbf{p}) = \sum_{i\in\mathbb{M}} \left(\frac{\mathcal{O}_i^{\text{theo}}(\mathbf{p}) - \mathcal{O}_i^{\text{exp}}}{\boxed{\sigma_i^{\text{total}}}} \right)^2 = \sum_{i\in\mathbb{M}} R_i^2(\mathbf{p})$$

$$\ldots + \sigma_{\text{model,x}}^{(\text{amplitude})} = \mathcal{C}_x \left(\frac{Q}{\Lambda}\right)^{\nu+1}, \; x \in \{\text{NN}, \pi\text{N}\}$$

Estimating the model error

$$\chi^2(\mathbf{p}) = \sum_{i\in\mathbb{M}} \left(\frac{\mathcal{O}_i^{\text{theo}}(\mathbf{p}) - \mathcal{O}_i^{\text{exp}}}{\boxed{\sigma_i^{\text{total}}}} \right)^2 = \sum_{i\in\mathbb{M}} R_i^2(\mathbf{p})$$

$$\ldots + \sigma_{\text{model,x}}^{(\text{amplitude})} = \mathcal{C}_x \left(\frac{Q}{\Lambda} \right)^{\nu+1}, \; x \in \{\text{NN}, \pi\text{N}\}$$

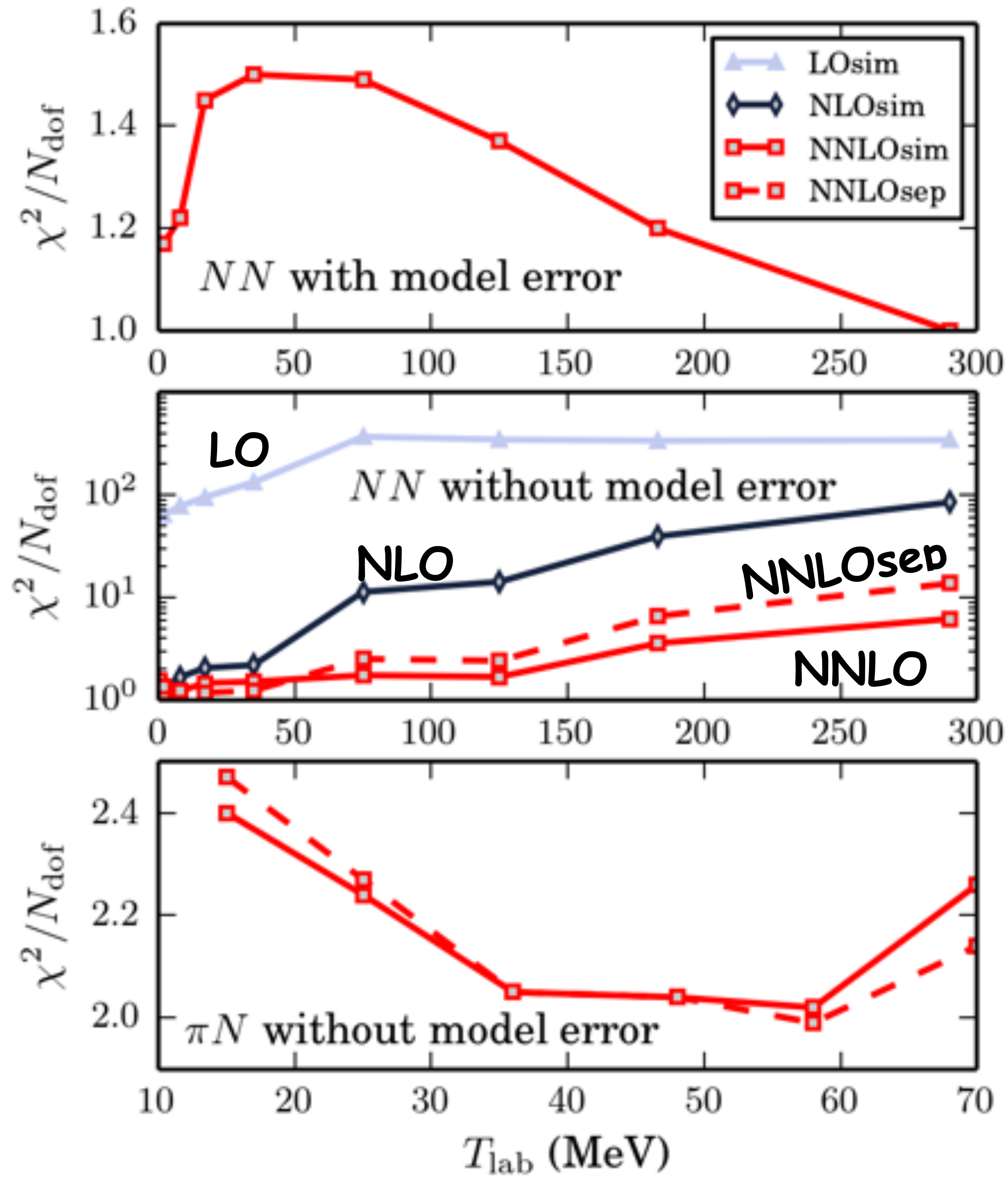

Estimating the model error

$$\chi^2(\mathbf{p}) = \sum_{i\in\mathbb{M}} \left(\frac{\mathcal{O}_i^{\text{theo}}(\mathbf{p}) - \mathcal{O}_i^{\text{exp}}}{\boxed{\sigma_i^{\text{total}}}} \right)^2 = \sum_{i\in\mathbb{M}} R_i^2(\mathbf{p})$$

$$\ldots + \sigma_{\text{model,x}}^{(\text{amplitude})} = \mathcal{C}_x \left(\frac{Q}{\Lambda}\right)^{\nu+1}, \; x \in \{\text{NN}, \pi\text{N}\}$$

$$M(\mathbf{q},\mathbf{k}) = \frac{1}{2}\{(a+b) + (a-b)\boldsymbol{\sigma}_1\cdot(\hat{\mathbf{q}}\times\hat{\mathbf{k}})\boldsymbol{\sigma}_2\cdot(\hat{\mathbf{q}}\times\hat{\mathbf{k}})$$
$$+ (c+d)(\boldsymbol{\sigma}_1\cdot\hat{\mathbf{q}})(\boldsymbol{\sigma}_2\cdot\hat{\mathbf{q}}) + (c-d)(\boldsymbol{\sigma}_1\cdot\hat{\mathbf{k}})(\boldsymbol{\sigma}_2\cdot\hat{\mathbf{k}})$$
$$- e(\boldsymbol{\sigma}_1+\boldsymbol{\sigma}_2)\cdot(\hat{\mathbf{q}}\times\hat{\mathbf{k}}) - f(\boldsymbol{\sigma}_1-\boldsymbol{\sigma}_2)\cdot(\hat{\mathbf{q}}\times\hat{\mathbf{k}})\}$$

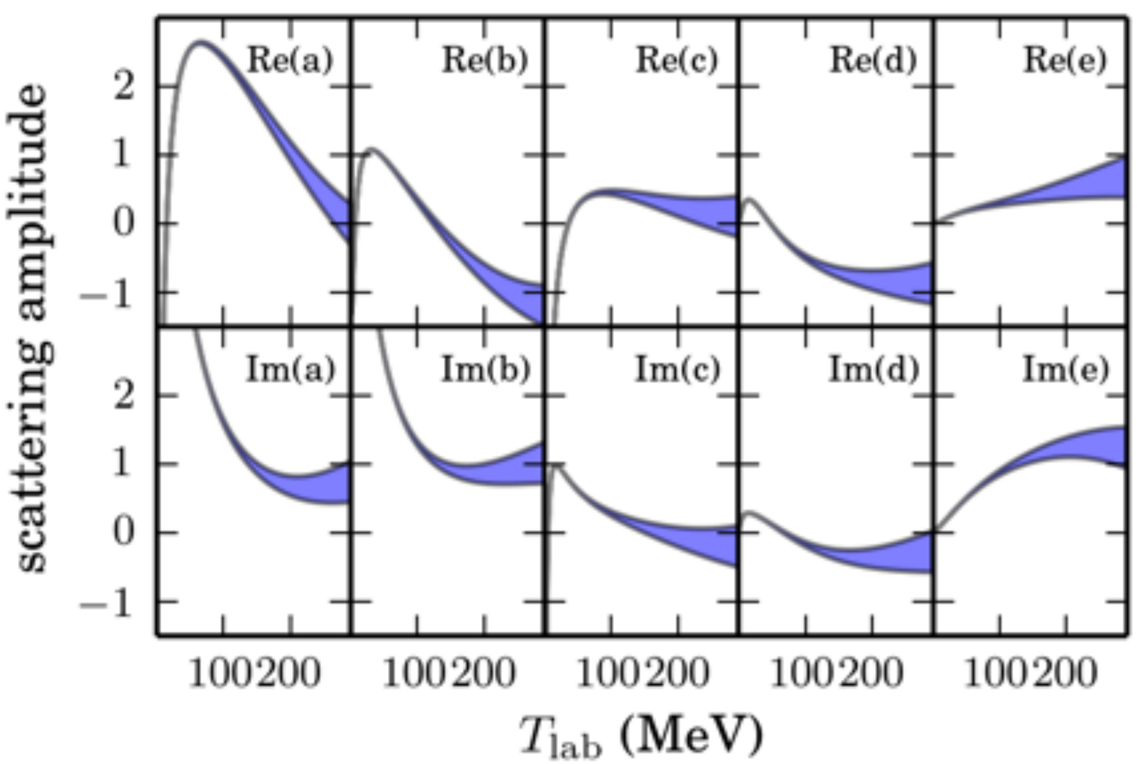

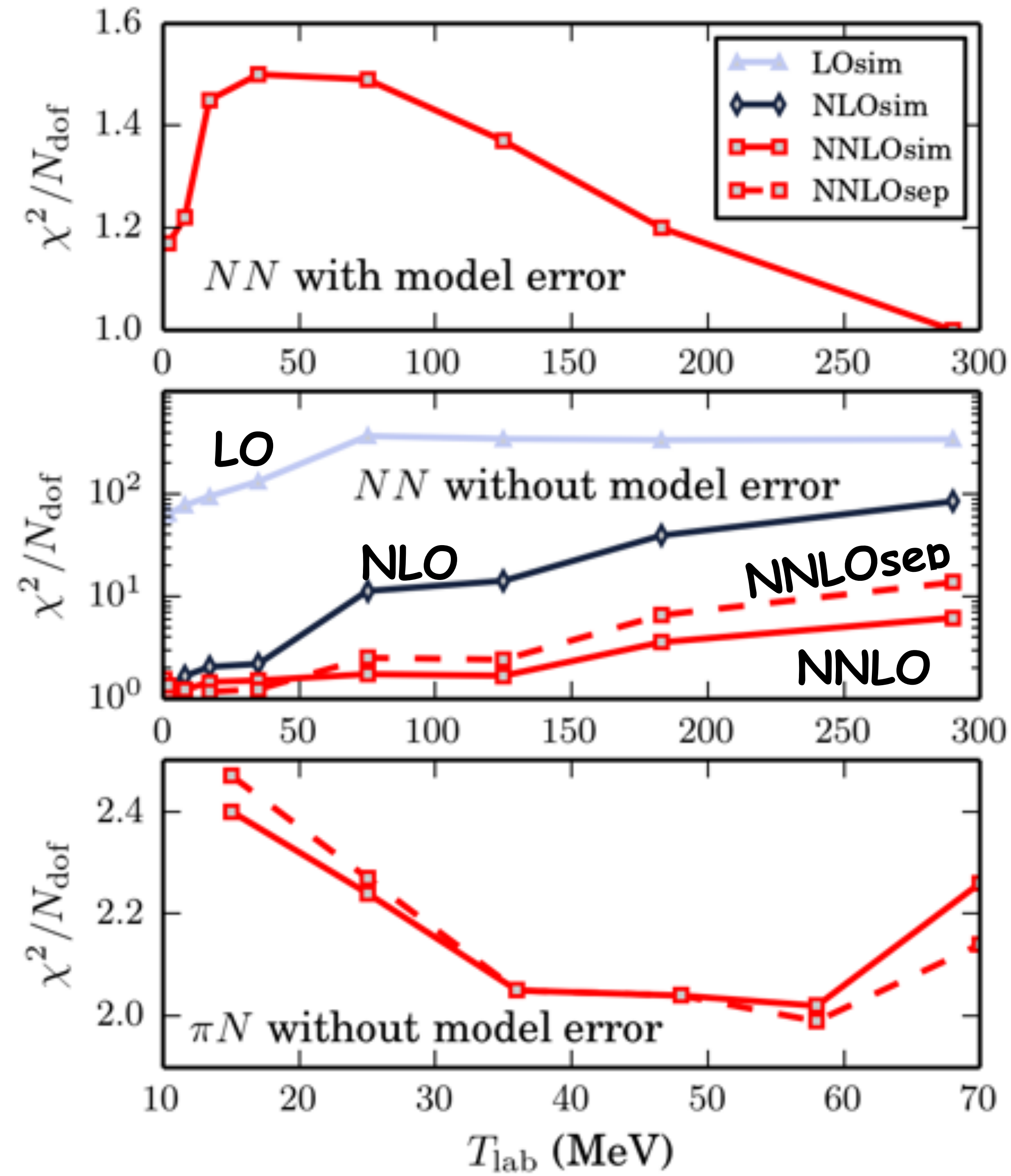

Uncertainty Quantification

Statistical uncertainty in the parameter vector at the optimum is given by the surface of the objective function.

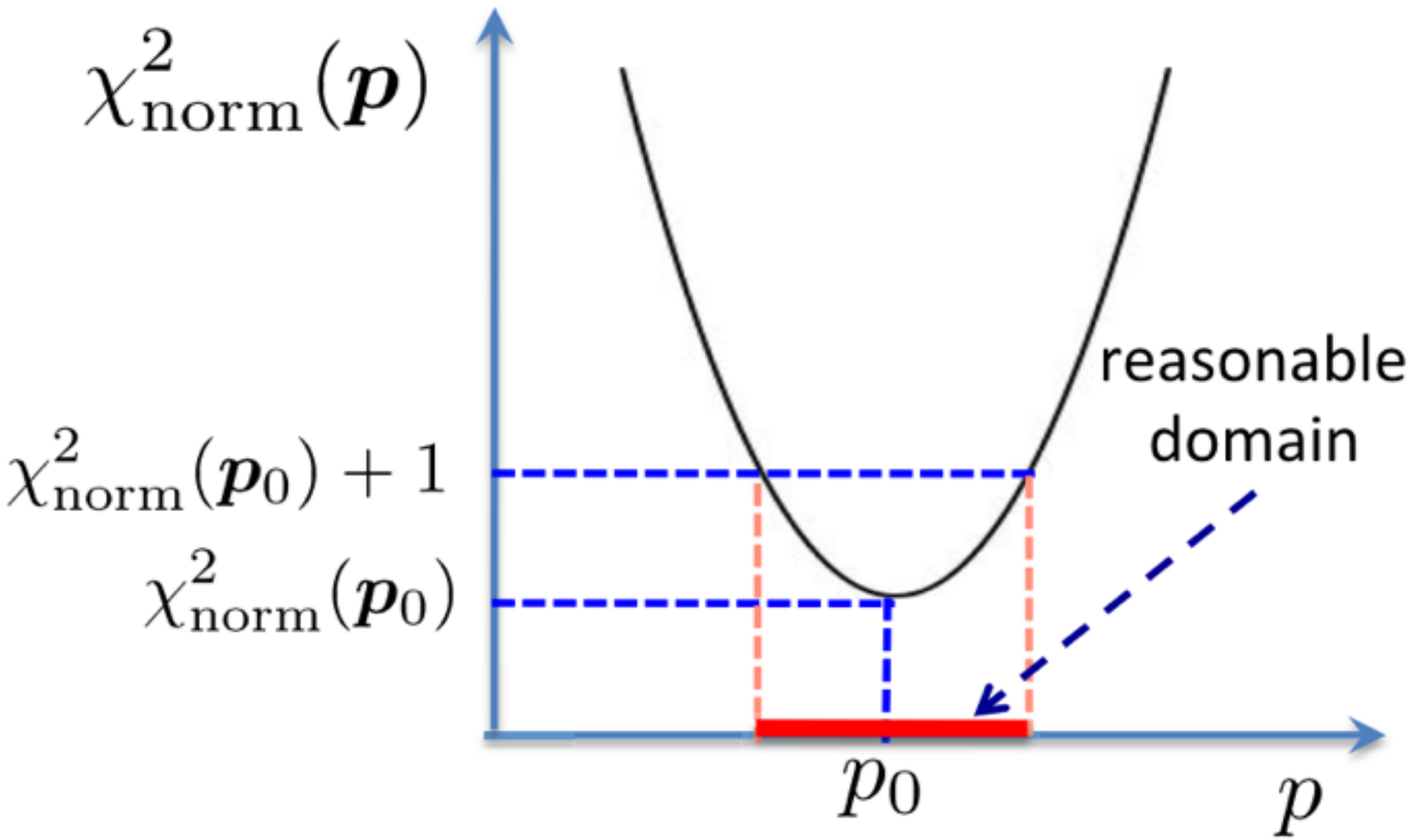

Computational Experience With Confidence Regions and Confidence Intervals for Nonlinear Least Squares
J. R. Donaldson and R. B. Schnabel *Technometrics 29* 67 (1987)

Error estimates of theoretical models: a guide
J Dobaczewski, W Nazarewicz and P-G Reinhard, *J. Phys.G* 41 074001 (2014)

Uncertainty Quantification

Statistical uncertainty in the parameter vector at the optimum is given by the surface of the objective function.

$$\mathbf{p}_\star = \arg\min_{\mathbf{p}} \chi^2(\mathbf{p})$$

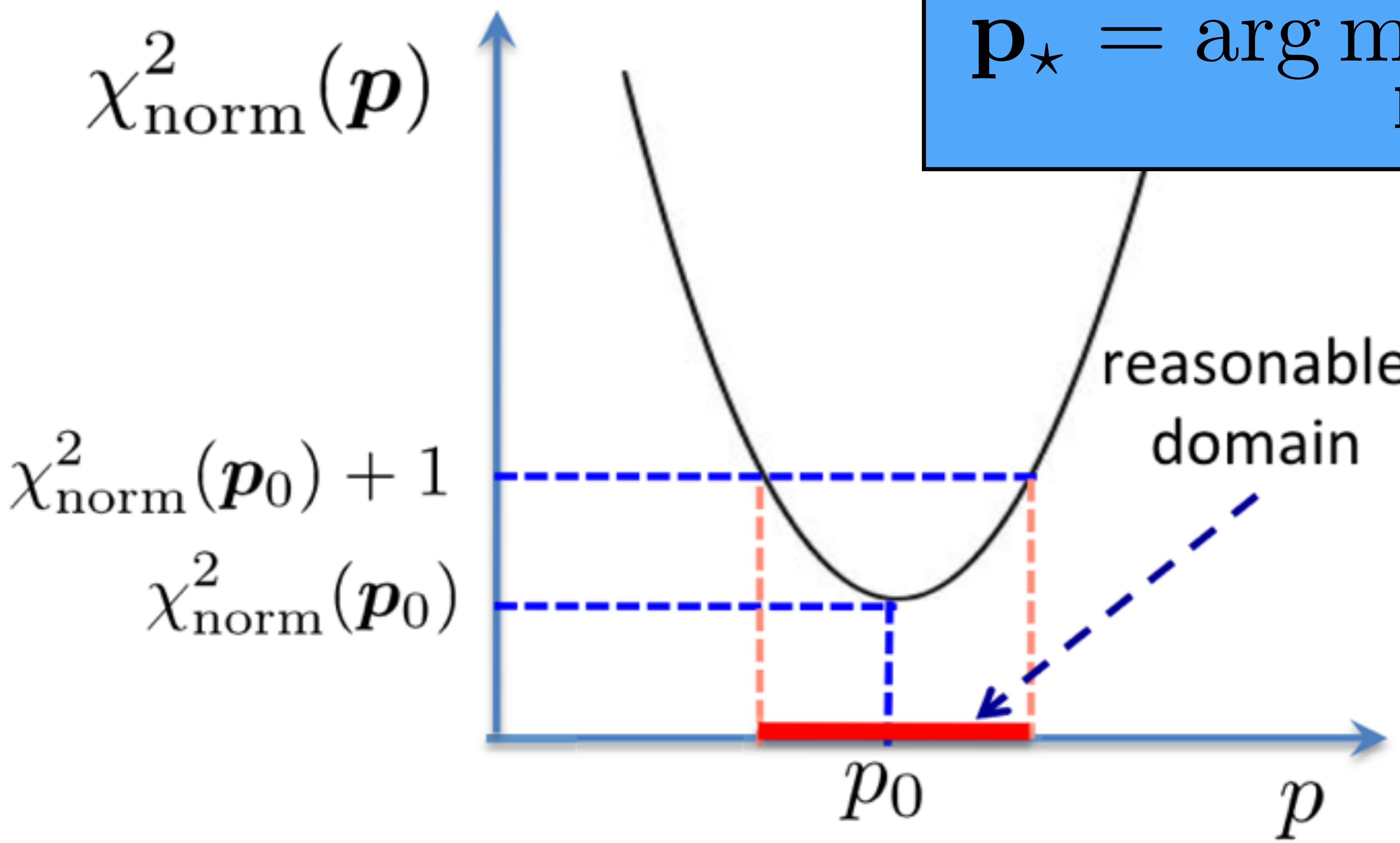

Computational Experience With Confidence Regions and Confidence Intervals for Nonlinear Least Squares
J. R. Donaldson and R. B. Schnabel *Technometrics 29* 67 (1987)

Error estimates of theoretical models: a guide
J Dobaczewski, W Nazarewicz and P-G Reinhard, *J. Phys.G* 41 074001 (2014)

Uncertainty Quantification

$$\chi^2(\mathbf{p}_\star + \Delta\mathbf{p}) - \chi^2(\mathbf{p}_\star) \approx \frac{1}{2}(\Delta\mathbf{p})^T \mathbf{H}(\Delta\mathbf{p})$$

$$H_{ij} = \left.\frac{\partial^2 \chi^2(\mathbf{p})}{\partial p_i \partial p_j}\right|_{\mathbf{p}=\mathbf{p}_\star}.$$

$$\mathrm{Cov}(\mathbf{p}_\star) = 2\frac{\chi^2(\mathbf{p}_\star)}{\mathrm{N_{dof}}}\mathbf{H}^{-1}$$

n the parameter vector at the

rface of the objective function.

$$\mathbf{p}_\star = \arg\min_{\mathbf{p}} \chi^2(\mathbf{p})$$

$$\mathcal{O}_A(\mathbf{p}_\star + \Delta\mathbf{p}) \approx \mathcal{O}_A(\mathbf{p}_\star) + (\Delta\mathbf{p})^T\mathbf{J} + \frac{1}{2}(\Delta\mathbf{p})^T\mathbf{H}(\Delta\mathbf{p})$$
$$= \mathcal{O}_A(\mathbf{p}_\star) + \mathbf{x}^T\mathbf{U}^T\mathbf{J} + \frac{1}{2}\mathbf{x}^T\mathbf{U}^T\mathbf{H}\mathbf{U}\mathbf{x}$$
$$\equiv \mathcal{O}_A(\mathbf{p}_\star) + \mathbf{x}^T\tilde{\mathbf{J}} + \frac{1}{2}\mathbf{x}^T\tilde{\mathbf{H}}\mathbf{x},$$

le

$\chi^2_{\mathrm{norm}}(\boldsymbol{p}$

$\chi^2_{\mathrm{norm}}(\boldsymbol{p}_0)$

$$\mathrm{Cov(A,B)} \equiv \mathbb{E}[(\mathcal{O}_\mathrm{A}(\mathbf{p}) - \mathbb{E}[\mathcal{O}_\mathrm{A}(\mathbf{p})])(\mathcal{O}_\mathrm{B}(\mathbf{p}) - \mathbb{E}[\mathcal{O}_\mathrm{B}(\mathbf{p})])]$$
$$\approx \mathbb{E}[(\tilde{J}_{A,i}x_i + \frac{1}{2}\tilde{H}_{A,ij}x_ix_j - \frac{1}{2}\tilde{H}_{A,ii}\sigma_i^2)$$
$$\times (\tilde{J}_{B,k}x_k + \frac{1}{2}\tilde{H}_{B,kl}x_kx_l - \frac{1}{2}\tilde{H}_{B,kk}\sigma_k^2)]$$
$$= \tilde{\mathbf{J}}_A^T\boldsymbol{\Sigma}\tilde{\mathbf{J}}_B + \frac{1}{2}(\boldsymbol{\sigma}^2)^T(\tilde{\mathbf{H}}_A \circ \tilde{\mathbf{H}}_B)\boldsymbol{\sigma}^2$$

Computat ... uares
J. R. Dona

Error estimates of theoretical models: a guide
J Dobaczewski, W Nazarewicz and P-G Reinhard, *J. Phys.G* 41 074001 (2014)

Error Propagation

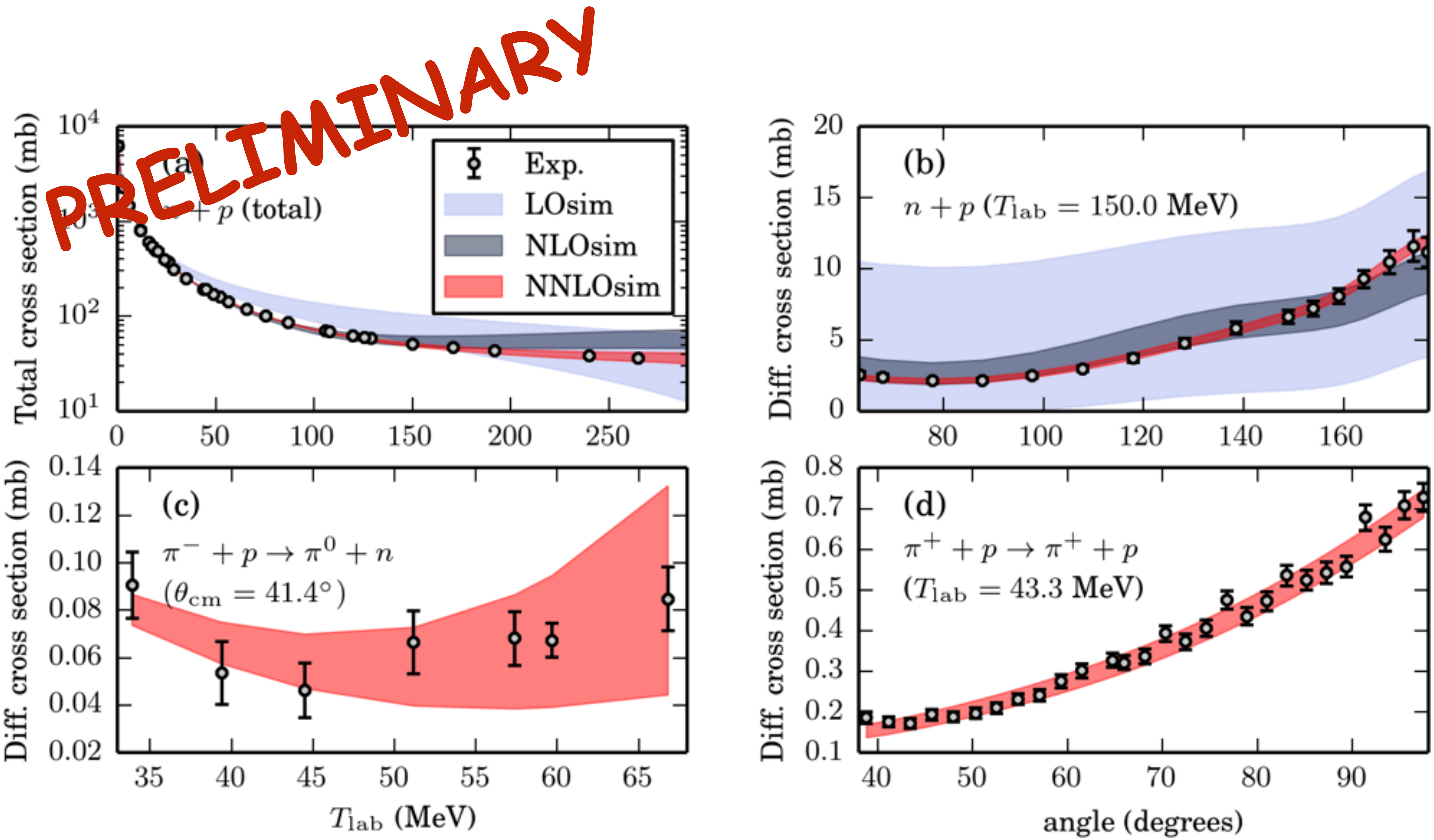

Simultaneous Optimization is Key

PRELIMINARY

TABLE VII. Obtained πN parameters and their statistical uncertainties for the NNLO potentials. c_i, d_i and e_i are in units of GeV^{-1}, GeV^{-2} and GeV^{-3} respectively.

	NNLOsep	NNLOsim
c_1	−0.68(50)	+0.22(29)
c_2	+3.0(14)	+5.1(10)
c_3	−4.12(32)	−3.56(13)
c_4	+5.35(81)	+3.933(85)
$d_1 + d_2$	+6.22(44)	+5.320(94)

Observable	NNLO$_{sim}$	NNLO$_{sep}$	Exp
$E_{gs}(^4HE)$ [MeV]	-28.26^{+4}_{-5}	-28^{+8}_{-18}	-28.30(1)
$r_{pt-p}(^4He)$ [fm]	1.445^{+2}_{-2}	1.44^{+15}_{-28}	1.455(7)

Simultaneous Optimization is Key

PRELIMINARY

TABLE VII. Obtained πN parameters and their statistical uncertainties for the NNLO potentials. c_i, d_i and e_i are in units of GeV^{-1}, GeV^{-2} and GeV^{-3} respectively.

	NNLOsep	NNLOsim
c_1	$-0.68(50)$	$+0.22(29)$
c_2	$+3.0(14)$	$+5.1(10)$
c_3	$-4.12(32)$	$-3.56(13)$
c_4	$+5.35(81)$	$+3.933(85)$
$d_1 + d_2$	[illegible]	[illegible]

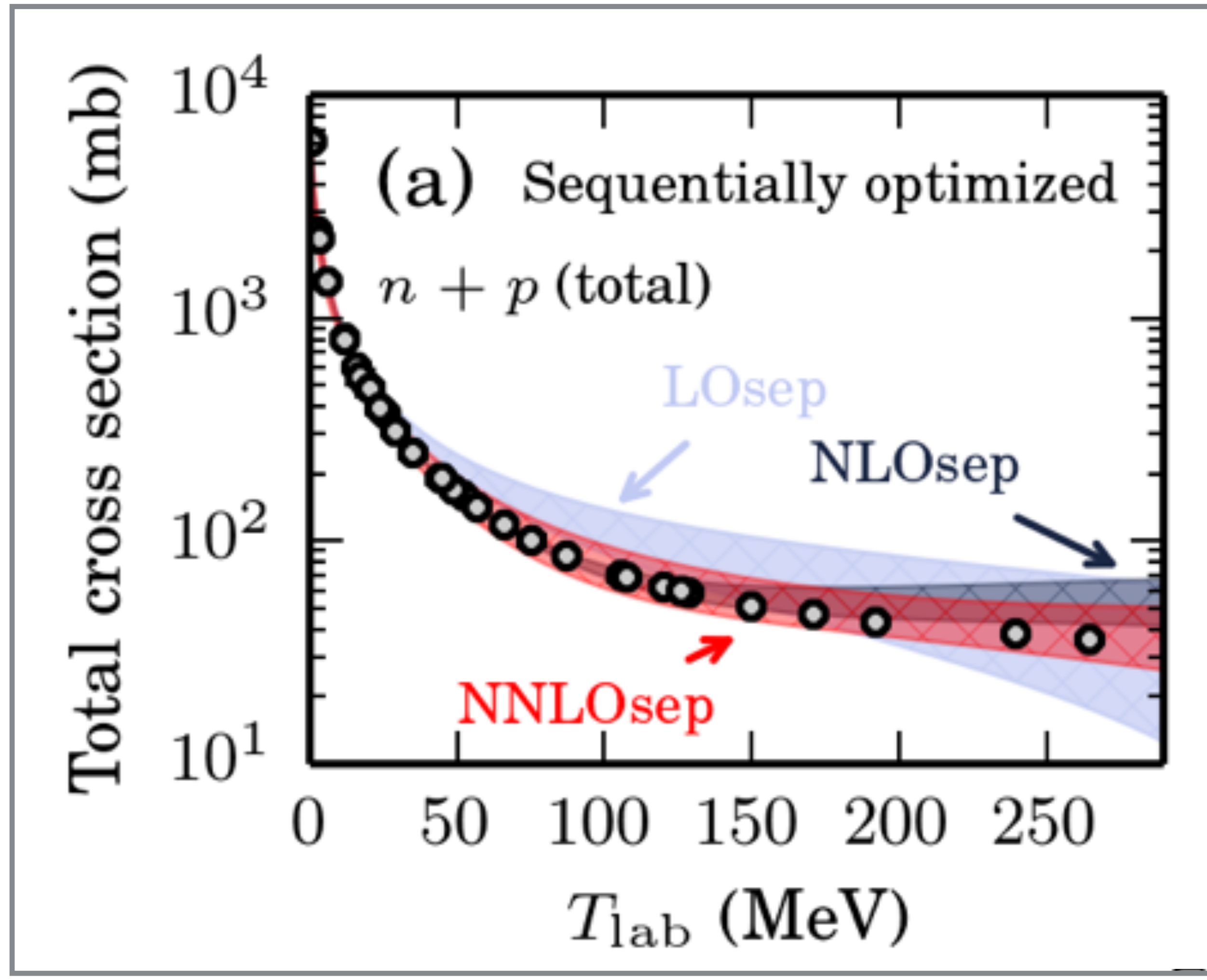

Observable	NNLO$_{sim}$	NNLO$_{sep}$	Exp
$E_{gs}(^4He)$ [MeV]	-28.26^{+4}_{-5}	-28^{+8}_{-18}	-28.30(1)
$r_{pt-p}(^4He)$ [fm]	1.445^{+2}_{-2}	1.44^{+15}_{-28}	1.455(7)

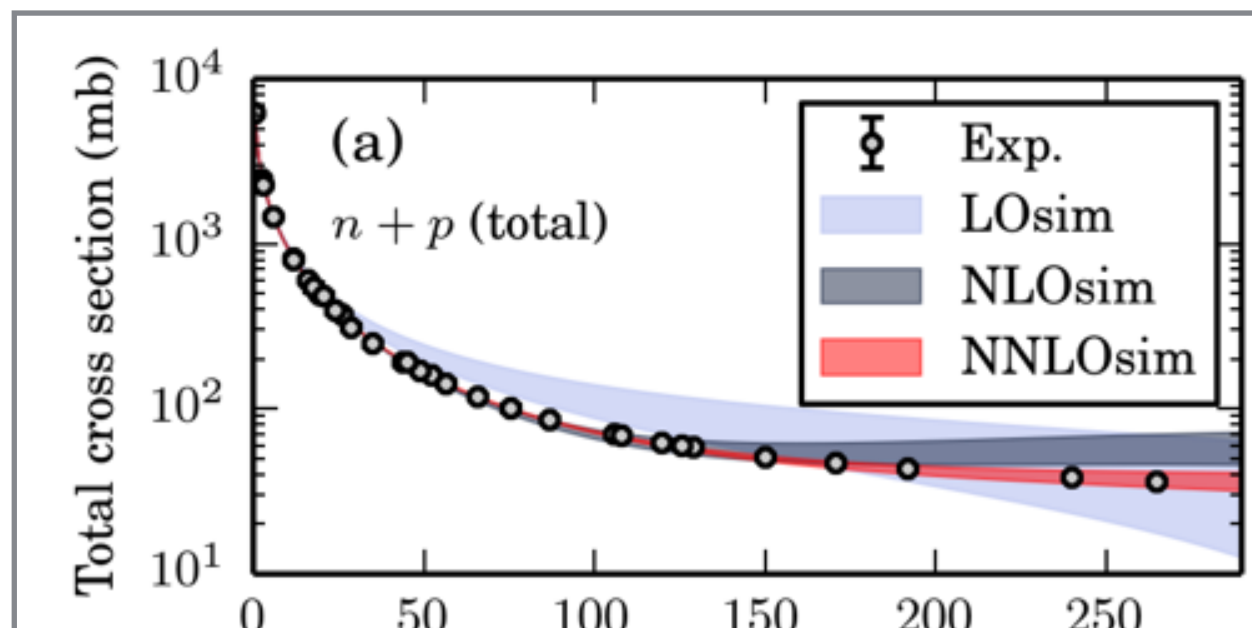

Covariance Analysis

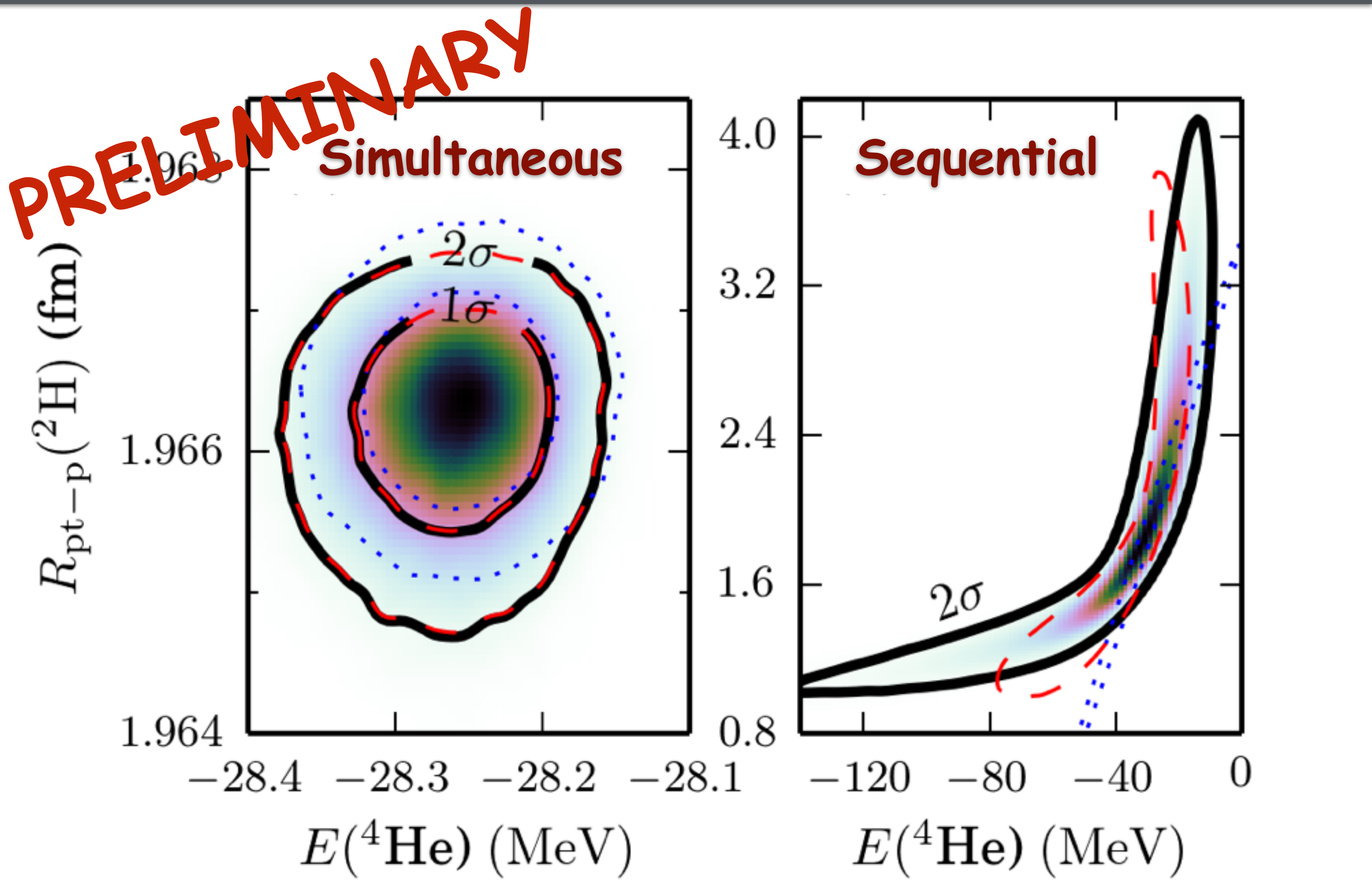

what goes wrong: *radii, binding energies, spectra, …*

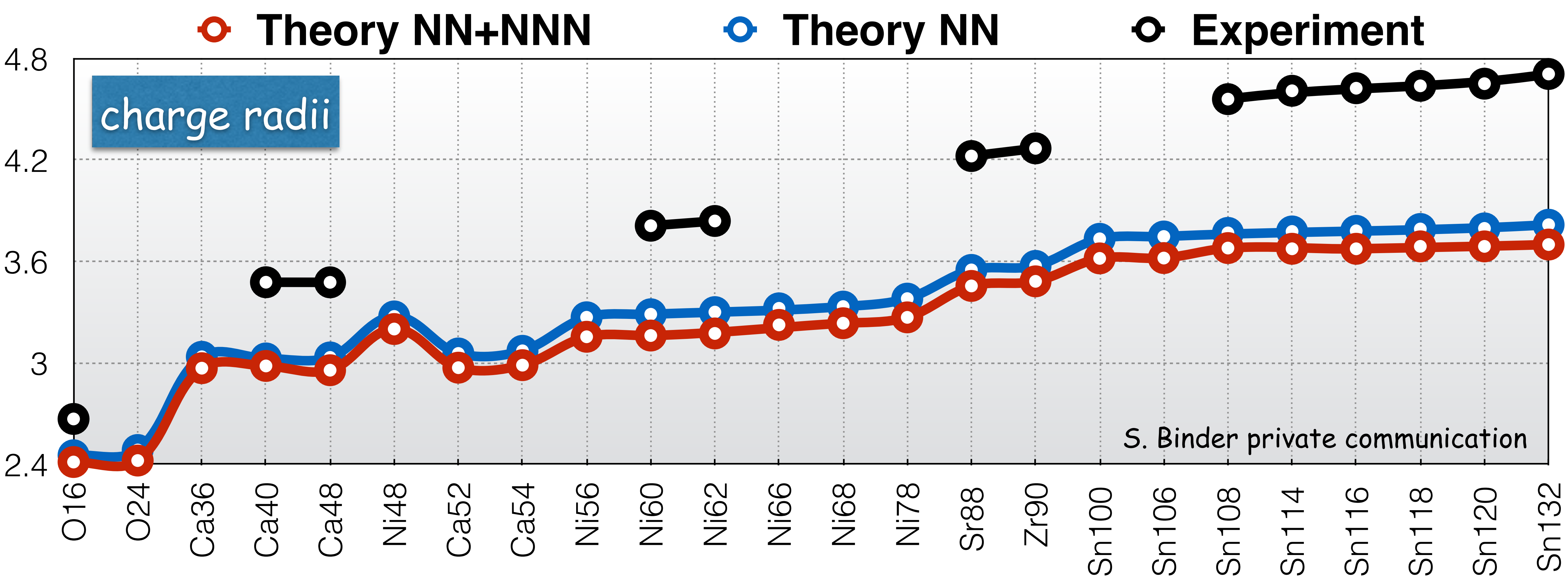

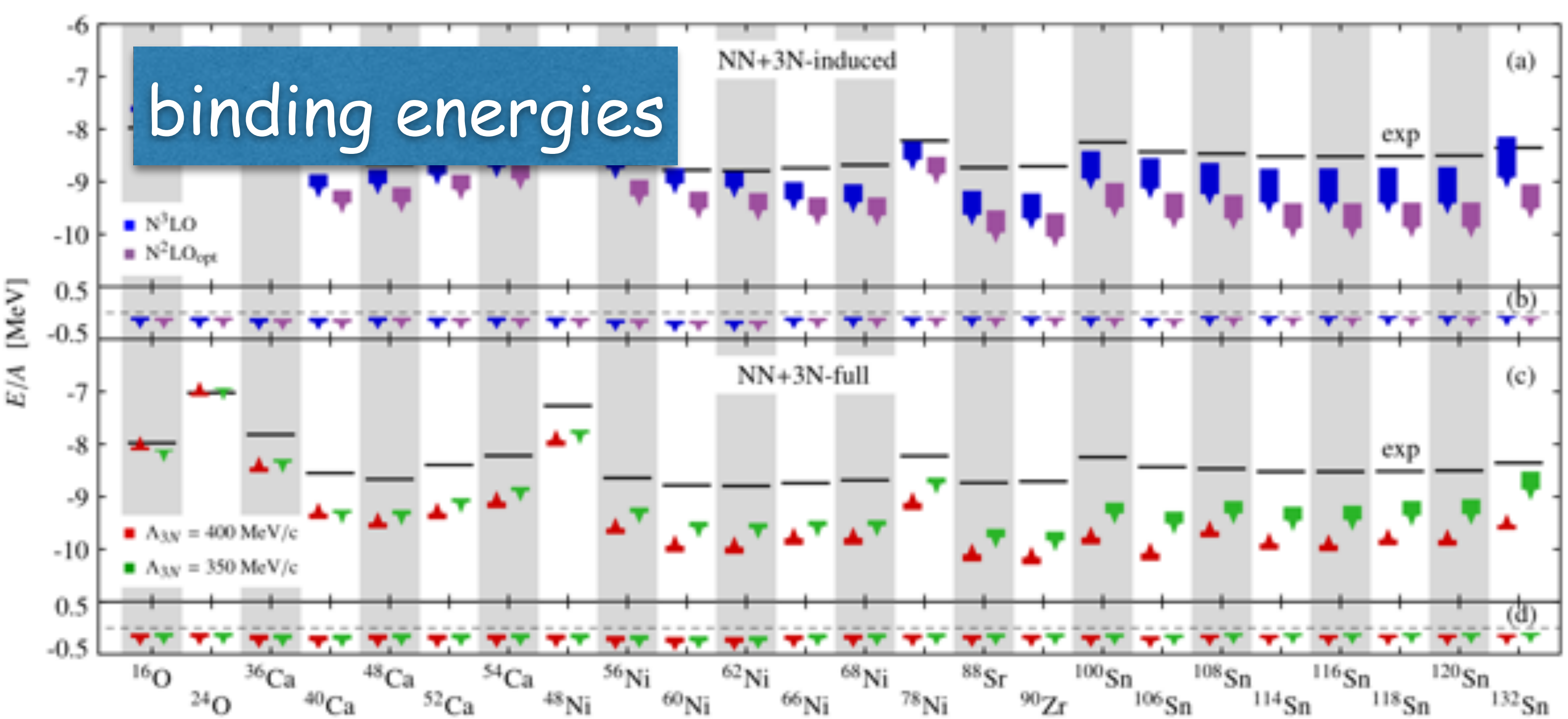

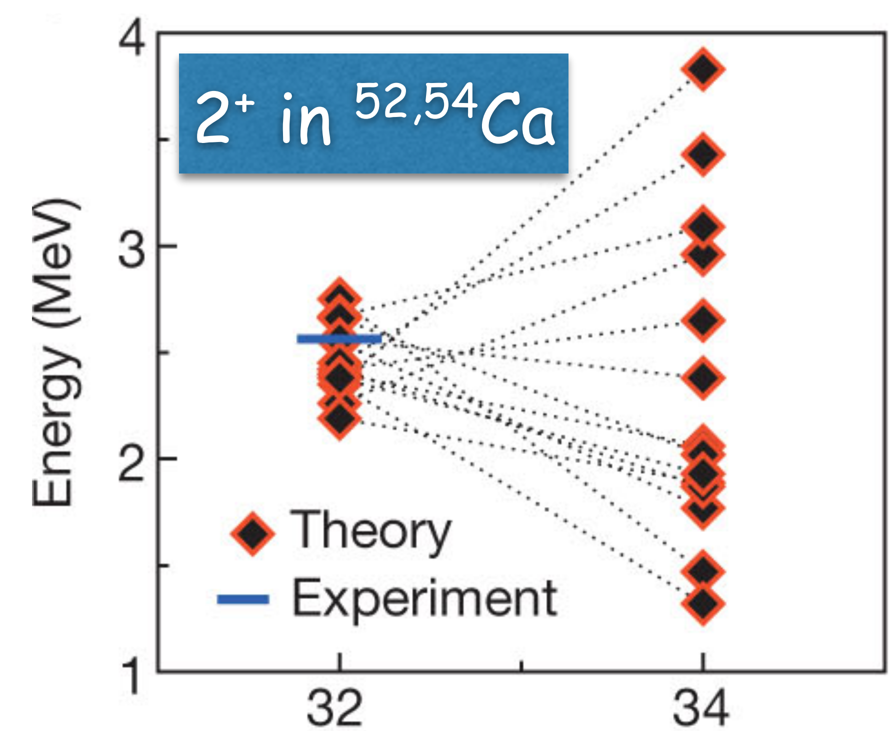

S. Binder et al. Phys. Lett. B 736, 119 (2014)

D. Steppenbeck et al. Nature 502 , 207-210 (2013)

what goes wrong: *radii, binding energies, spectra, …*

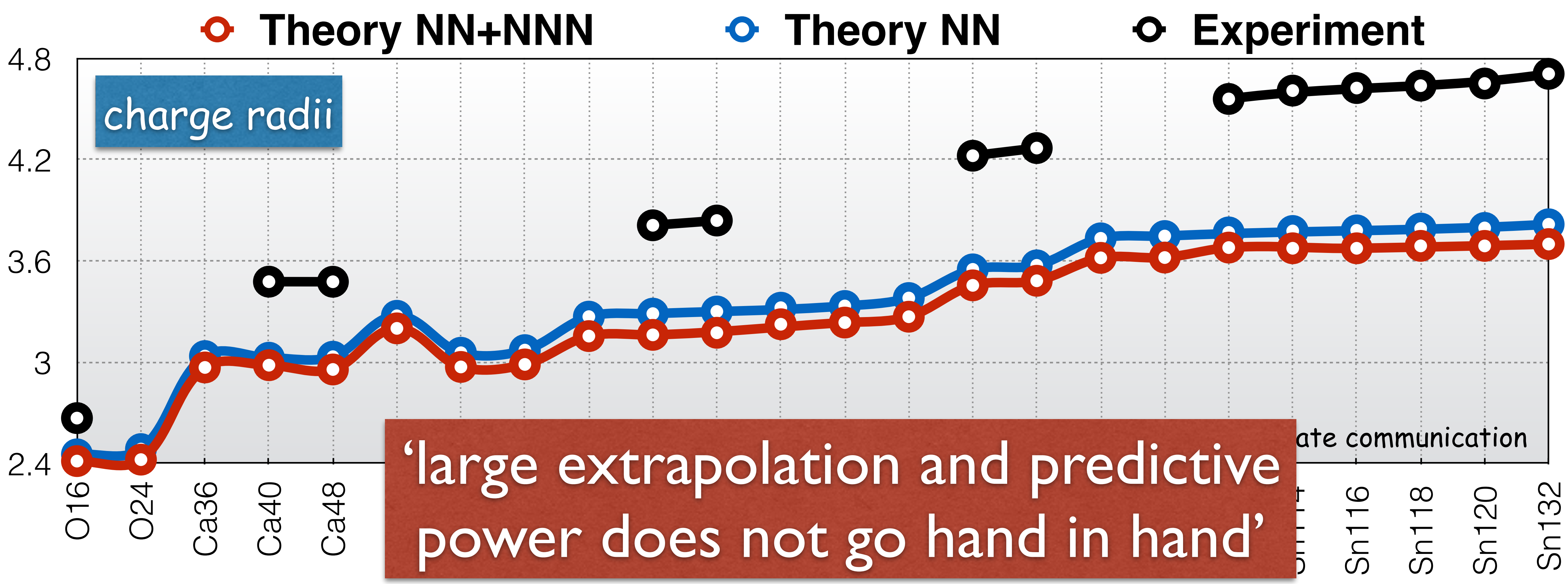

‘large extrapolation and predictive power does not go hand in hand’

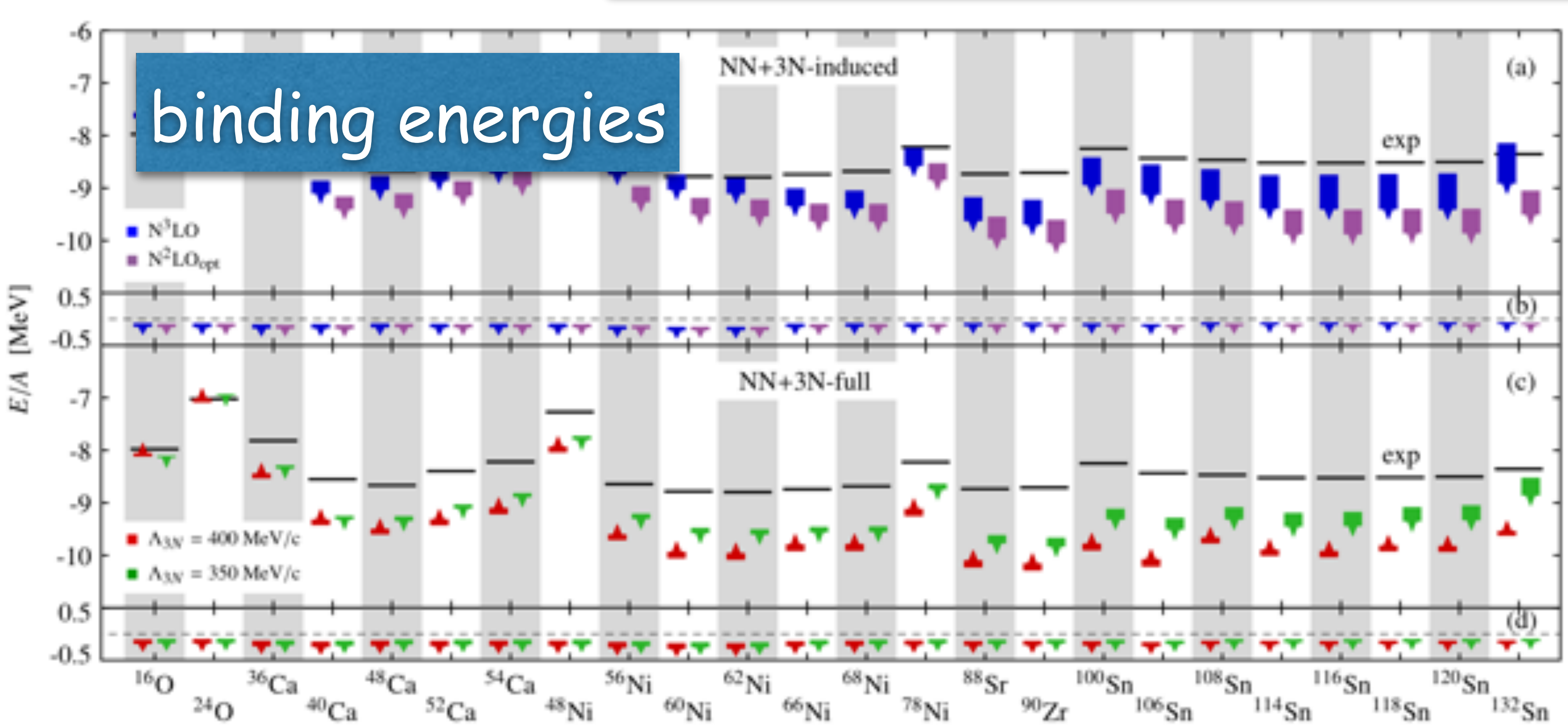

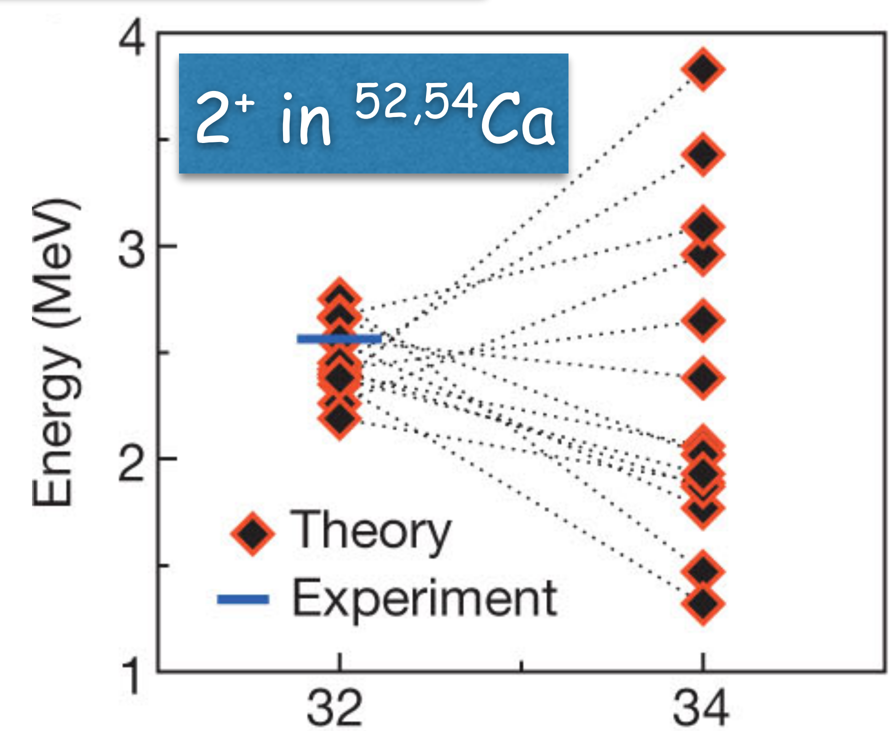

S. Binder et al. Phys. Lett. B 736, 119 (2014)

D. Steppenbeck et al. Nature 502 , 207-210 (2013)

NNLO$_{\text{sat(uration)}}$ and *"in-medium optimization": design*

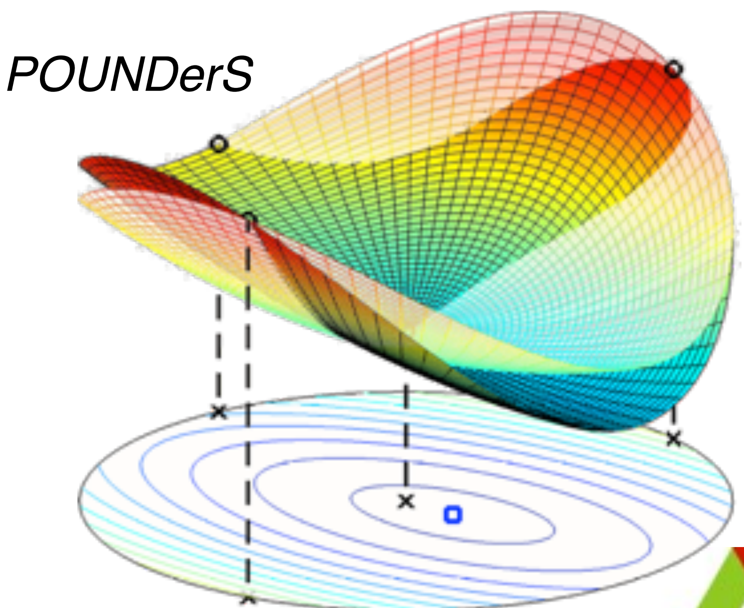

Argonne
NATIONAL LABORATORY

Interaction: NN+3NF(non-local) NNLO cutoff=450 MeV

Optimization: vary all LECs in NN+3NF simultaneously

Design goal: describe binding energies and radii for A=2, 3, 4, p-shell, and sd-shell

$$\min_{\vec{x}} \left[f(\vec{x}) = \sum_{q=1}^{N} \left(\frac{O(\vec{x})_q - O_q^{\exp}}{w_q} \right)^2 \right]$$

AE et al. accepted PRC(R)

NNLO$_{\text{sat(uration)}}$ and *"in-medium optimization"*: *design*

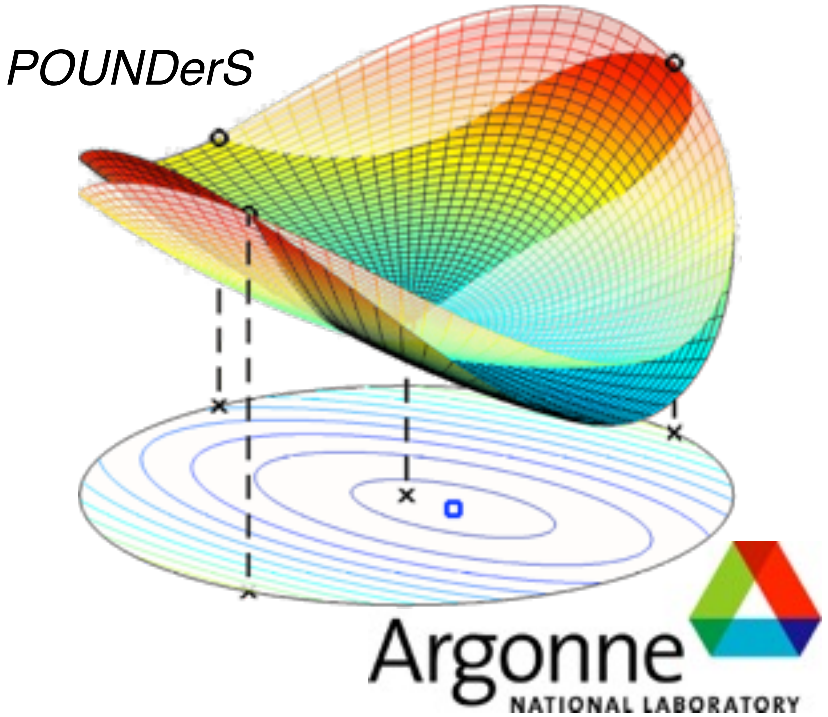

Interaction: NN+3NF(non-local) NNLO cutoff=450 MeV

Optimization: vary all LECs in NN+3NF simultaneously

Design goal: describe binding energies and radii for A=2, 3, 4, p-shell, and sd-shell

$$\min_{\vec{x}} \left[f(\vec{x}) = \sum_{q=1}^{N} \left(\frac{O(\vec{x})_q - O_q^{\exp}}{w_q} \right)^2 \right]$$

Nucleon-nucleon scattering data up to Tlab=35 MeV

Scattering lengths and effective ranges in the $^1S_0$ channels

NCSM and CCSD(Nmax=8) solutions of binding energies and charge radii for a selected set of light nuclei

AE et al. accepted PRC(R)

NNLO$_{\mathrm{sat(uration)}}$ and *"in-medium optimization"*: *design*

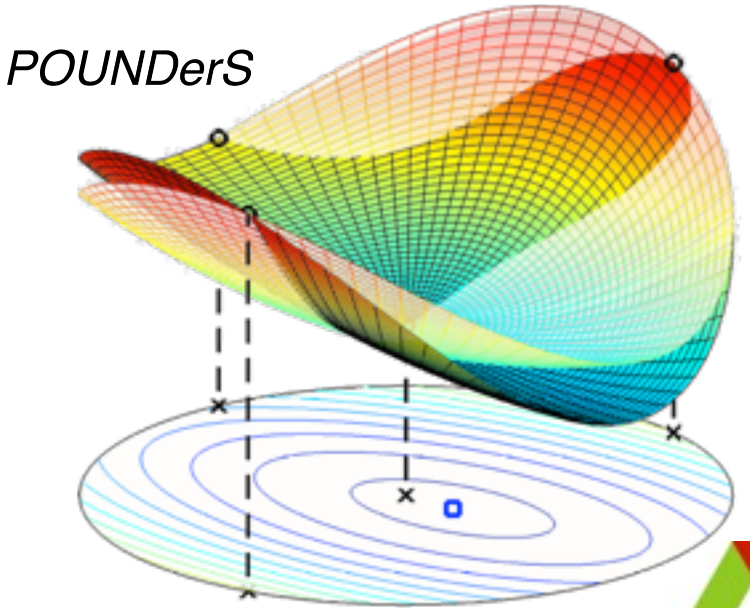

Interaction: NN+3NF(non-local) NNLO cutoff=450 MeV

Optimization: vary all LECs in NN+3NF simultaneously

Design goal: describe binding energies and radii for A=2, 3, 4, p-shell, and sd-shell

$$\min_{\vec{x}} \left[f(\vec{x}) = \sum_{q=1}^{N} \left(\frac{O(\vec{x})_q - O_q^{\mathrm{exp}}}{w_q} \right)^2 \right]$$

Nucleon-nucleon scattering data up to Tlab=35 MeV

Scattering lengths and effective ranges in the $^1S_0$ channels

NCSM and CCSD(Nmax=8) solutions of binding energies and charge radii for a selected set of light nuclei

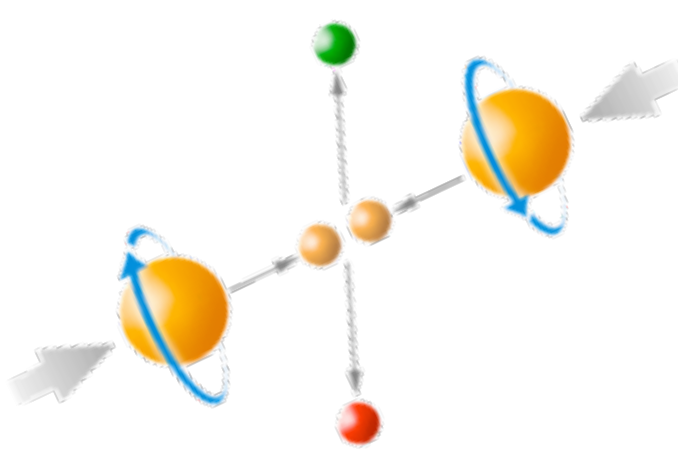

AE et al. accepted PRC(R)

NNLO$_{\mathrm{sat(uration)}}$ and *"in-medium optimization"*: *design*

POUNDerS

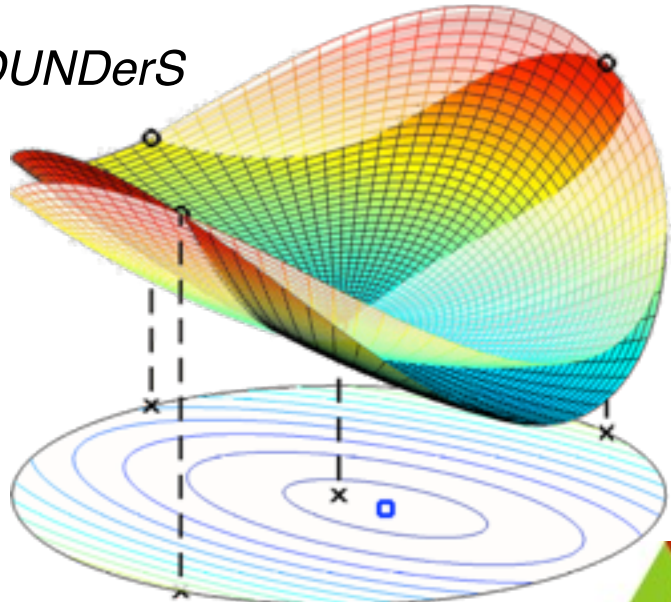

Argonne NATIONAL LABORATORY

Interaction: NN+3NF(non-local) NNLO cutoff=450 MeV

Optimization: vary all LECs in NN+3NF simultaneously

Design goal: describe binding energies and radii for A=2, 3, 4, p-shell, and sd-shell

$$\min_{\vec{x}} \left[f(\vec{x}) = \sum_{q=1}^{N} \left(\frac{O(\vec{x})_q - O_q^{\exp}}{w_q} \right)^2 \right]$$

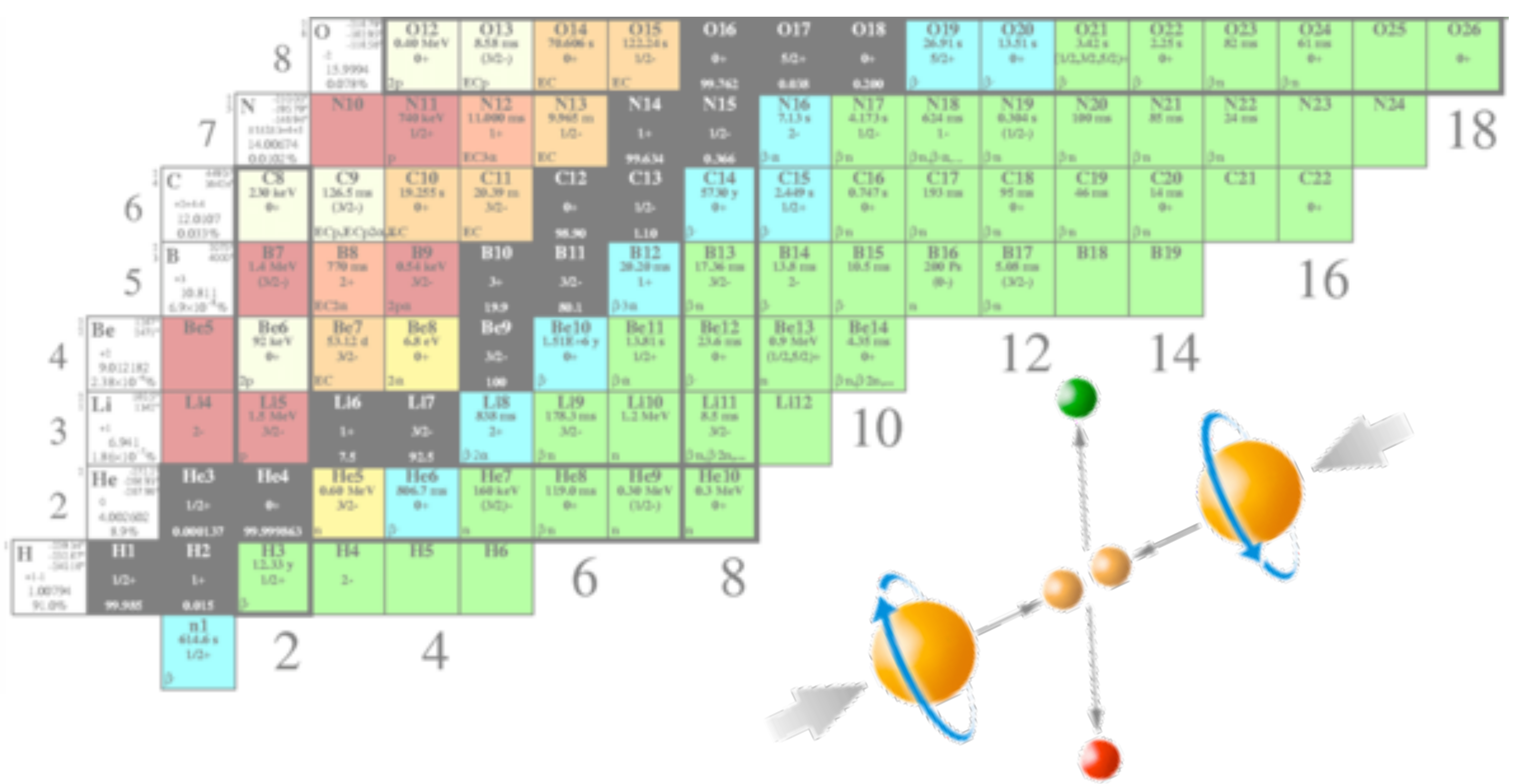

Nucleon-nucleon scattering data up to Tlab=35 MeV

Scattering lengths and effective ranges in the $^1S_0$ channels

NCSM and CCSD(Nmax=8) solutions of binding energies and charge radii for a selected set of light nuclei

AE et al. accepted PRC(R)

in-medium optimization: implementation

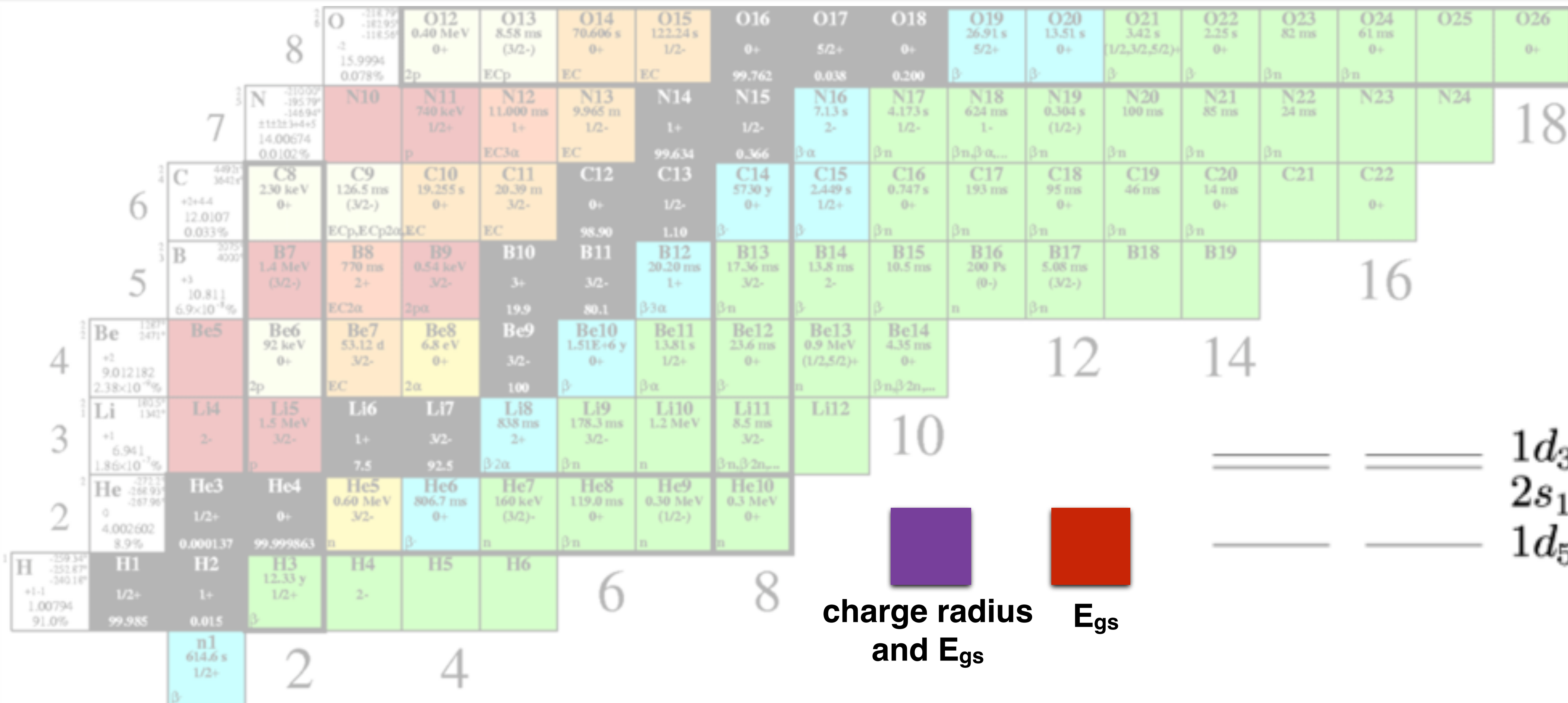

charge radius and E_{gs}

E_{gs}

No-Core Shell Model

- Nmax=40/20
- hw=36 MeV

Coupled Cluster

- 3NF in NO2B
- Nmax=8
- hw=22 MeV

for each iteration (3 min) calculate…

…NN-scattering observables and effective ranges

…NCSM results for A=2,3,4 nuclei.

…CCSD results for A=14,16,22,24,25 nuclei.
A nucleus-dependent estimates was employed to account for the effects of a larger model spaces and triples-cluster corrections

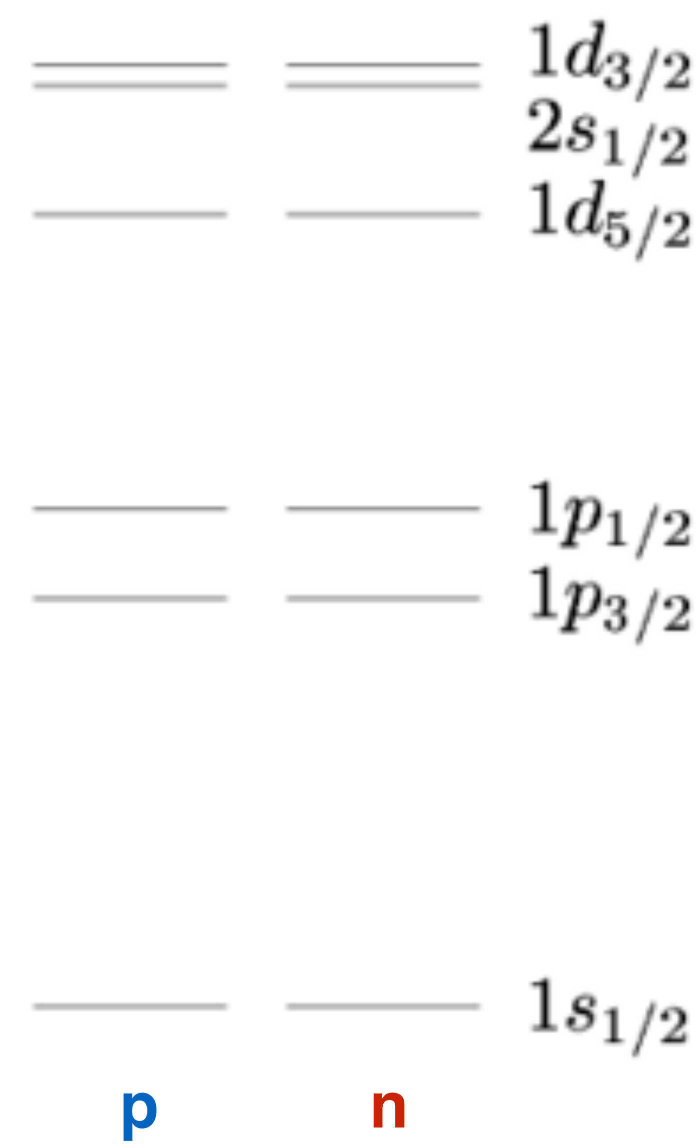

in-medium optimization: implementation

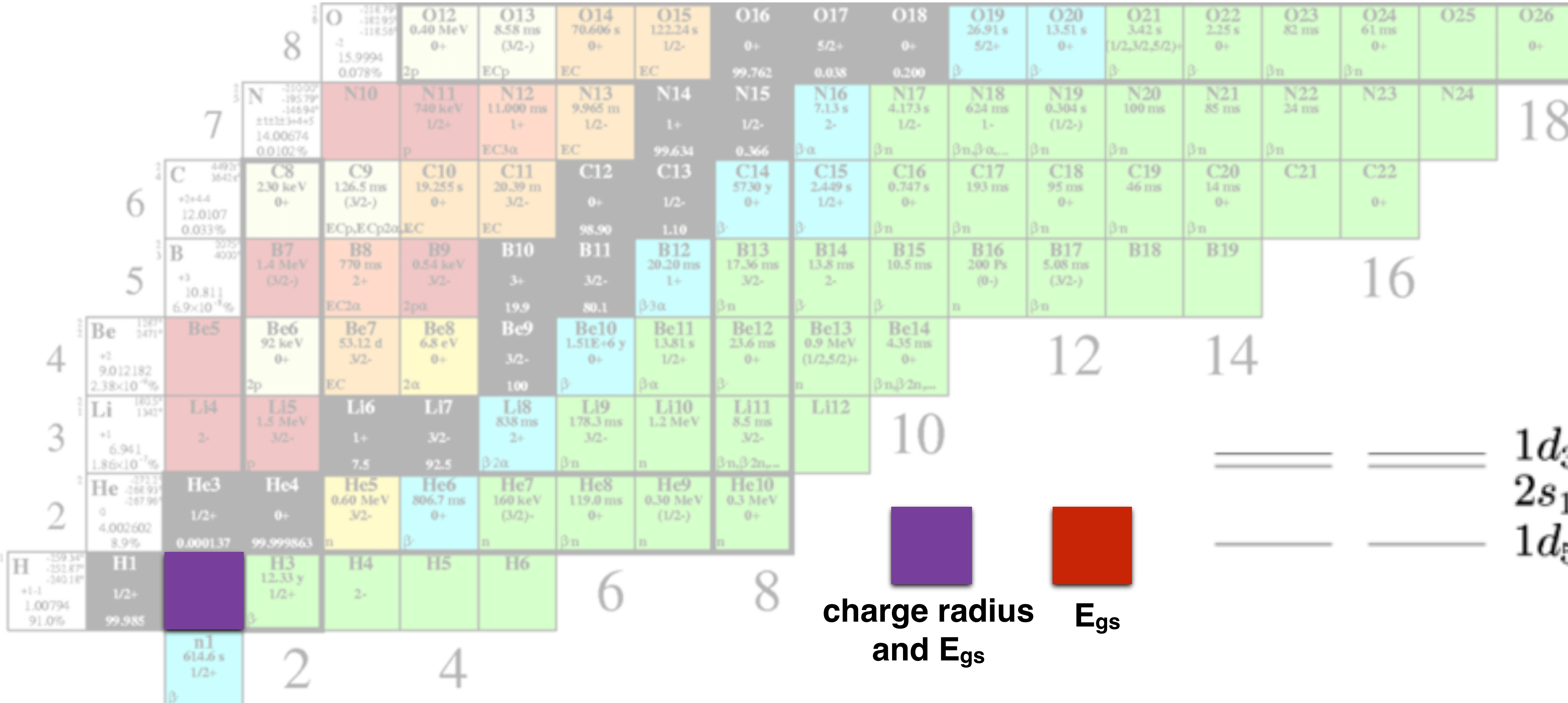

No-Core Shell Model
- Nmax=40/20
- hw=36 MeV

Coupled Cluster
- 3NF in NO2B
- Nmax=8
- hw=22 MeV

for each iteration (3 min) calculate…

…NN-scattering observables and effective ranges

…NCSM results for A=2,3,4 nuclei.

…CCSD results for A=14,16,22,24,25 nuclei.
A nucleus-dependent estimates was employed to account for the effects of a larger model spaces and triples-cluster corrections

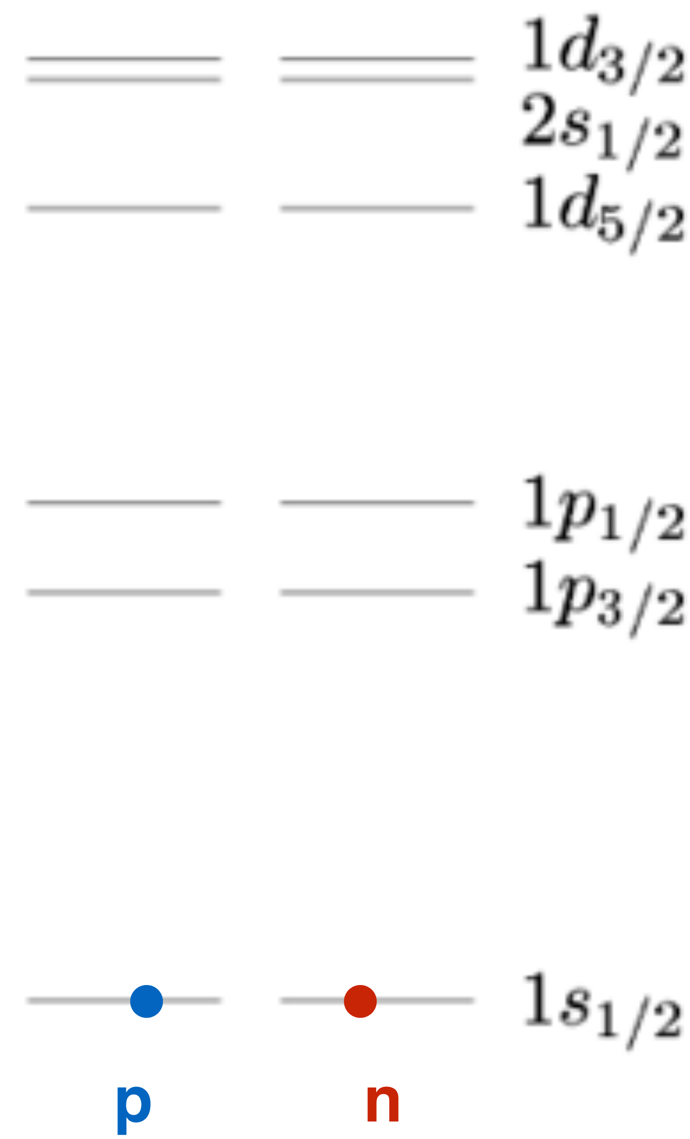

in-medium optimization: implementation

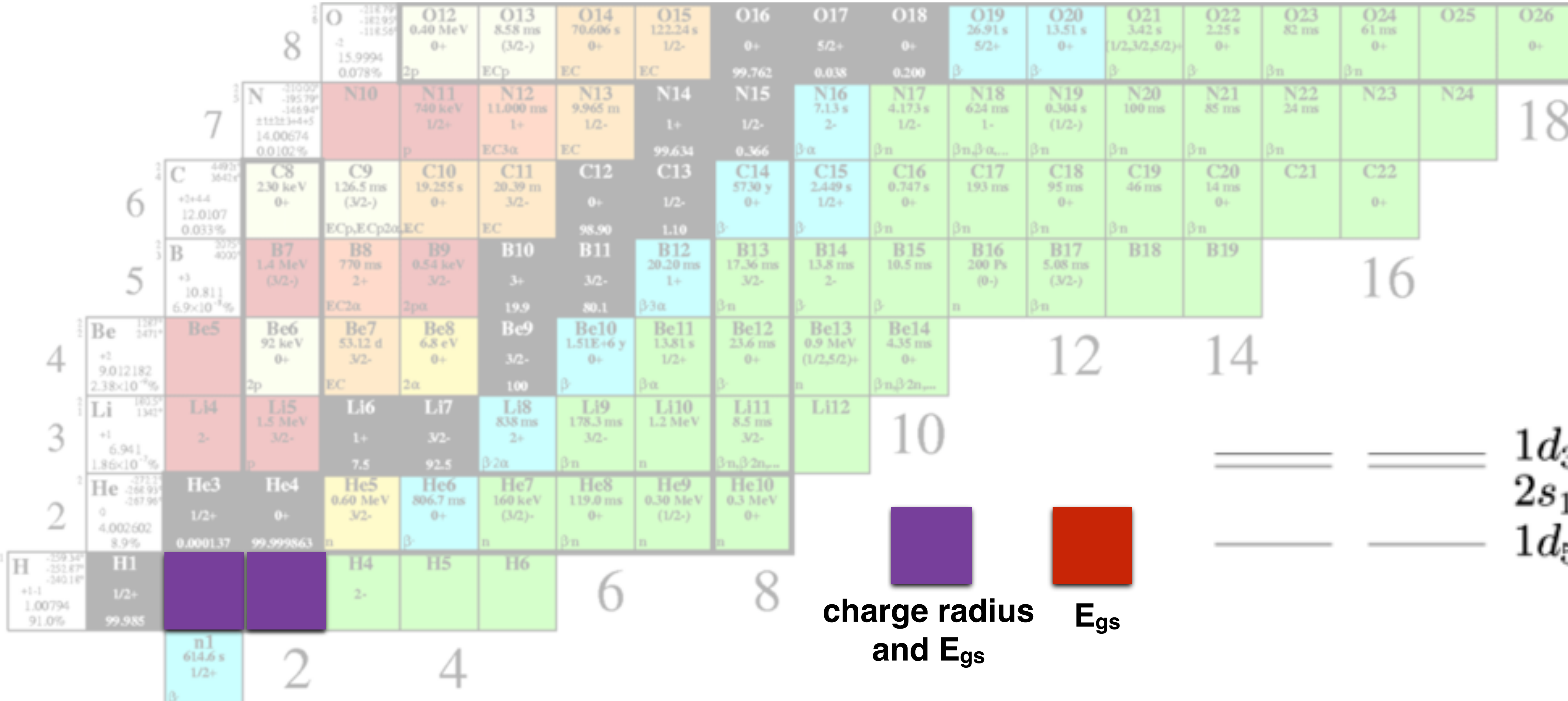

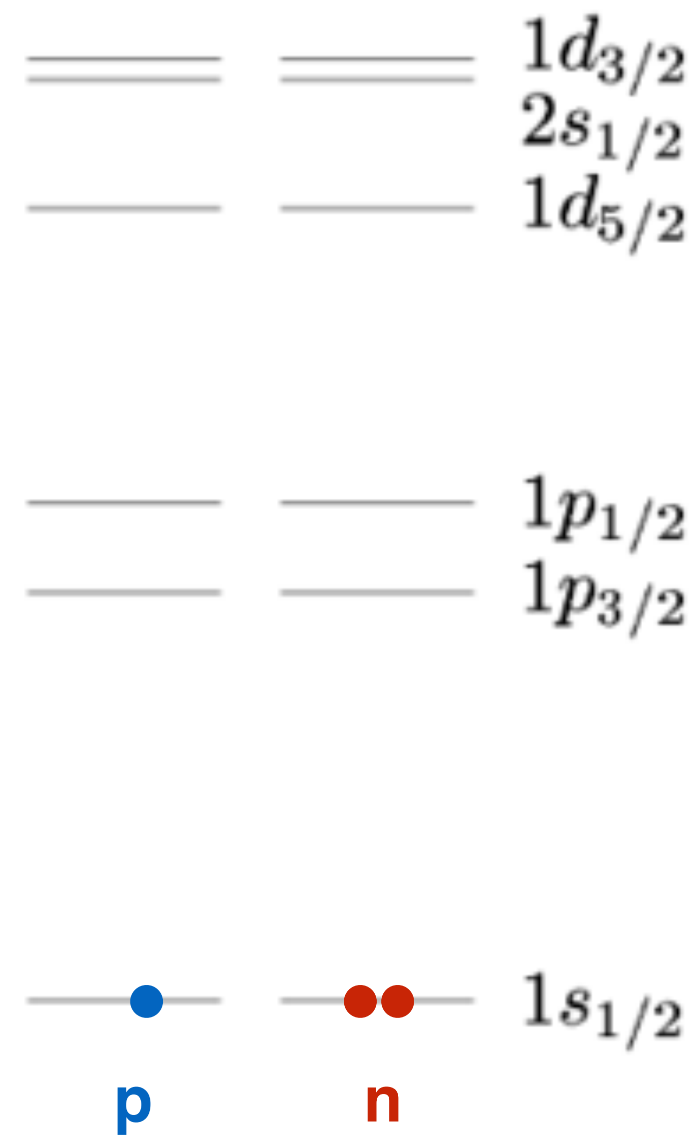

No-Core Shell Model
- Nmax=40/20
- hw=36 MeV

Coupled Cluster
- 3NF in NO2B
- Nmax=8
- hw=22 MeV

for each iteration (3 min) calculate…

…NN-scattering observables and effective ranges

…NCSM results for A=2,3,4 nuclei.

…CCSD results for A=14,16,22,24,25 nuclei.
A nucleus-dependent estimates was employed to account for the effects of a larger model spaces and triples-cluster corrections

in-medium optimization: implementation

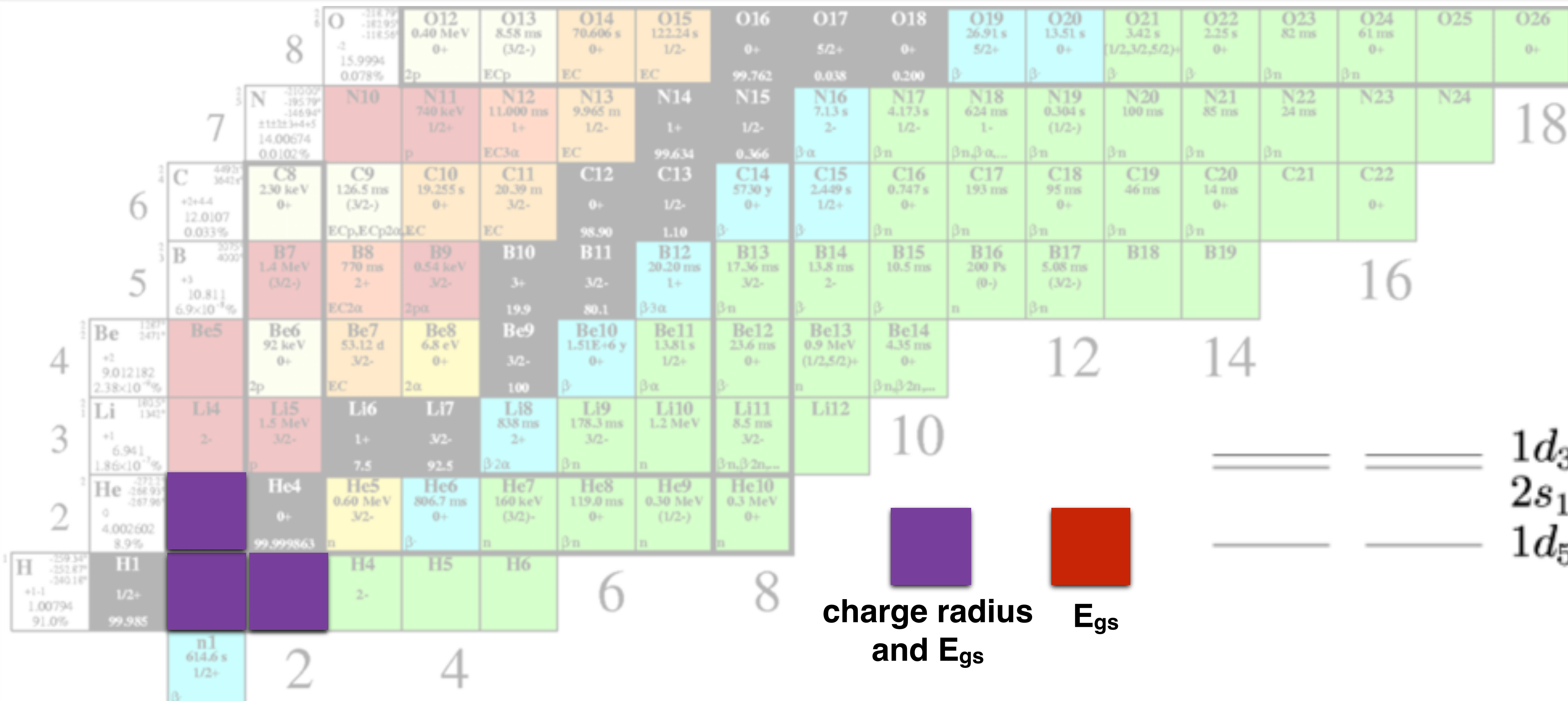

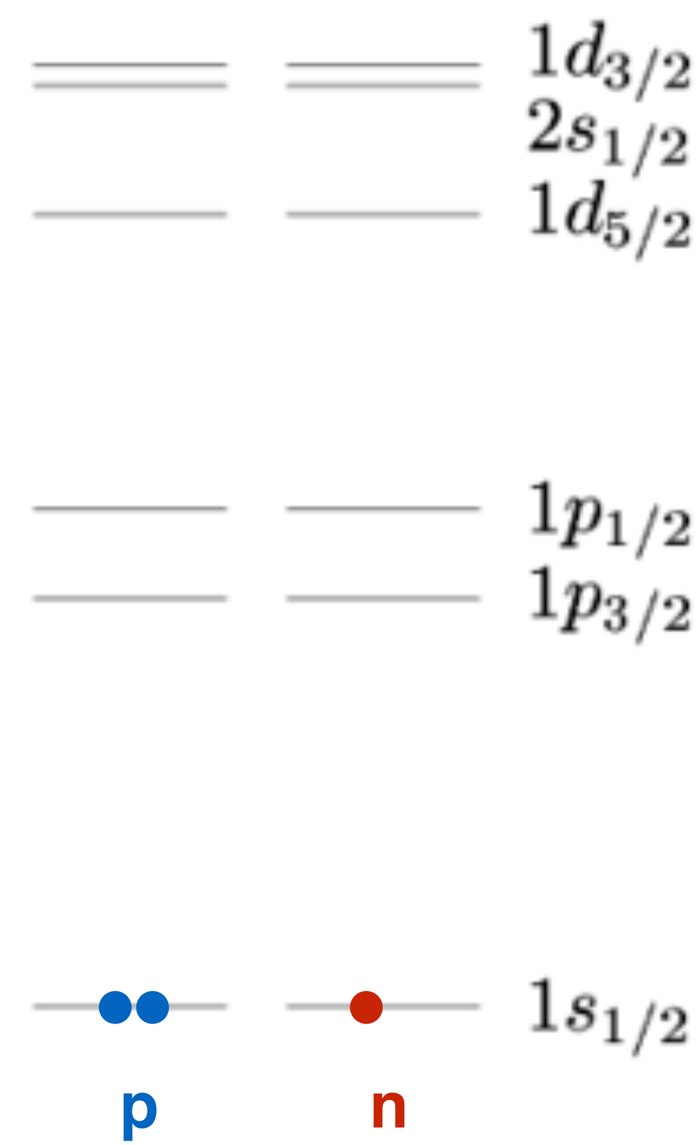

No-Core Shell Model
- Nmax=40/20
- hw=36 MeV

Coupled Cluster
- 3NF in NO2B
- Nmax=8
- hw=22 MeV

for each iteration (3 min) calculate…

…NN-scattering observables and effective ranges

…NCSM results for A=2,3,4 nuclei.

…CCSD results for A=14,16,22,24,25 nuclei.
A nucleus-dependent estimates was employed to account for the effects of a larger model spaces and triples-cluster corrections

in-medium optimization: implementation

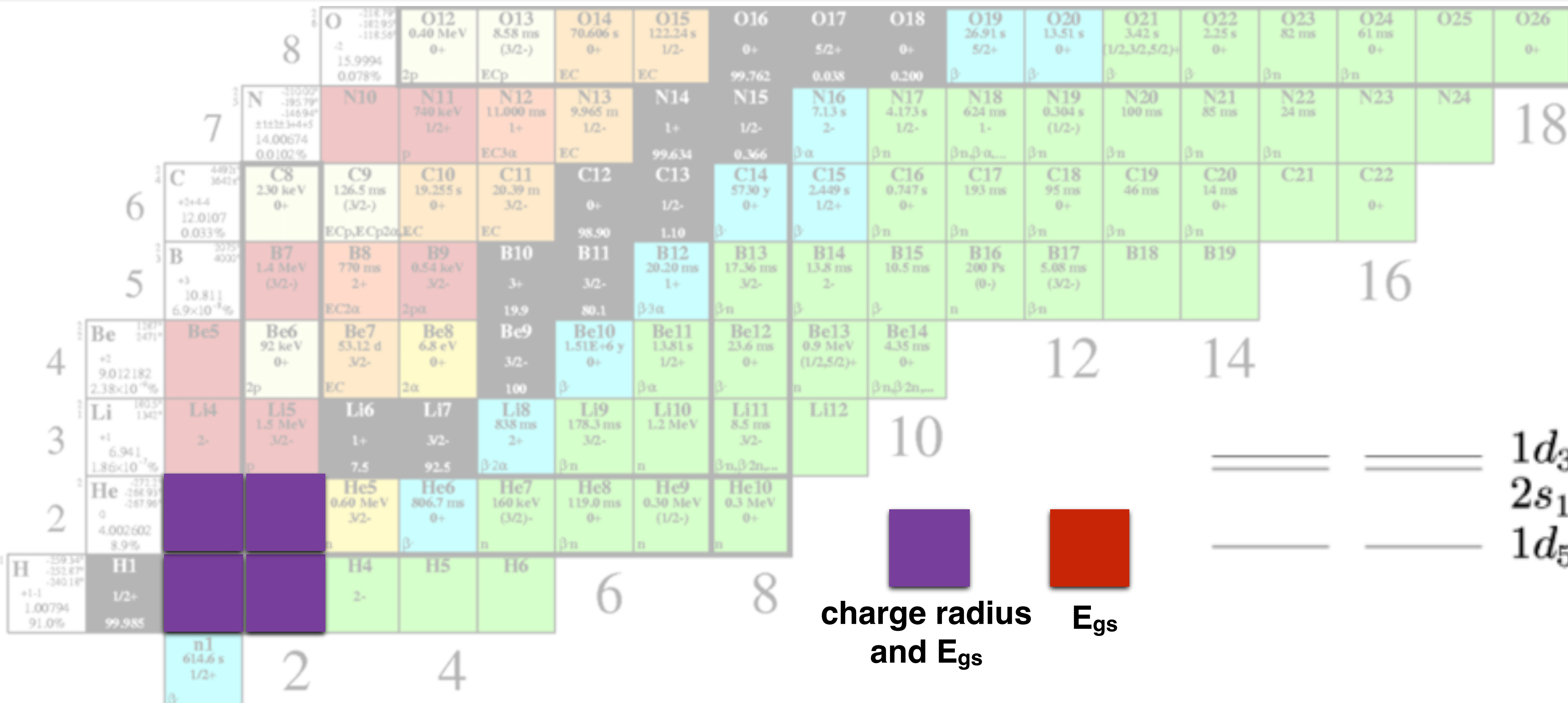

No-Core Shell Model
- Nmax=40/20
- hw=36 MeV

Coupled Cluster
- 3NF in NO2B
- Nmax=8
- hw=22 MeV

for each iteration (3 min) calculate…

…NN-scattering observables and effective ranges

…NCSM results for A=2,3,4 nuclei.

…CCSD results for A=14,16,22,24,25 nuclei.
A nucleus-dependent estimates was employed to account for the effects of a larger model spaces and triples-cluster corrections

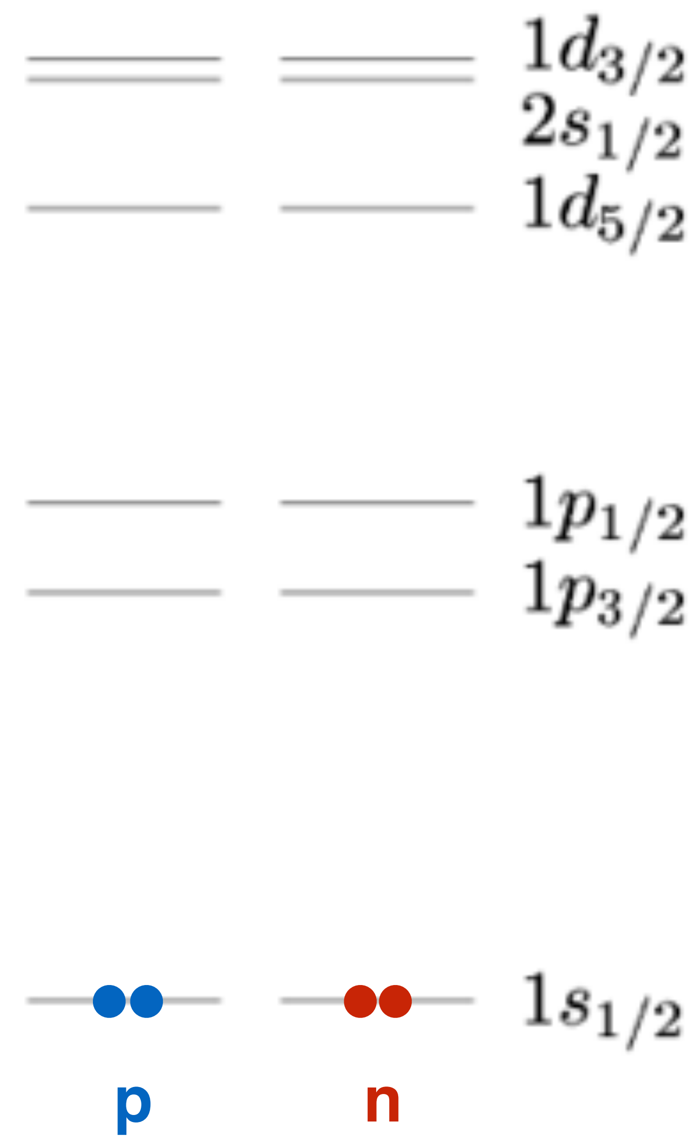

in-medium optimization: implementation

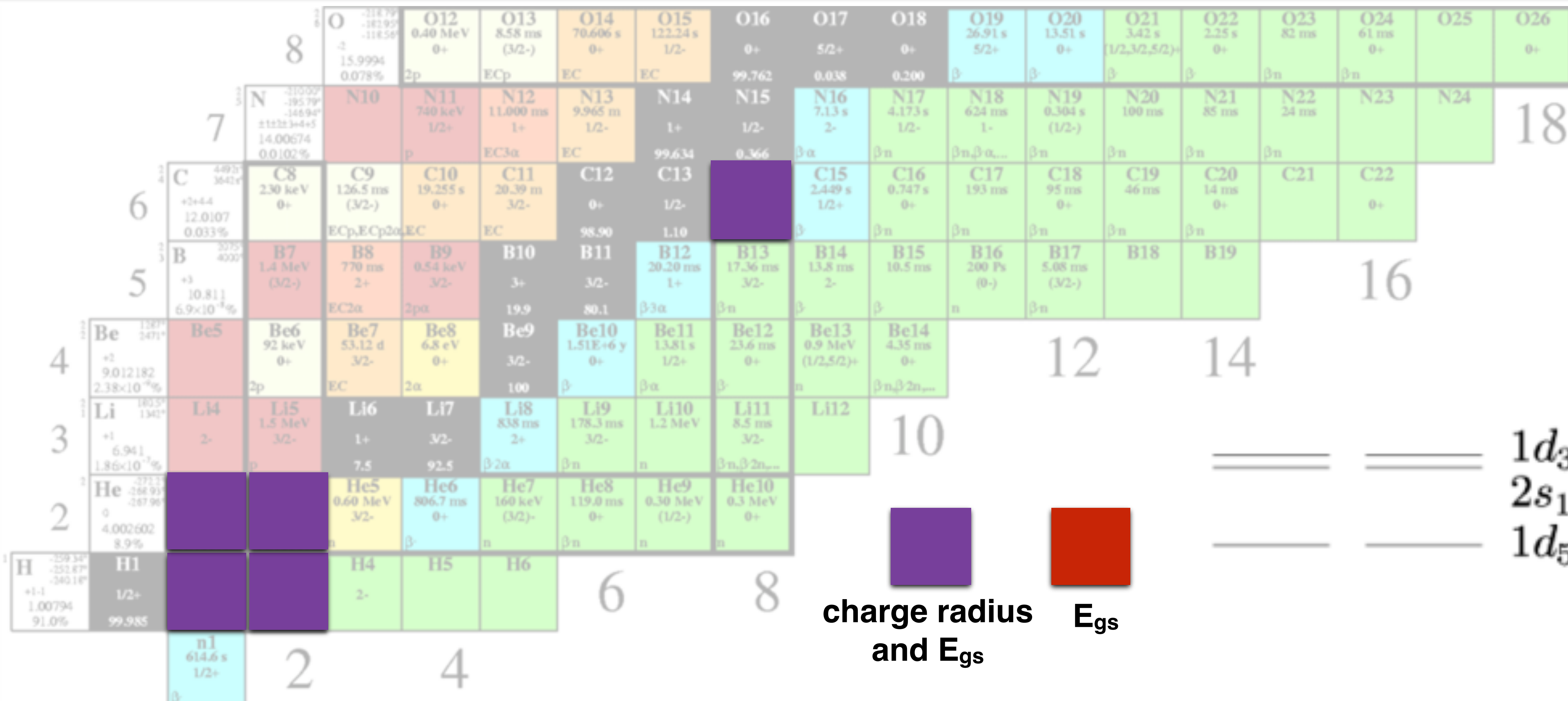

No-Core Shell Model
- Nmax=40/20
- hw=36 MeV

Coupled Cluster
- 3NF in NO2B
- Nmax=8
- hw=22 MeV

for each iteration (3 min) calculate…

…NN-scattering observables and effective ranges

…NCSM results for A=2,3,4 nuclei.

…CCSD results for A=14,16,22,24,25 nuclei.
A nucleus-dependent estimates was employed to account for the effects of a larger model spaces and triples-cluster corrections

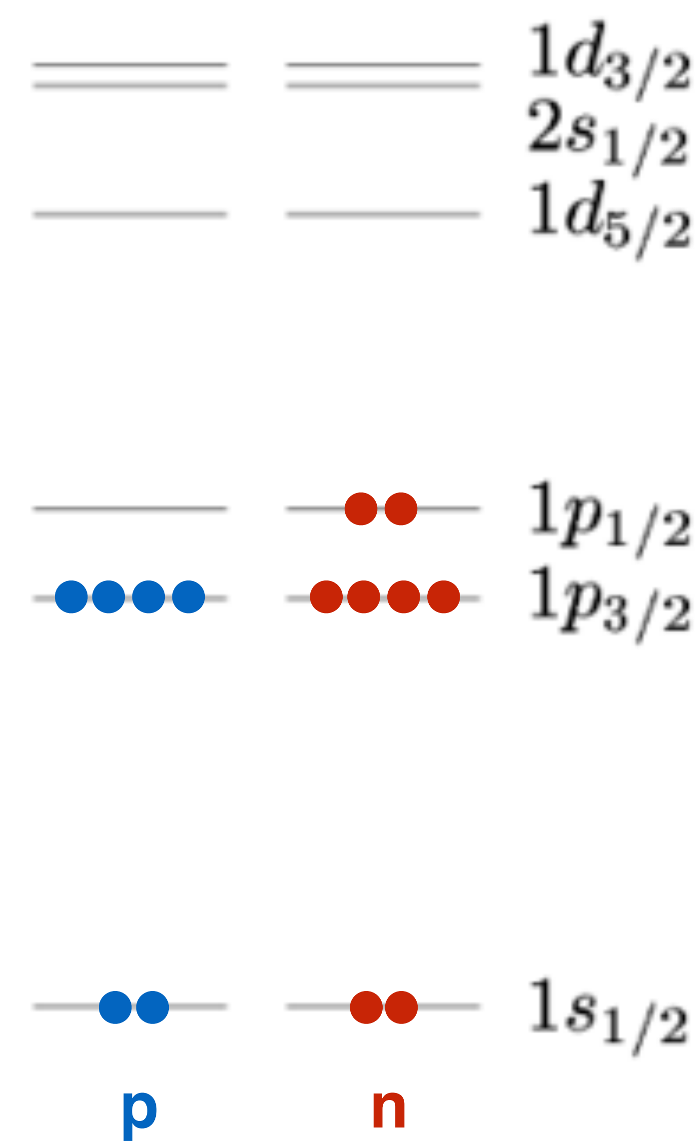

in-medium optimization: implementation

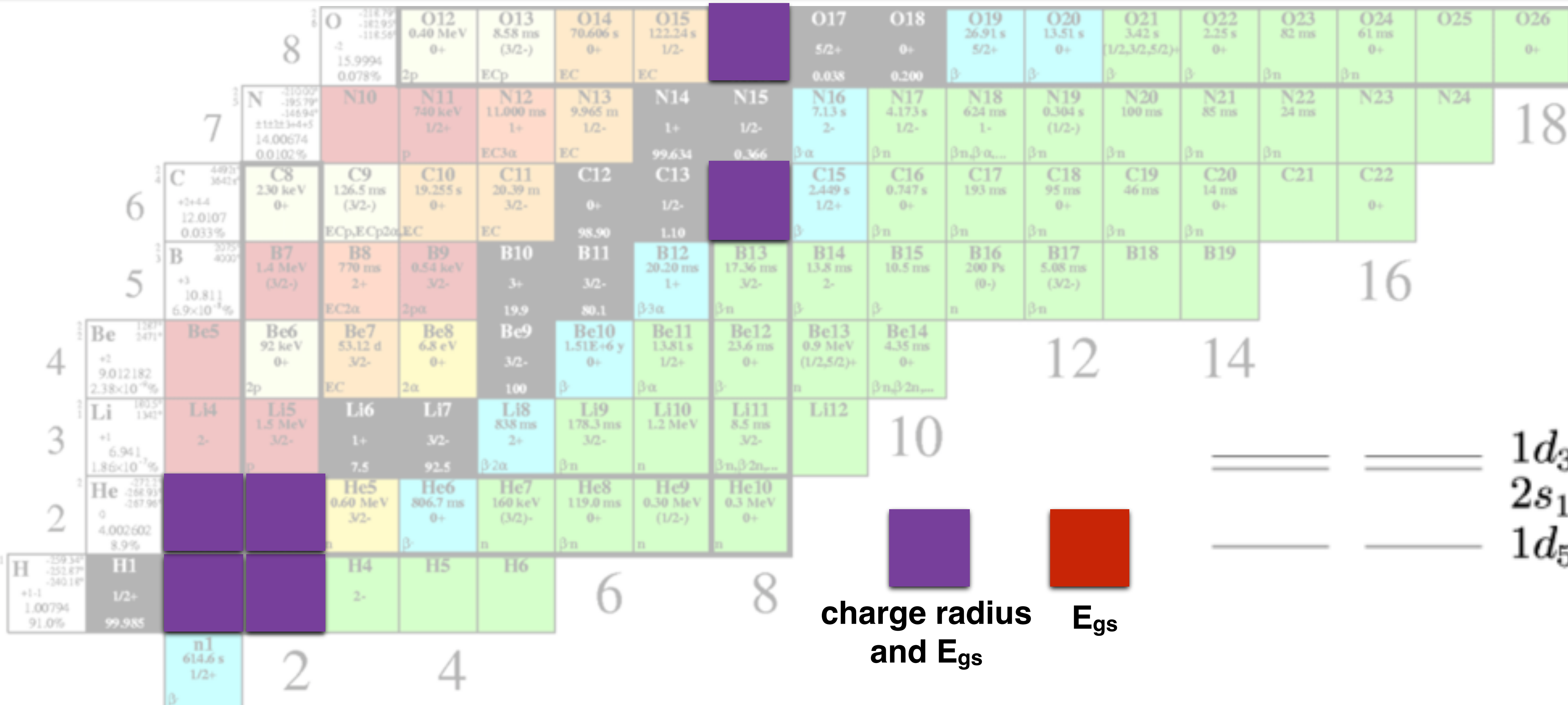

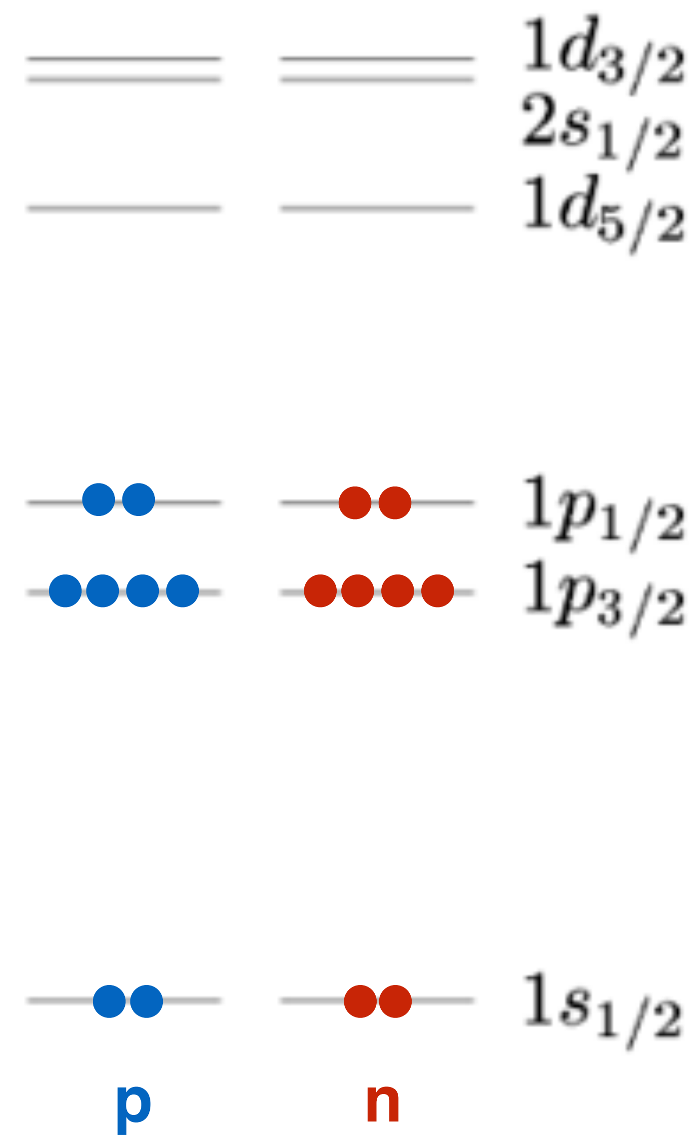

No-Core Shell Model
- Nmax=40/20
- hw=36 MeV

Coupled Cluster
- 3NF in NO2B
- Nmax=8
- hw=22 MeV

for each iteration (3 min) calculate…

…NN-scattering observables and effective ranges

…NCSM results for A=2,3,4 nuclei.

…CCSD results for A=14,16,22,24,25 nuclei.
A nucleus-dependent estimates was employed to account for the effects of a larger model spaces and triples-cluster corrections

in-medium optimization: implementation

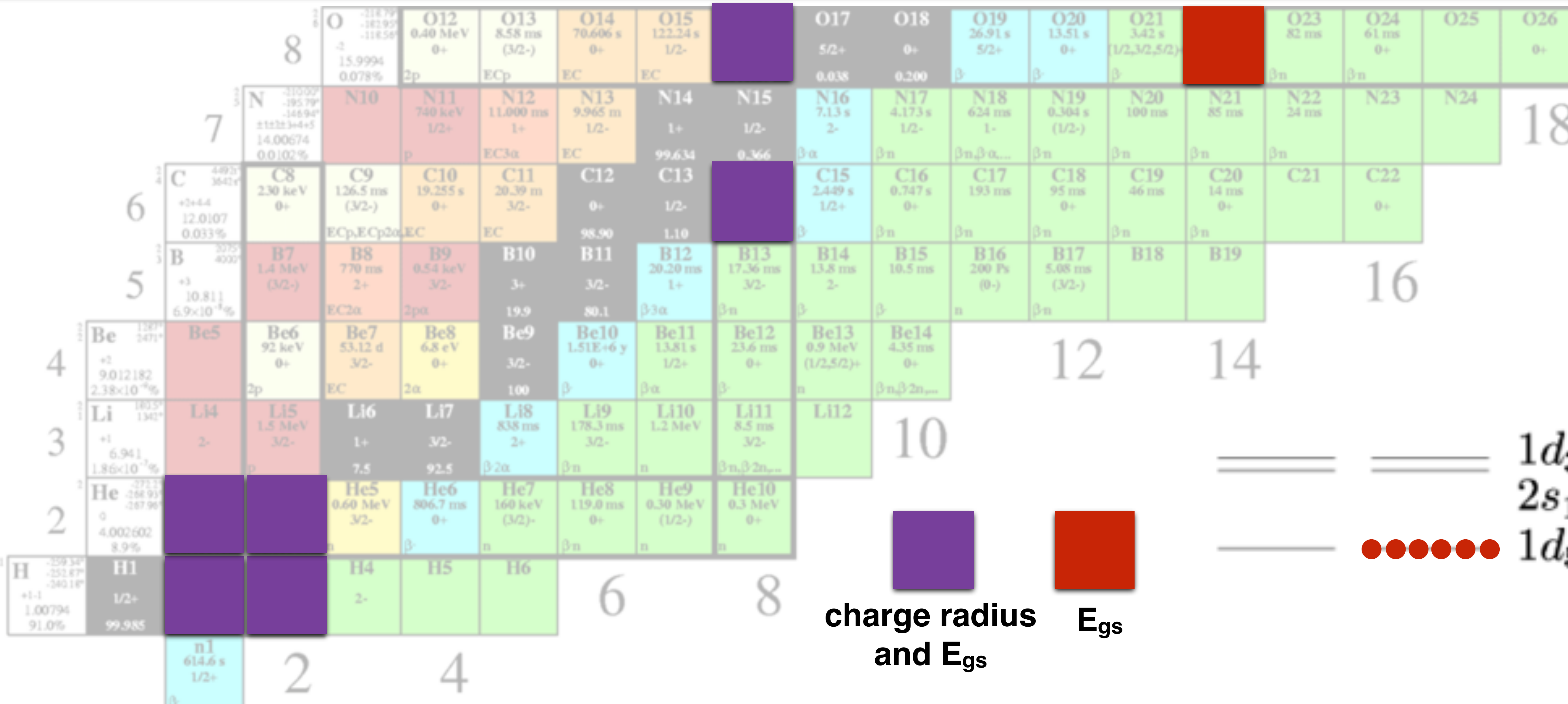

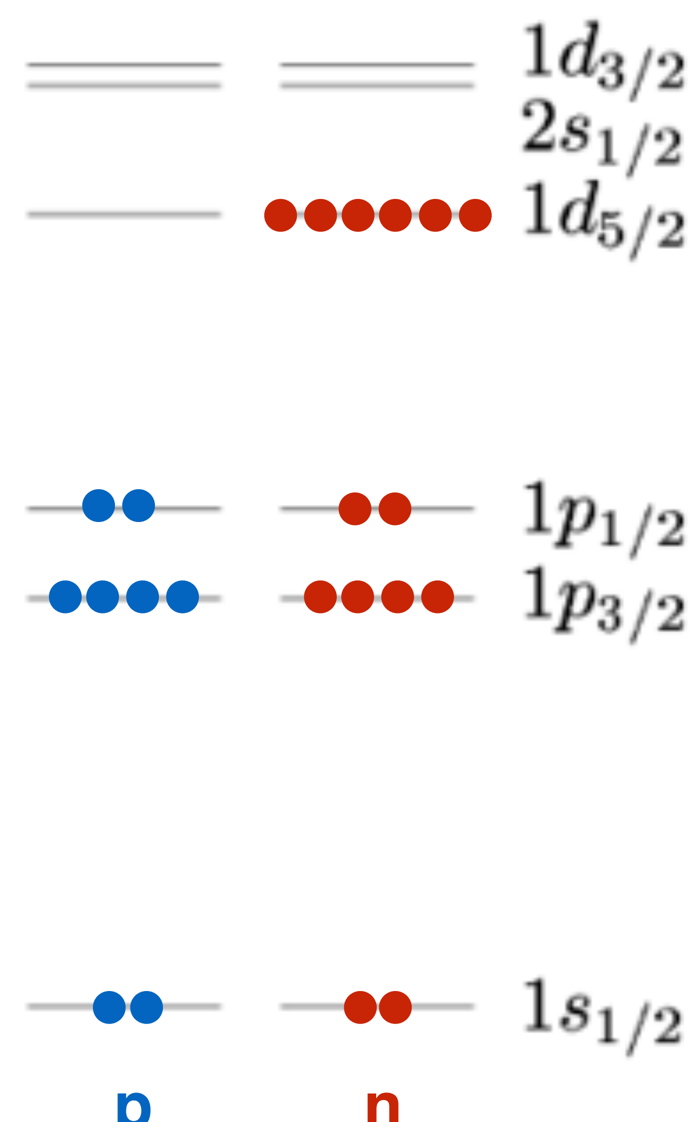

No-Core Shell Model
- Nmax=40/20
- hw=36 MeV

Coupled Cluster
- 3NF in NO2B
- Nmax=8
- hw=22 MeV

for each iteration (3 min) calculate…

…NN-scattering observables and effective ranges

…NCSM results for A=2,3,4 nuclei.

…CCSD results for A=14,16,22,24,25 nuclei.
A nucleus-dependent estimates was employed to account for the effects of a larger model spaces and triples-cluster corrections

in-medium optimization: implementation

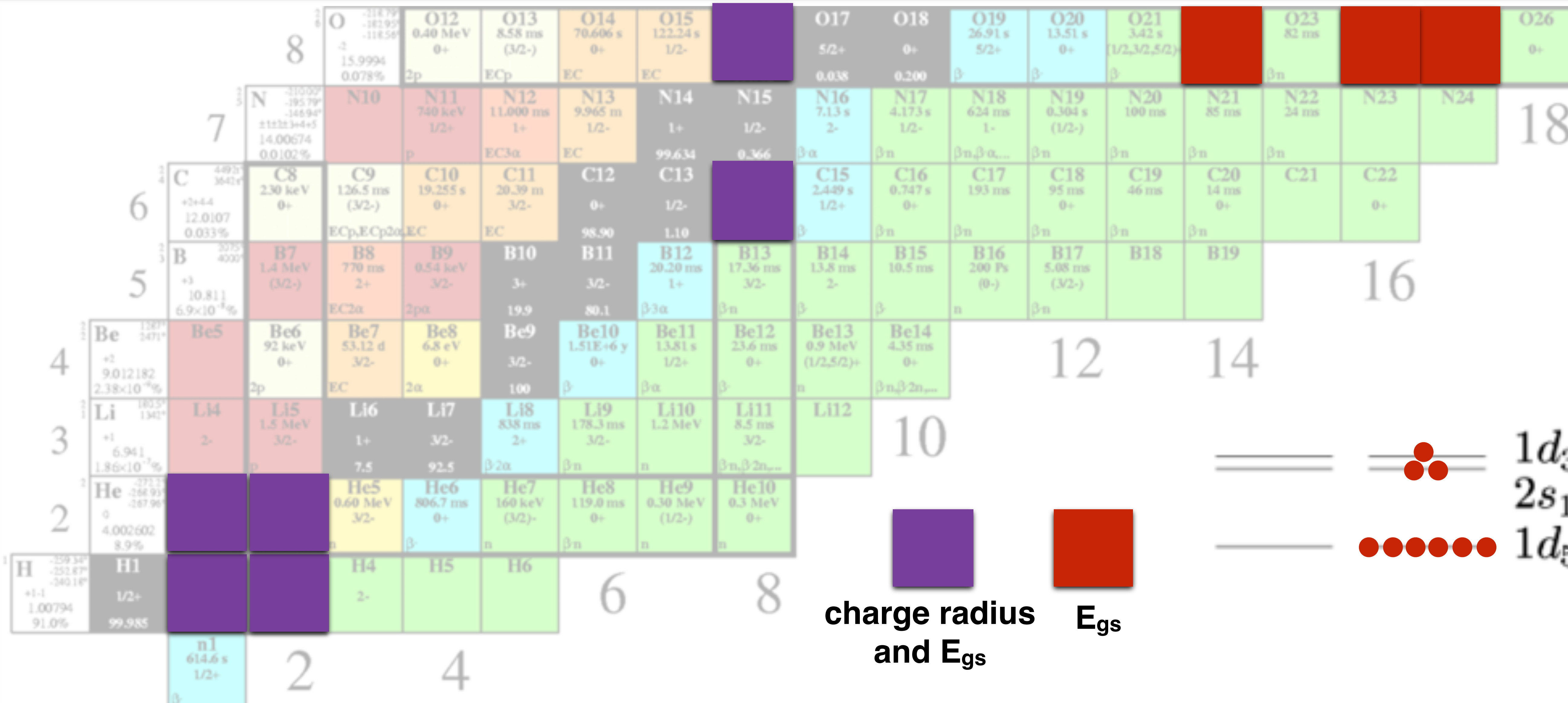

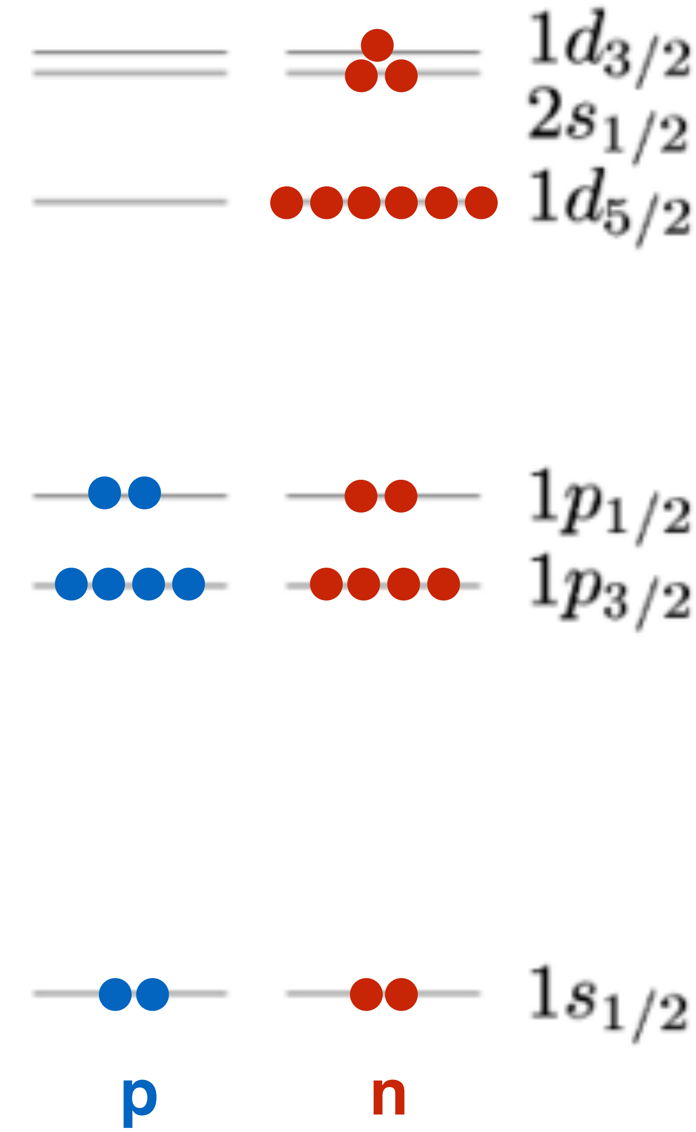

No-Core Shell Model
- Nmax=40/20
- hw=36 MeV

Coupled Cluster
- 3NF in NO2B
- Nmax=8
- hw=22 MeV

for each iteration (3 min) calculate…

…NN-scattering observables and effective ranges

…NCSM results for A=2,3,4 nuclei.

…CCSD results for A=14,16,22,24,25 nuclei.
A nucleus-dependent estimates was employed to account for the effects of a larger model spaces and triples-cluster corrections

in-medium optimization: implementation

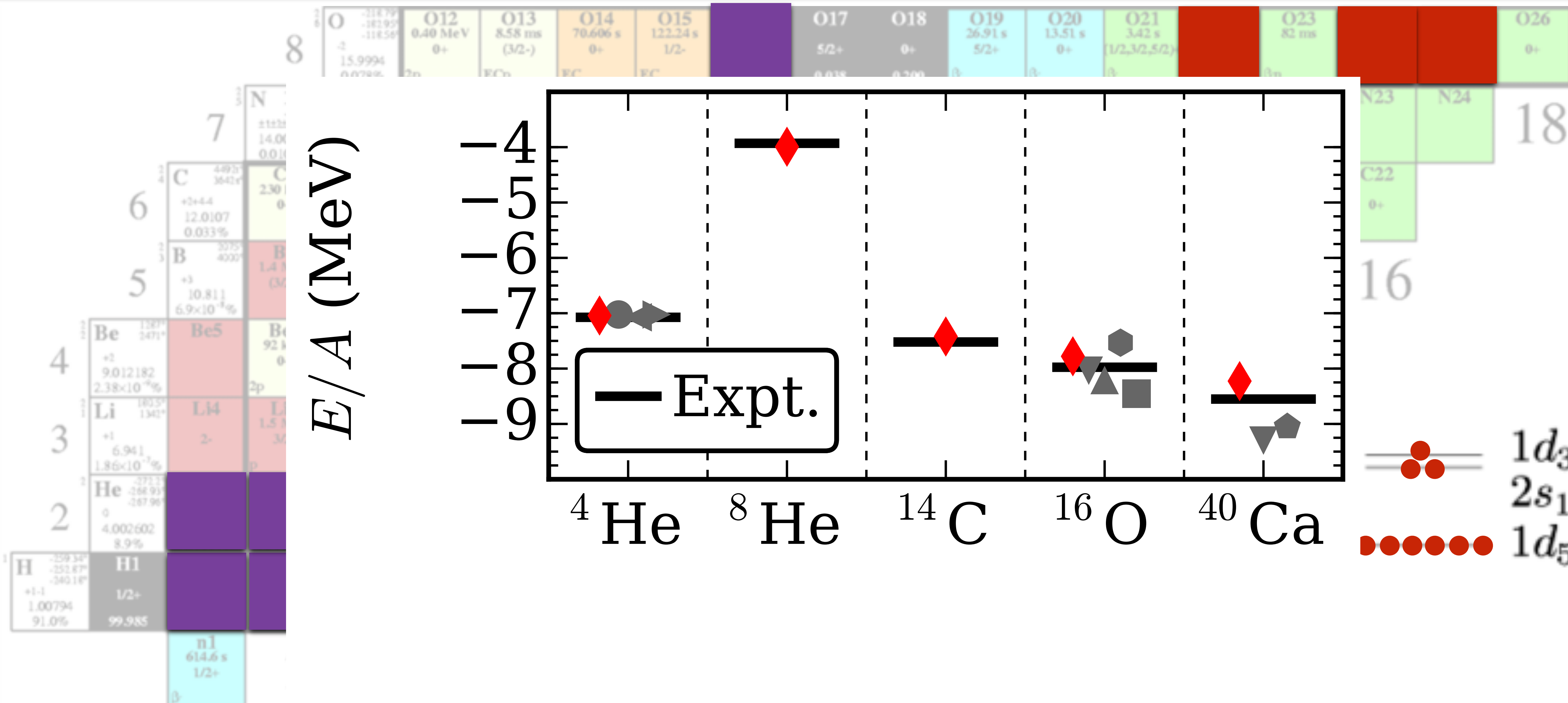

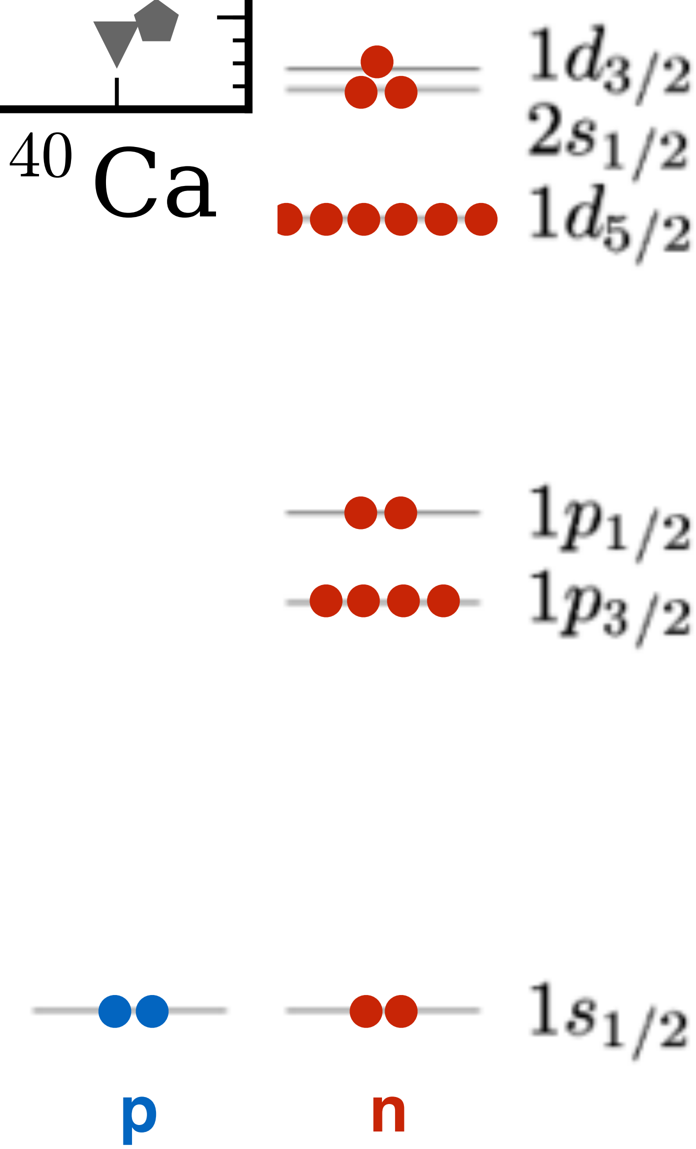

No-Core Shell Mo

- Nmax=40/2
- hw=36 MeV

Coupled Cluster

- 3NF in NO2B
- Nmax=8
- hw=22 MeV

A nucleus-dependent estimates was employed to account for the effects of a larger model spaces and triples-cluster corrections

in-medium optimization: implementation

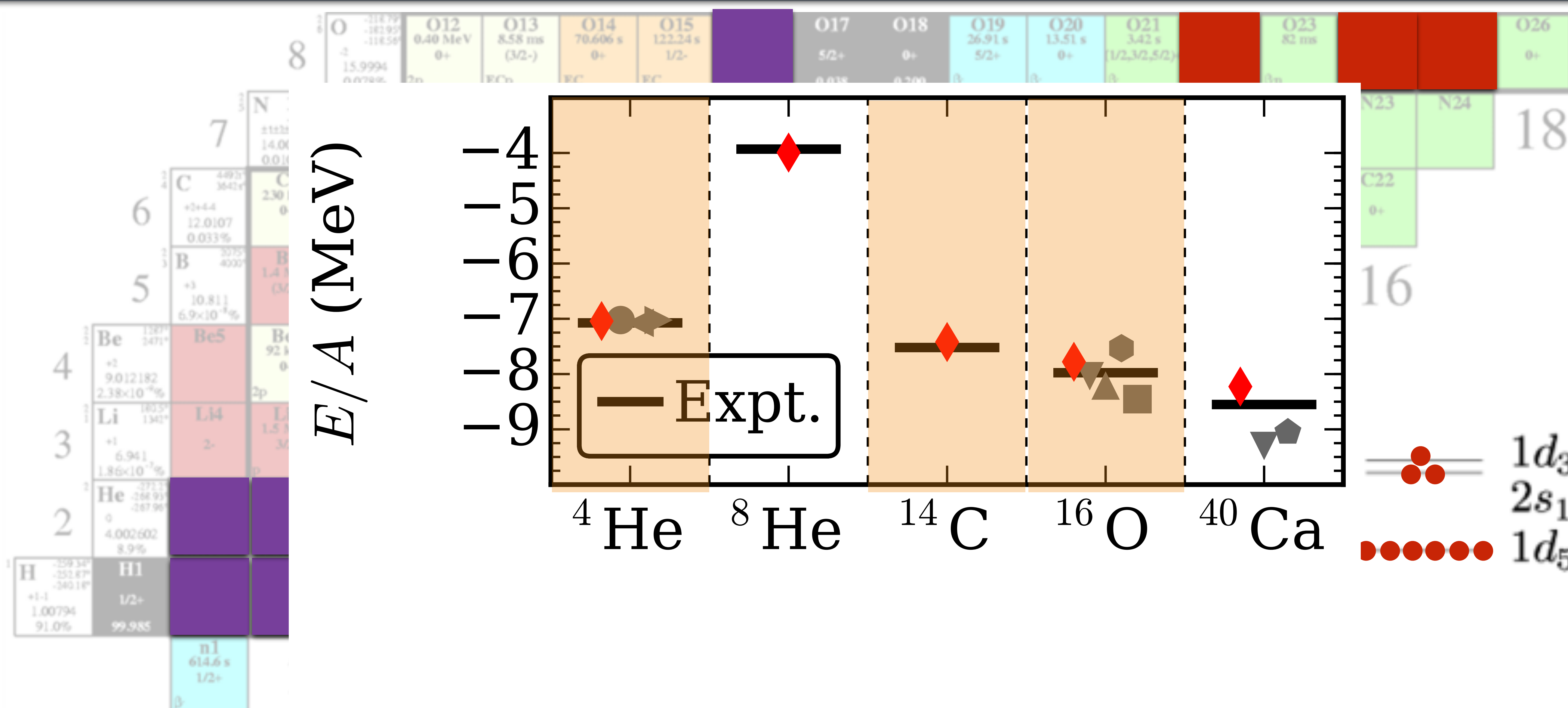

No-Core Shell M
- Nmax=40/2
- hw=36 MeV

Coupled Cluster
- 3NF in NO2B
- Nmax=8
- hw=22 MeV

A nucleus-dependent estimates was employed to account for the effects of a larger model spaces and triples-cluster corrections

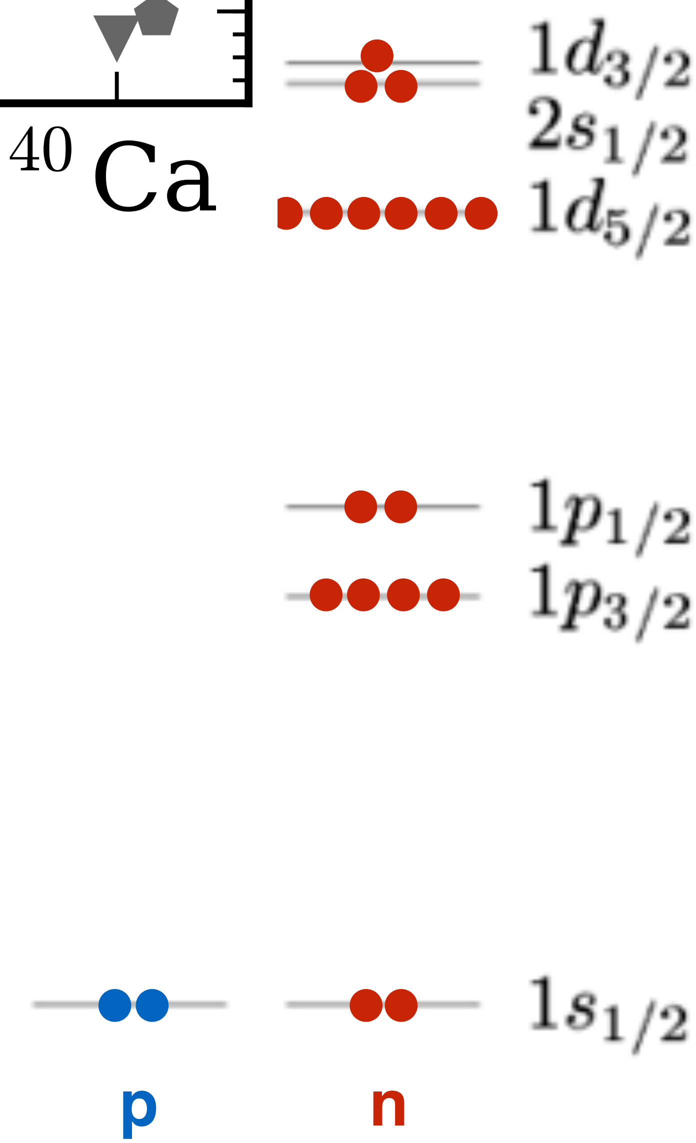

in-medium optimization: implementation

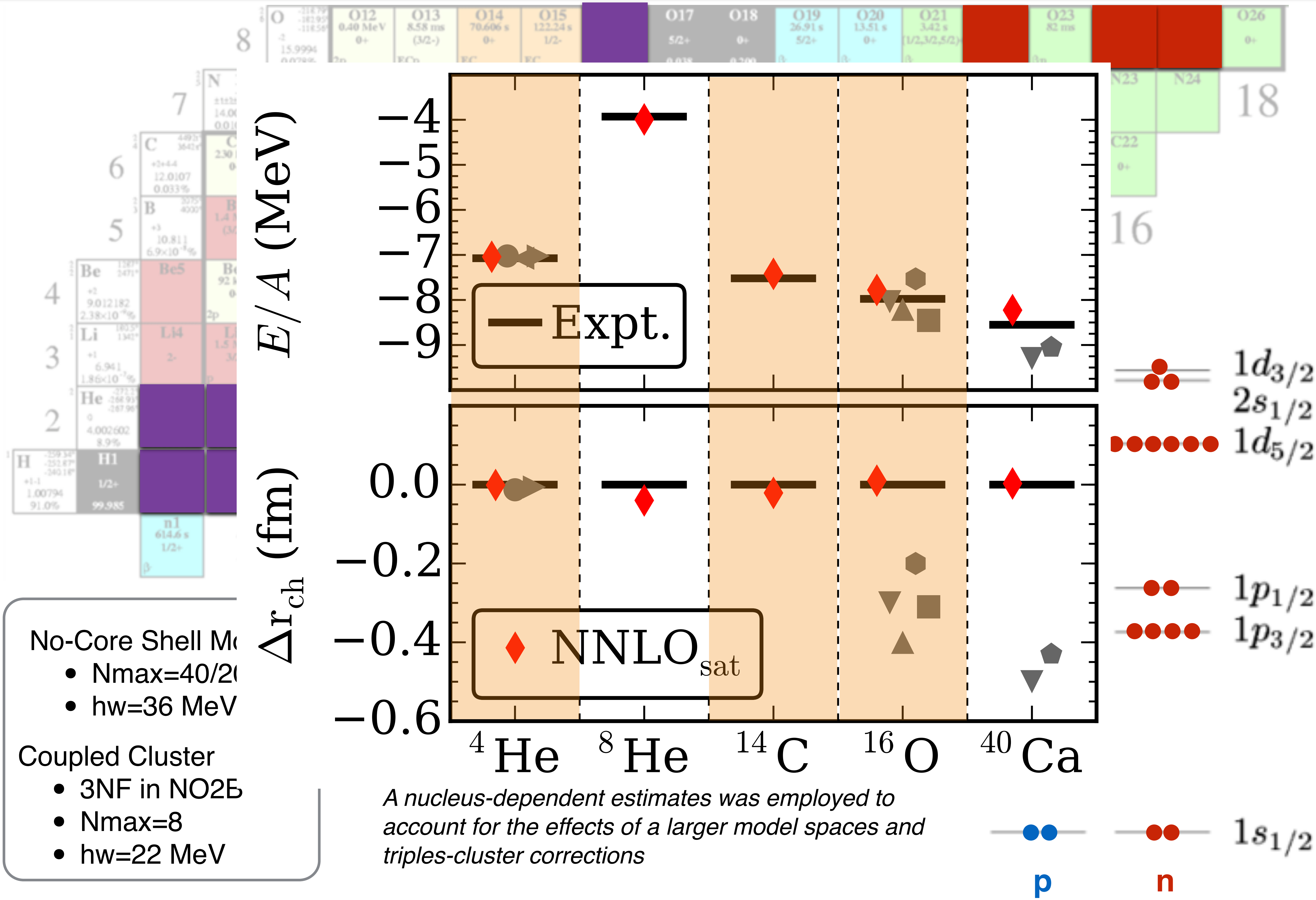

No-Core Shell Mo

- Nmax=40/2(
- hw=36 MeV

Coupled Cluster

- 3NF in NO2B
- Nmax=8
- hw=22 MeV

A nucleus-dependent estimates was employed to account for the effects of a larger model spaces and triples-cluster corrections

NNLO$_{sat}$ phase shifts and scattering observables

Phase shifts are very reasonable in the low energy range.

For higher energies, NNLO$_{sat}$ falls on the envelope of NNLO

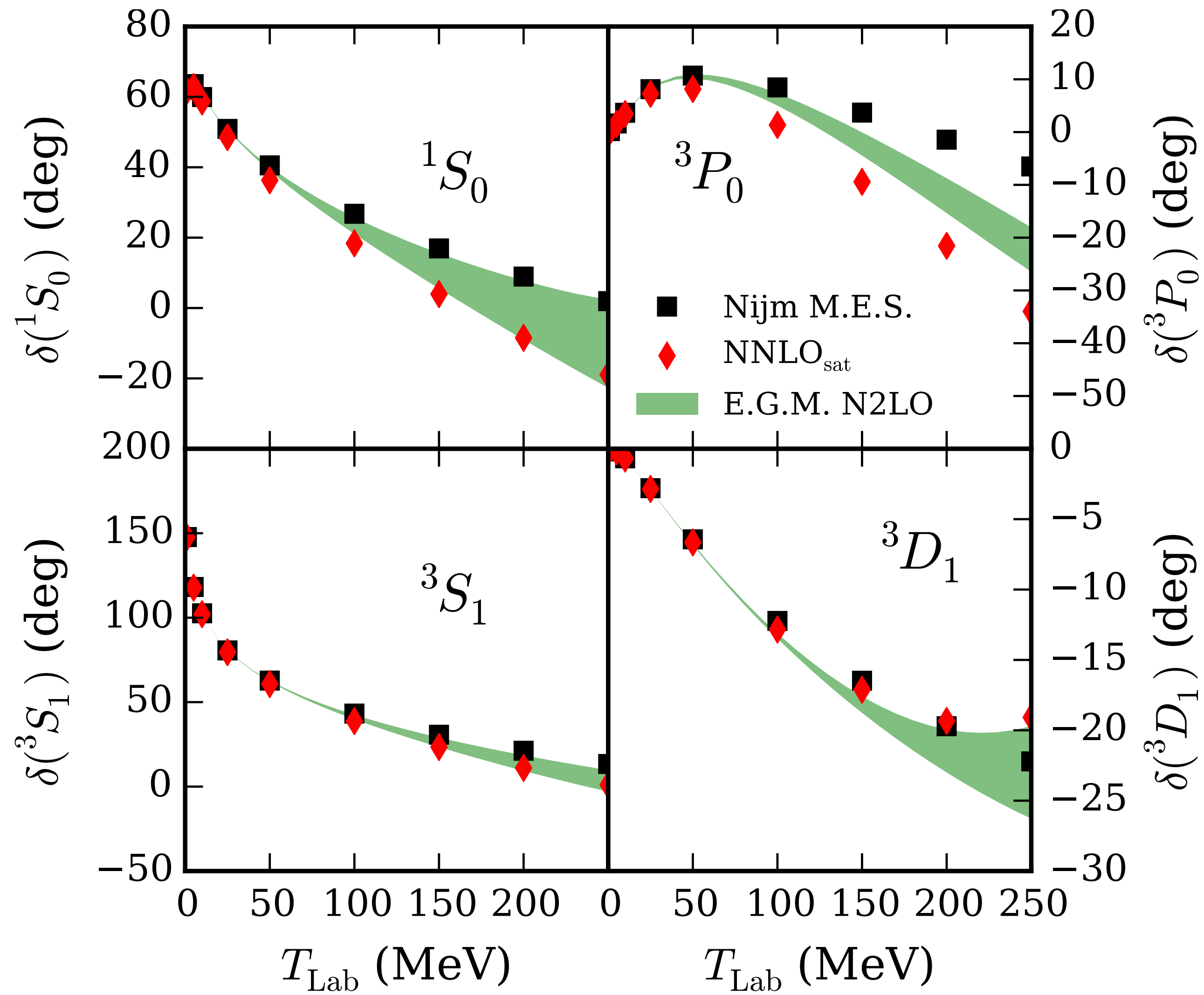

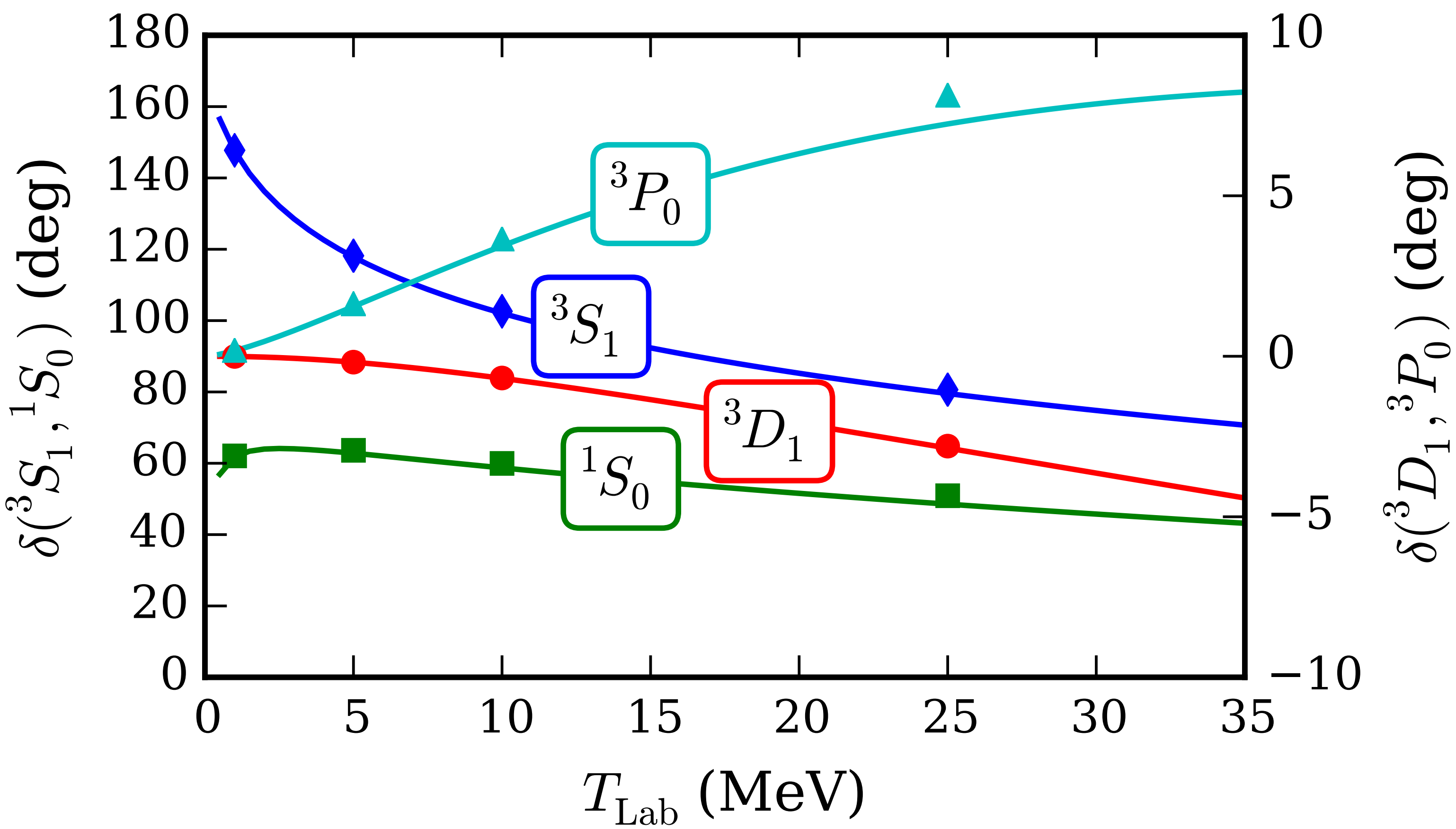

Chi square per datum

T_{Lab}	pp	np
0-35	6	3
35-125	164	7
125-183	118	18
183-290	314	16

without systematic uncertainty

$NNLO_{sat}$ and the reproduction of input data

NCSM Energies and charge radii with NNLOsat

Observable	Theory	Experiment	D/Exp (%)
$E_{gs}(^2H)$	-2.224574	2.224575(9) MeV	0.0
$r_{pt\text{-}p}(^2H)$	1.978	1.97535(85) fm	0.1
$Q_D(^2H)$	0.270	0.2859(3) fm^2	5.6
$P_D(^2H)$	3.46%	—	—
$E_{gs}(^3H)$	-8.52	-8.482 MeV	0.4
$r_{ch}(^3H)$	1.78	1.7591(363) fm	1.1
$E_{gs}(^3He)$	-7.76	-7.718 MeV	0.5
$r_{ch}(^3He)$	1.99	1.9661(30) fm	1.2
$E_{gs}(^4He)$	-28.43	-28.296 MeV	0.5
$r_{ch}(^4He)$	1.70	1.6755(28) fm	1.5

CCSD Energies and charge radii with NNLOsat

Observable	Theory	Experiment	D/Exp (%)
$E_{gs}(^{14}C)$	103.6	105.285 MeV	1.6
$r_{ch}(^{14}C)$	2.48	2.5025(87) fm	0.9
$E_{gs}(^{16}O)$	124.4	127.619 MeV	2.5
$r_{ch}(^{16}O)$	2.71	2.6991(52) fm	0.4
$E_{gs}(^{22}O)$	160.8	162.028(57) MeV	0.8
$E_{gs}(^{24}O)$	168.1	168.96(12) MeV	0.5
$E_{gs}(^{25}O)$	167.4	168.18(10) MeV	0.5

$^1S_0$ effective range expansion

Observable	Theory	Experiment	D/Exp (%)
a_{nn}	-18.93	-18.9(4) fm	0.2
r_{nn}	2.855	2.75(11) fm	3.8
a_{np}	-23.728	-23.740(20) fm	0.0
r_{np}	2.798	2.77(5) fm	1.0
a_{pp}	-7.8258	-7.8196(26) fm	0.0
r_{pp}	2.855	2.790(14) fm	2.3

$|\langle ^3He \| E_1^A \| ^3H \rangle| = 0.6343$
(empirical = 0.6848(11))

$$\langle r_{\rm ch}^2 \rangle = \langle r_{\rm pp}^2 \rangle + \langle R_{\rm p}^2 \rangle + \frac{N}{Z}\langle R_{\rm n}^2 \rangle + \frac{3\hbar^2}{4m_p^2c^2}$$

R_p=0.8775 fm
$(R_n)^2$=-0.1149 fm^2
Darwin-Foldy=0.033 fm^2

NNLO$_{sat}$ and the reproduction of input data

NCSM Energies and charge radii with NNLOsat

Observable	Theory	Experiment	D/Exp (%)
$E_{gs}(^2H)$	-2.224574	2.224575(9) MeV	0.0
$r_{pt\text{-}p}(^2H)$	1.978	1.97535(85) fm	0.1
$Q_D(^2H)$	0.270	0.2859(3) fm^2	5.6
$P_D(^2H)$	3.46%	—	—
$E_{gs}(^3H)$	-8.52	-8.482 MeV	0.4
$r_{ch}(^3H)$	1.78	1.7591(363) fm	1.1
$E_{gs}(^3He)$	-7.76	-7.718 MeV	0.5
$r_{ch}(^3He)$	1.99	1.9661(30) fm	
$E_{gs}(^4He)$	-28.43	-28.296 Me	
$r_{ch}(^4He)$	1.70	1.6755(28) f	

CCSD Energies and charge radii with NNLOsat

Observable	Theory	Experiment	D/Exp (%)
$E_{gs}(^{14}C)$	103.6	105.285 MeV	1.6
$r_{ch}(^{14}C)$	2.48	2.5025(87) fm	0.9
$E_{gs}(^{16}O)$	124.4	127.619 MeV	2.5
$r_{ch}(^{16}O)$	2.71	2.6991(52) fm	0.4
$E_{gs}(^{22}O)$	160.8	162.028(57) MeV	0.8
$E_{gs}(^{24}O)$	168.1	168.96(12) MeV	0.5
$E_{gs}(^{25}O)$	167.4	168.18(10) MeV	0.5

$^1S_0$ effective range expansion

Observable	Theory	Experimen	
a_{nn}	-18.93	-18.9(4) fm	
r_{nn}	2.855	2.75(11) fm	
a_{np}	-23.728	-23.740(20) fm	
r_{np}	2.798	2.77(5) fm	1.0
a_{pp}	-7.8258	-7.8196(26) fm	0.0
r_{pp}	2.855	2.790(14) fm	2.3

NNLO$_{sat}$
*reproduces the binding energies and the charge radii of selected psd-shell nuclei to **1%***

$\langle r^2_{\rm ch}\rangle = \langle r^2_{\rm pp}\rangle + \langle R^2_{\rm p}\rangle + \frac{}{Z}\langle R^2_{\rm n}\rangle + \frac{}{4m_p^2c^2}$

R_p=0.8775 fm
$(R_n)^2$=-0.1149 fm^2
Darwin-Foldy=0.033 fm^2

^{16}O charge density and negative parity states

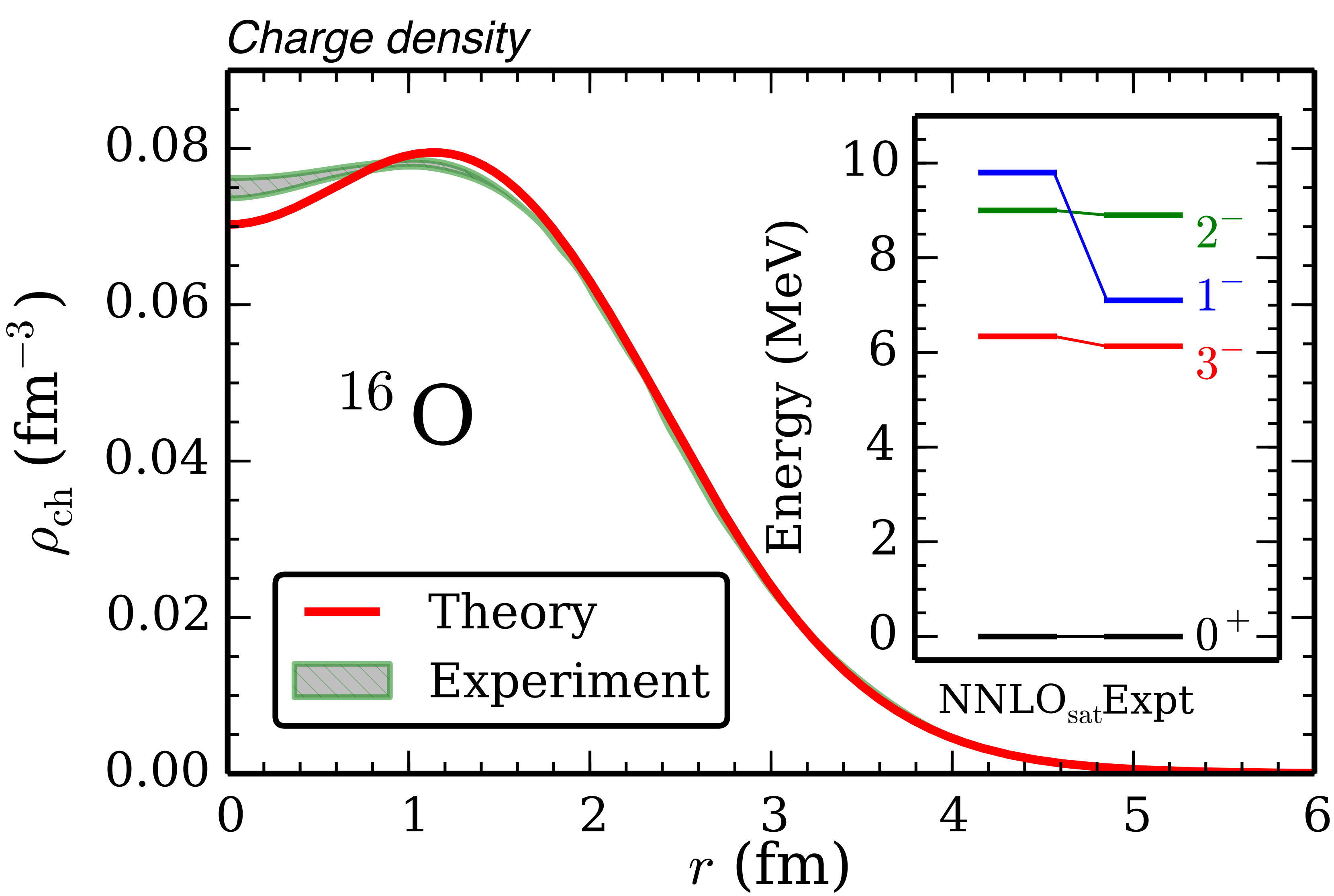

One-nucleon separation energies

	NNLOsat	Experiment
$S_n(^{17}O)$	4.0 MeV	4.14 MeV
$S_n(^{16}O)$	14.0 MeV	15.67 MeV
$S_p(^{17}F)$	0.5 MeV	0.60 MeV
$S_p(^{16}O)$	10.7 MeV	12.12 MeV

Λ-CCSD(T)
hw=22 MeV, Nmax=14
E3max=16
NO2B HF basis
+leading order
NNN contribution
to the total energy

ab initio challenge:
E(3^-)=6.34 MeV

NNLOsat
E(3^-)=6.13 MeV, 90%
1p-1h excitation ($p_{1/2}$-$d_{5/2}$)

1p-1h states sensitive to the particle-hole gap (A=16/17 separation energies)

Experimental charge distribution data: H. DeVries, et al At. Data Nucl. Data Tables 36, 494 (1987)

Spectra, binding energies and radii

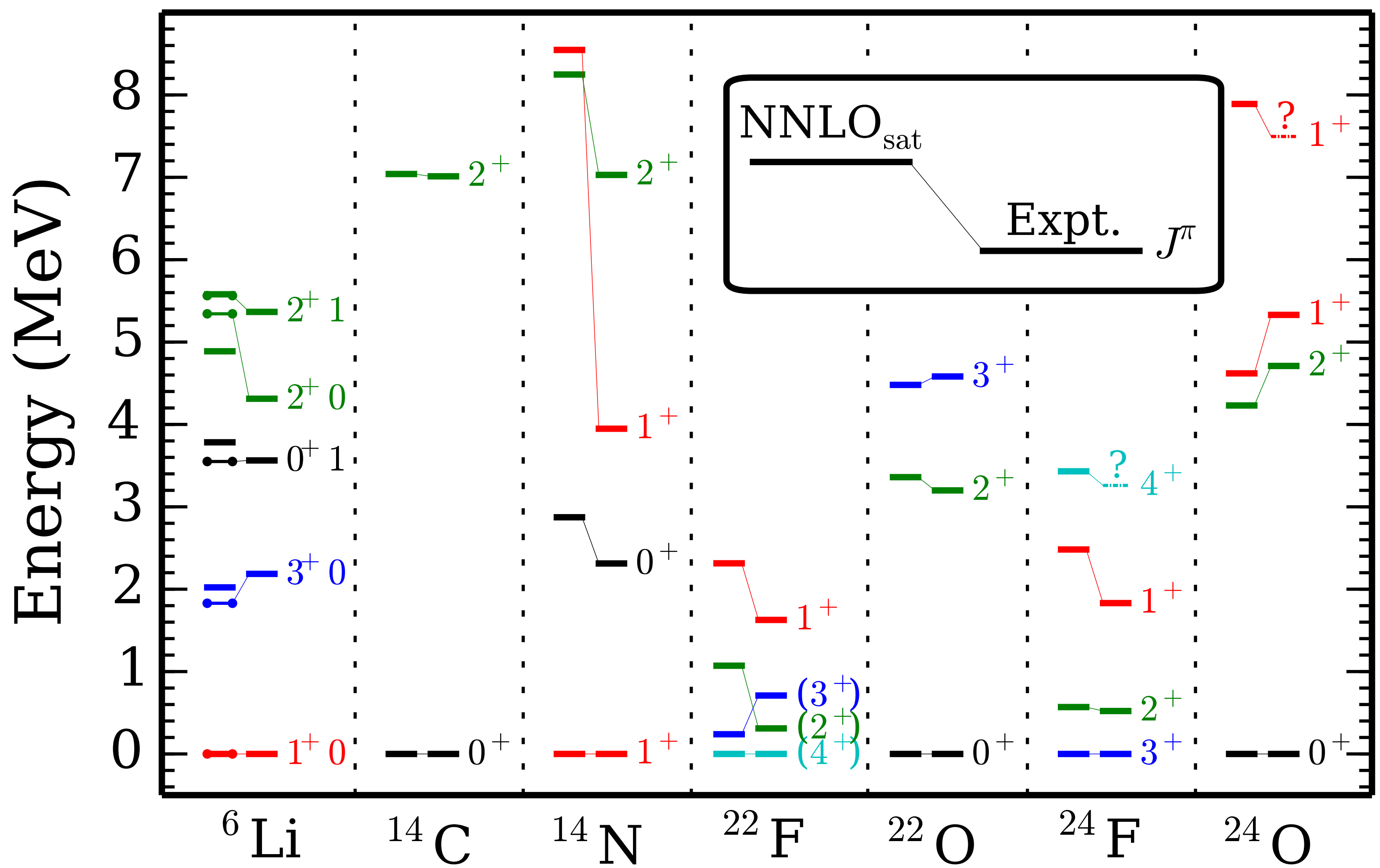

Λ-CCSD(T)
hw=22 MeV, Nmax=14
E3max=16
NO2B HF basis
+leading order
NNN contribution
to the total energy

Ground state energies in MeV:

	NNLO$_{sat}$	Exp.
^{6}Li	32.4	32.0
^{8}He	30.9	31.5
^{9}Li	43.9	45.3
^{14}N	103.7	104.7
^{22}F	163.0	167.7
^{24}F	175.1	179.1

Radii in fm:

	charge	matter	Exp.
^{8}He	1.91	—	1.959(16)
^{9}Li	2.22	—	2.217(35)
^{22}O	(2.72)	2.80	2.75(15)
^{24}O	(2.76)	2.95	—

^{18}O spectra compressed
E(2$^+$)=0.7 MeV (exp. 1.9 MeV)

Spectra, binding energies and radii

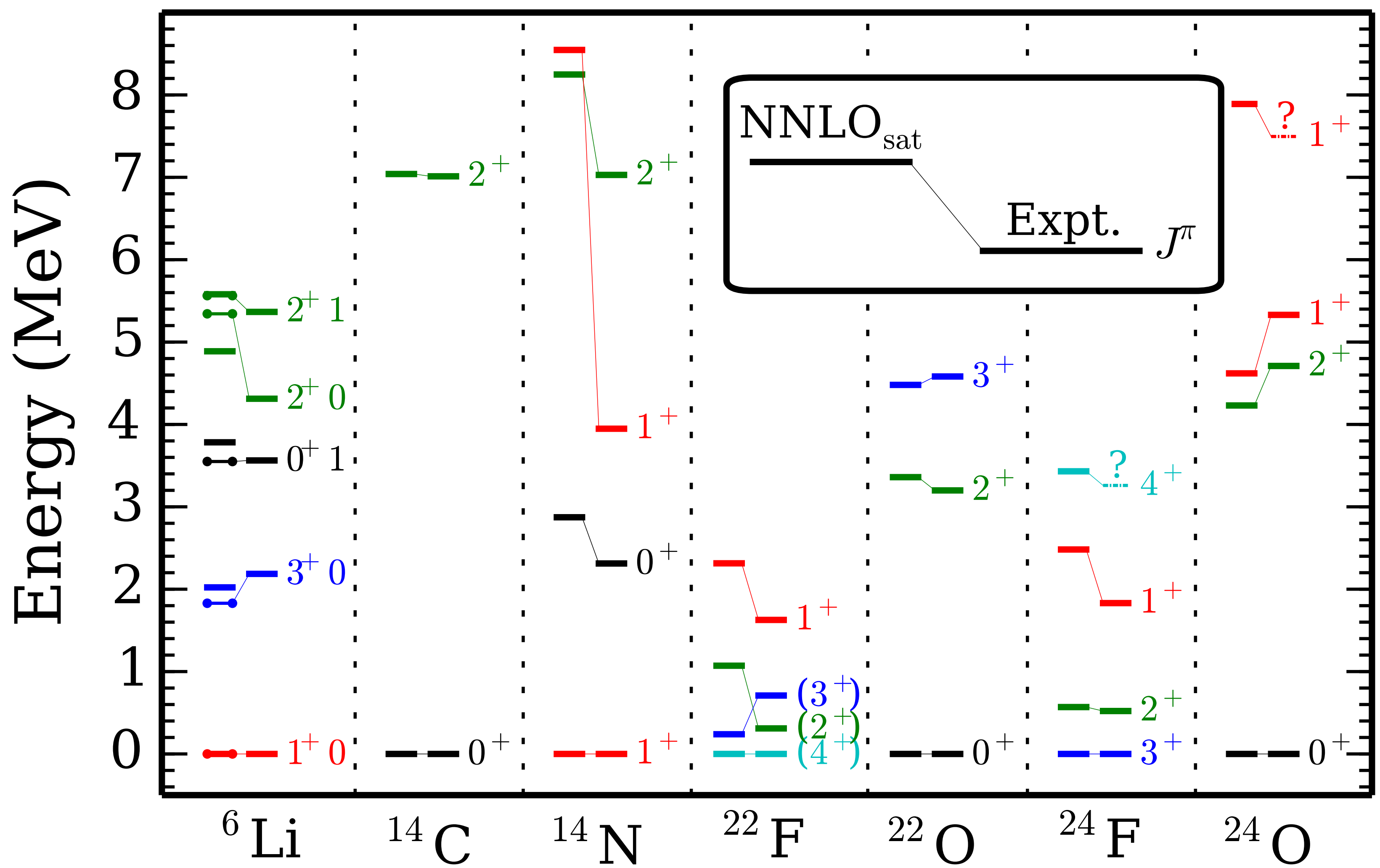

Calcium-40

	E_{gs} (MeV)	r_{ch} (fm)	E(3$^-$) (MeV)
NNLOsat	326	3.48	3.81
Experimen	342	3. 48	3.74

Λ-CCSD(T)
hw=22 MeV, Nmax=14
E3max=16
NO2B HF basis
+leading order
NNN contribution
to the total energy

Ground state energies in MeV:

	NNLO$_{sat}$	Exp.
^{6}Li	32.4	32.0
^{8}He	30.9	31.5
^{9}Li	43.9	45.3
^{14}N	103.7	104.7
^{22}F	163.0	167.7
^{24}F	175.1	179.1

Radii in fm:

	charge	matter	Exp.
^{8}He	1.91	—	1.959(16)
^{9}Li	2.22	—	2.217(35)
^{22}O	(2.72)	2.80	2.75(15)
^{24}O	(2.76)	2.95	—

^{18}O spectra compressed
E(2$^+$)=0.7 MeV (exp. 1.9 MeV)

NNLO$_{\mathrm{sat}}$ and symmetric nuclear matter

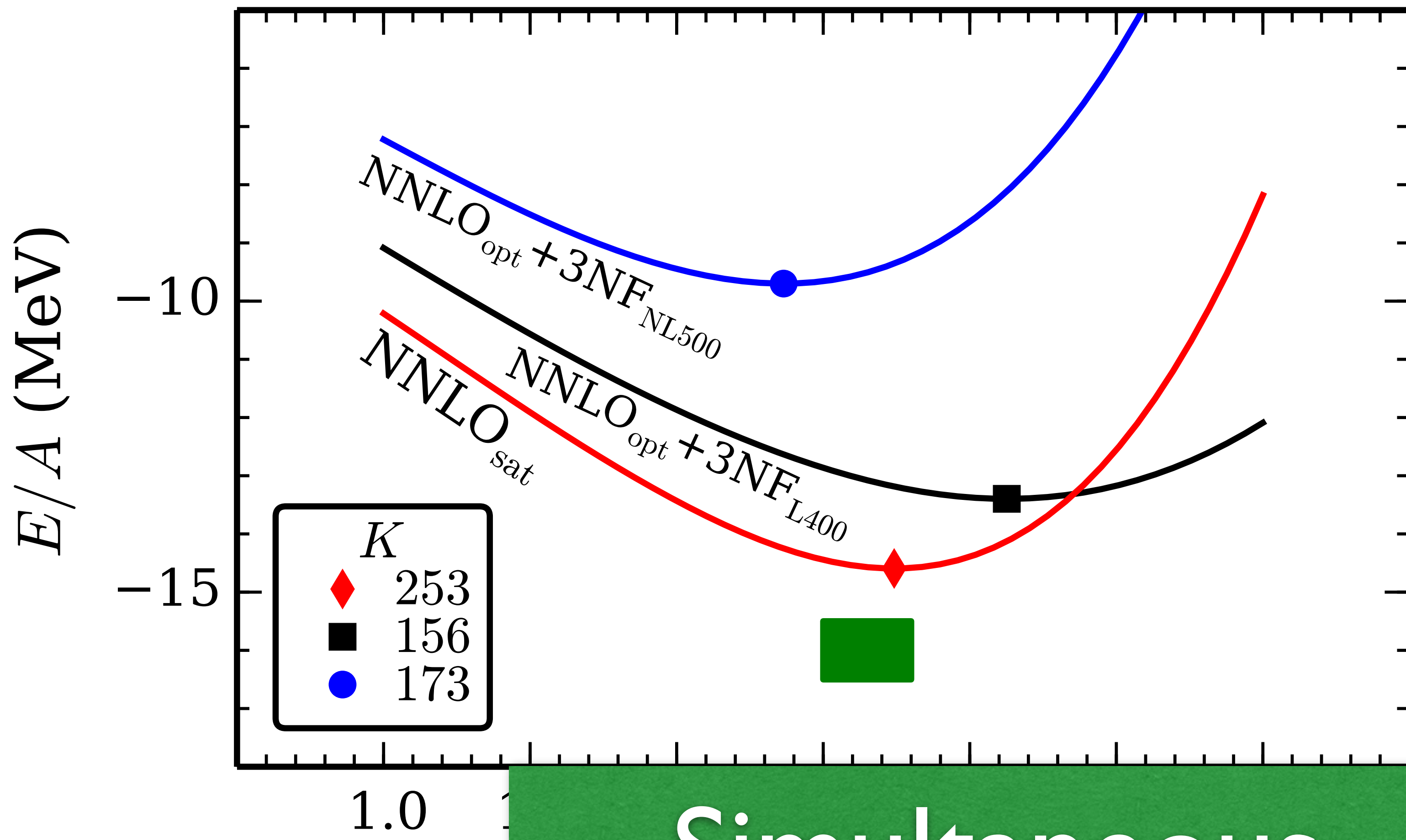

Simultaneous optimization is key!

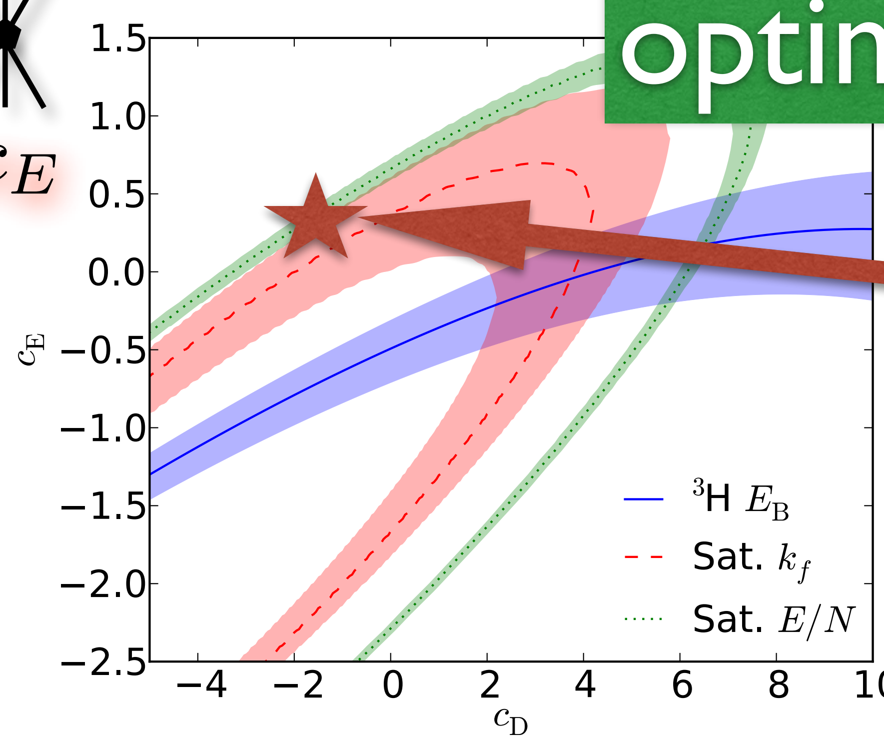

NNLO$_{\mathrm{opt}}$ + 3NF$_{\mathrm{NL500}}$:

E/A=-15.5 MeV & k_f=1.4 fm^{-1}
^{3}H =-13.5 MeV (!)

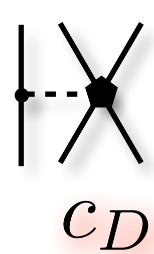

Coupled-cluster calculations of nucleonic matter

G. Hagen et al.

PHYSICAL REVIEW C 89, 014319 (2014)

NNLO$_{\mathrm{sat}}$ saturation properties

E/A = -14.59 MeV
k_f = 1.35 fm-1
ρ_0 = 0.17 fm-3

incompressibility

$$K = 9\rho_0^2 \frac{d^2(E/A)}{d\rho^2}\bigg|_{\rho=\rho_0}$$

inversely proportional to the compressibility.

cannot be measured directly, but related to e.g. the giant monopole resonance ('breathing mode') in finite nuclei.

J. P. Blaizot Phys. Rep. 64, 171 (1980)

NNLO$_{sat}$ and symmetric nuclear matter

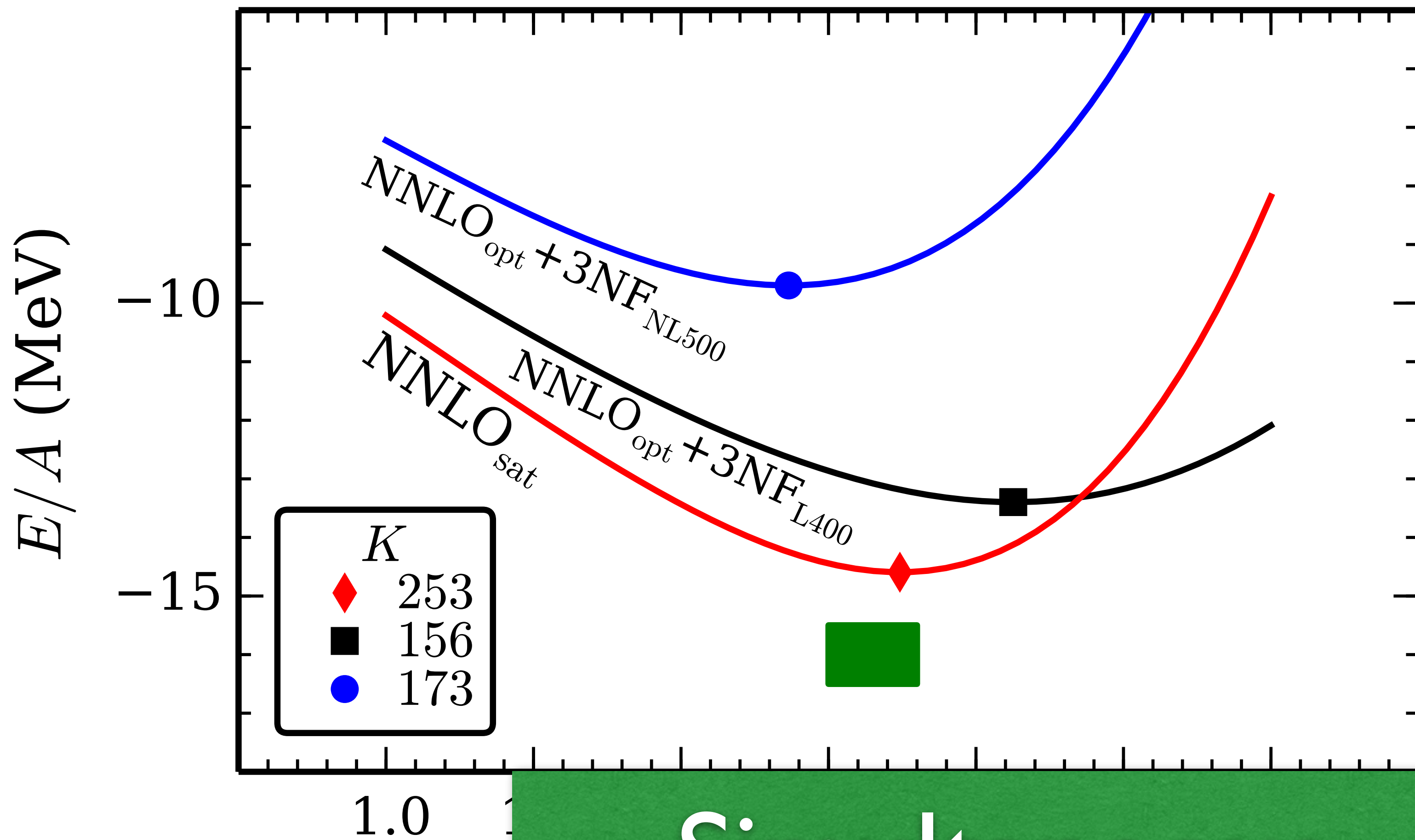

Simultaneous optimization is key!

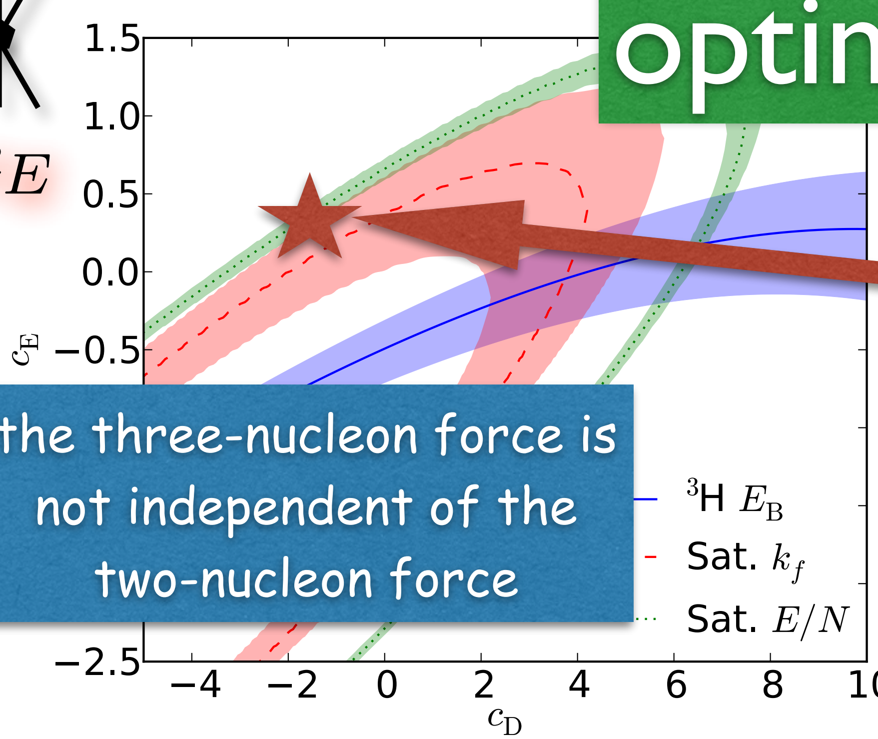

the three-nucleon force is not independent of the two-nucleon force

NNLO$_{opt}$ + 3NF$_{NL500}$:

E/A=-15.5 MeV & k_f=1.4 fm^{-1}
^{3}H =-13.5 MeV (!)

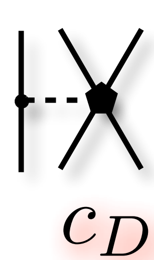

Coupled-cluster calculations of nucleonic matter

G. Hagen et al.

PHYSICAL REVIEW C 89, 014319 (2014)

NNLO$_{sat}$ saturation properties

E/A = -14.59 MeV
k_f = 1.35 fm-1
ρ_0 = 0.17 fm-3

incompressibility

$$K = 9\rho_0^2 \frac{d^2(E/A)}{d\rho^2}\bigg|_{\rho=\rho_0}$$

inversely proportional to the compressibility.

cannot be measured directly, but related to e.g. the giant monopole resonance ('breathing mode') in finite nuclei.

J. P. Blaizot Phys. Rep. 64, 171 (1980)

Summary and conclusions

- *"We are tightening the experiment-theory feedback loop"*
- *Progress in ab initio nuclear physics using a **consistently in-medium optimized force: NNLO$_{sat}$.*** *(designed for masses and radii)*
- *In ^{48}Ca, we have constructed a **bridge to nuclear density functional theory** and predicted intervals for relevant observables.*
- *Next step: the optimization of **N3LO NN+3NF.***
- *Much effort is going into estimating the **uncertainty budget** of chiral interactions and many-body calculations.*
- *Advanced **optimization/regression technology in place** for uncertainty quantification in few-nucleon sector.*
- *Work in progress to include **NNN scattering in optimization.***

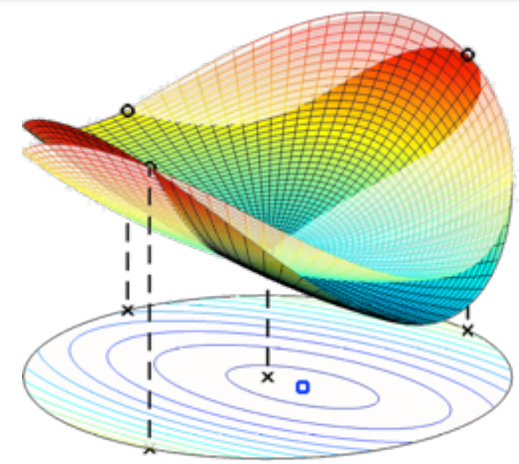

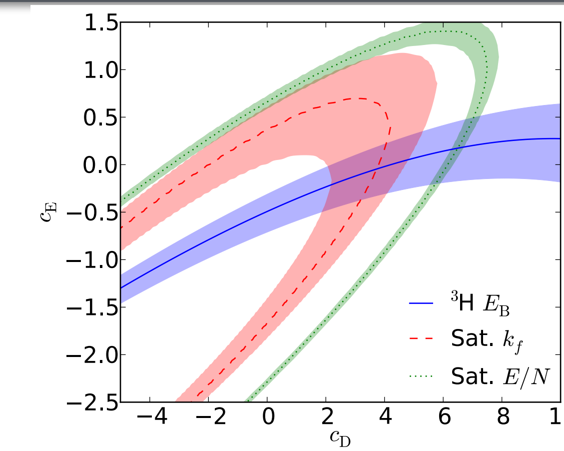

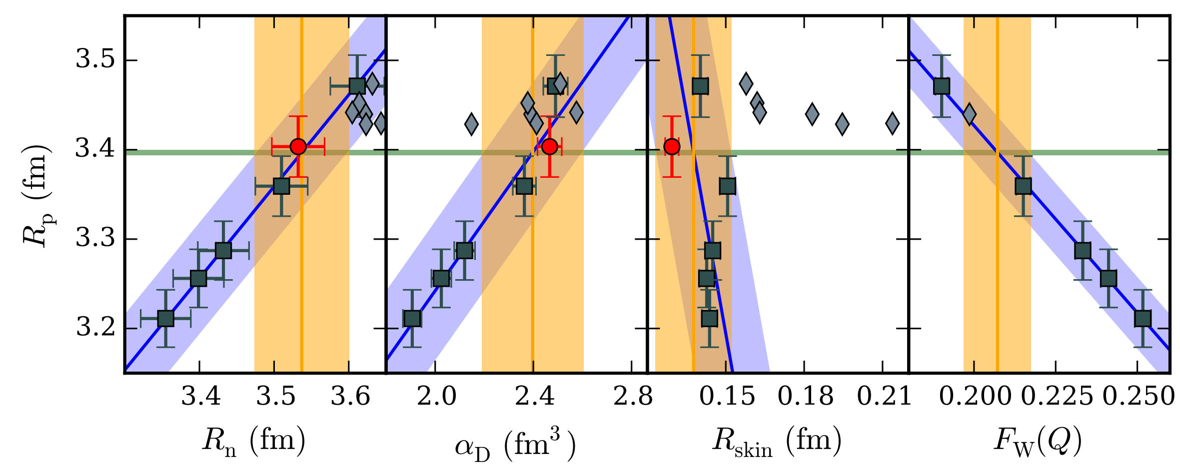

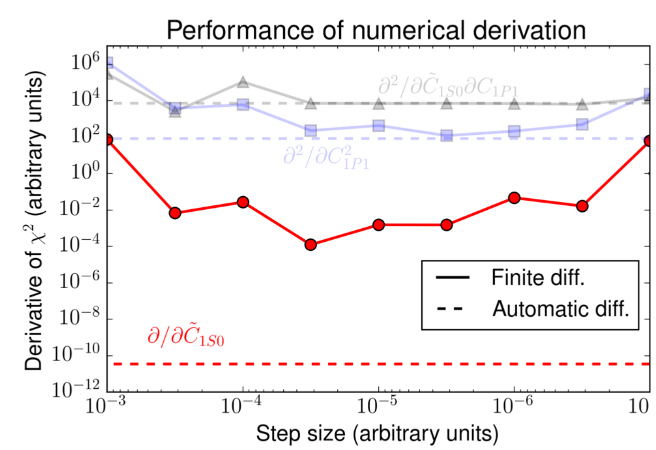

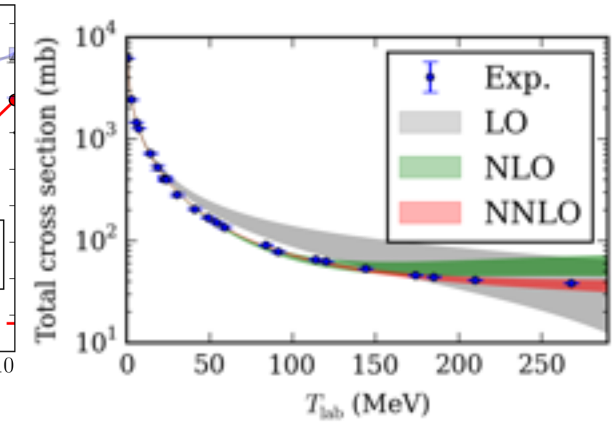

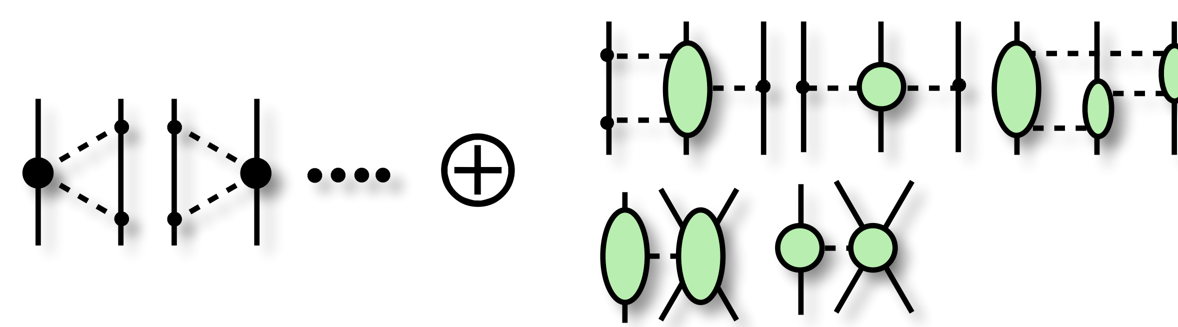

THANK YOU FOR YOUR ATTENTION

Collaborators:

Boris Carlsson (UiO/Chalmers)
Christian Forssén (Chalmers)
Gaute Hagen (UT/ORNL)
Morten Hjorth-Jensen (UiO/MSU)
Gustav Jansen (UT/ORNL)
Ruprecht Machleidt (UI)
Petr Navrátil (TRIUMF)
Witold Nazarewicz (MSU/UT/ORNL)
Thomas Papenbrock (UT/ORNL)
Kyle Wendt (UT/ORNL)

Sonia Bacca (TRIUMF)
Nir Barnea (HU)
Christian Drischler (TUD)
Kai Hebeler (TUD)
Mirko Miorelli (TRIUMF)
Giusephina Orlandini (INFN/TIFPA)
Achim Schwenk (TUD)

<u>and special thanks to the Bachelor students:</u>
Dag Fahlin Strömberg (Chalmers)
Oskar Lilja (Chalmers)
Mattias Lindby (Chalmers)
Björn A. Mattsson(Chalmers)

Appendix